Power Stability Investigation and Control of Rail Way Power Supply System using Particles Swarm Optimization of Proportional Integral Controller (Case Study:- Lebu to Adama line)

Bedasa Tolera Tolesa

A Thesis Submitted to

The Department of Electrical Power and Control Engineering

School of Electrical Engineering and Computing

Presented in Partial Fulfillment of the Requirement for the Degree of Master's in Electrical Power and Control Engineering

(Power System Engineering)

Office of Graduate Studies

Adama Science and Technology University

July 2023

Adama, Ethiopia

Power Stability Investigation and Control of Rail Way Power Supply System using Particles Swarm Optimization of Proportional Integral Controller (Case Study:-Lebu to Adama line)

Bedasa Tolera Tolesa

Advisor: Tafesse Asirat (PhD.)

A Thesis Submitted to

The Department of Electrical Power and Control Engineering School of Electrical Engineering and Computing

Presented in Partial Fulfillment of the Requirement for the Degree of Master's in Electrical Power and Control Engineering

(Power System Engineering)

Office of Graduate Studies

Adama Science and Technology University

July 2023

Adama, Ethiopia

DECLARATION

I hereby declare that this Master Thesis entitled "Power Stability Investigation and Control of Rail Way Power Supply System using PSO-PI Controller (Lebu to Adama line)" is my original work. That is, it has not been submitted for the award of any academic degree, diploma or certificate in any other university. All sources of materials that are used for this thesis have been duly acknowledged through citation.

Bedasa Tolera	___________	__________
Name of the Student	Signature	Date

RECOMMENDATION

I, the advisor of this thesis, hereby certify that I have read the revised version of the thesis entitled "Power Stability Investigation and Control of Rail Way Power Supply System using PSO-PI Controller (Lebu to Adama line)" prepared under my guidance by **Bedasa Tolera** submitted in partial fulfillment of the requirements for the degree of Mater's of Science in Power Engineering. Therefore, I recommend the submission of revised version of the thesis to the department following the applicable procedures.

Tafesse Asirat (PhD.)	________________________	_____________________
Major Advisor	Signature	Date

APPROVAL SHEET

I, the advisors of the thesis entitled "Power Stability Investigation and Control of Rail Way Power Supply System using PSO-PI Controller (Lebu to Adama line)" and developed by **Bedasa Tolera**, here by certify that the recommendation and suggestions made by the board of examiners are appropriately incorporated into the final version of the thesis.

Major Advisor	Signature	Date

We, the undersigned, members of the Board of Examiners of the thesis by **Bedasa Tolera** have read and evaluated the thesis entitled "Power Stability Investigation and Control of Rail Way Power Supply System using PSO-PI Controller (Lebu to Adama line)" and examined the candidate during open defense. This is, therefore, to certify that the thesis is accepted for partial fulfillment of the requirement of the degree of Master of Science in Power Engineering.

Chairperson	Signature	Date
Internal Examiner	Signature	Date
External Examiner	Signature	Date

Finally, approval and acceptance of the thesis is contingent upon submission of its final copy to the Office of Postgraduate Studies (OPGS) through the Department Graduate Council (DGC) and School Graduate Committee (SGC).

Department Head	Signature	Date
School Dean	Signature	Date
Office of Postgraduate Studies, Dean	Signature	Date

ACKNOWLEDGMENT

I want to start by giving God, the Almighty, praise and thanks for his favors during my research.

My advisor and mentor, **Dr. Tafesse Asirat**, has always provided me with invaluable advice and support, and it gives me great pleasure to convey my sincere gratitude to him. I am very appreciative of the excellent advice, motivation, and suggestions that he has provided me while I have been working on this thesis.

In addition to my advisor, I'd like to thank my friends, especially **Mr. Temesgen Getahun** (substation technician operation) for making my study and completion of this thesis at the university so pleasurable and competent. They created an academic and incredibly nice study environment.

Without acknowledging the greatest source of my strength, my family and relatives, for their unending love, support and encouragement, my acknowledgement would fall short. Without you there, it would not have been possible.

Table of Contents

LIST OF FIGURES

LIST OF TABLES

LIST OF ACRONYMS

Abbreviations	Descriptions
AC	Alternating Current
DC	Direct Current
ERC	Ethiopian Railway Corporation
FACTS	Flexible AC Transmission System
GA	Genetic Algorism
IEEE	Institute Of Electrical and Electronics Engineering
IPFC	Interline Power Flow Controller
MC	Magetic Circuit
PI	Proportional Integral
PSO	Particl swarm optimization
STATCOM	Static Compensator
SVC	Static Var Compensator
SVG	Static Var Generator
TCR	Thyristor-Controlled Reactor
TCSC	Thyristor-Controlled Series Capacitor
TCSR	Thyristor-Controlled Series Reactor
TCPST	Thyristor Controlled Phase Shifting Transformer
TCPAR	Thyristor Controlled Phase Angle Regulator
TCVR	Thyristor Controlled Voltage Regulator
TPSS	Traction Power Supply System
TSC	Thyristor-Switched Capacitor
TSR	Thyristor-Switched Reactor
TSSR	Thyristor-Switched Series Reactor
UPFC	Unified Power Flow Controller
VSC	Voltage Source Convertor

ABSTRACT

Due to the use of transformers, power electronic converters, and variable loads, power quality is the primary area of concern in electric traction systems. It always needs a power supply system that is effective, dependable, and economical. The 752.6 km long Ethio-Djibouti railway line connects Nagad, Djibouti, to Addis Ababa, Ethiopia, and is powered by a 25 kV, 50 Hz AC overhead power source. This thesis discusses traction power supply system modelling, power quality evaluation, and improvement for the Lebu to Adama railway line. The initial power factor in the ethio-dijibuti line in Lebu-Adama line is 0.67. The components of the traction power supply system's relevant data and parameters have been gathered, modelled, and examined. All significant traction power supply system components have undergone mathematical study and modelling, which includes both constant and variable power models. The traction power variation experienced by moving trains is accurately simulated by the variable power model. Analyses of train dynamics are also performed. A STATCOM has been analyzed, modelled as a controller, and applied to return good reactive power compensation and boost poor power factor while maintaining line voltage within the specified range. This STATCOM uses an algorithm based on instantaneous active and non-active current theory. To enhance performance, the PI controller's parameters are tuned using particle swarm optimization. In order to improve current and voltage, STATCOM is additionally simulated as an LCL filter-enhanced SVG-optimized model. The following phase is simulating the entire system using static and dynamic power models in the MATLAB/Simulink environment and contrasting it with the model of the existing system devoid of the controller. 99% of reactive power is compensated thanks to the usage of this approach, and a power factor of 0.9999 has been maintained throughout the motion. Furthermore, the overall harmonic distortion decreases to 0.5%, which is below the standards set by other countries. The dynamic performance parameters are also enhanced in this thesis study.

Keywords: *Power quality, Dynamic power model, STATCOM, non-active current, MATLAB/Simulink*

CHAPTER ONE

INTRODUCTION

1.1. Background

Trains are powered by electric power instead of fuel thanks to the Electric Traction System. Due to its many benefits, including fast speed, large capacity, cheap energy costs, and decreased carbon emissions, this type of electrification system is growing in popularity. Shoman and others, 2022 Ethiopia is presently extending parts of its electrified rail network, including the brand-new Addis Ababa-Djibouti Railway. This standard-gauge railway runs 752.26 kilometres from the capital of Ethiopia and the port of Djibouti. The system depends on a 25 kV 50 Hz AC overhead line direct feeding system with a return wire to provide the trains with dependable, high-quality electricity. For this train to operate properly, stable power is required (E. R. Corporation, 2021).

For reliable and secure electric power distribution to consumers, power system stability is a crucial component of power system functioning. A power system's ability to remain stable is referred to as its stability. Establish operational conditions and swiftly and safely recover from disruptions, such as load changes or faults. There are two basic types of power system stability. Those are dynamic and state stability. Static stability refers to the ability of a system or object to return to its original position or equilibrium after being displaced. In other words, it measures the system's tendency to resist change and maintain its balanced state.. In the presence of minor disturbances, such as alterations in load or generation, maintain operating conditions. Maintaining acceptable levels of voltage and frequency requires this kind of steadiness. Dynamic stability, on the other hand, is concerned with the system's response to external disturbances or changes over time. It refers to the ability of a system to return to its equilibrium position after being subjected to a disturbance or deviation.

Since transformers, motors, line impedances, multiple converters, and the moving nature of the system pose a number of quality issues, power quality is a major concern in electrified railway systems. Voltage fluctuation, low power factor, inadequate power flow control, voltage loss, and other issues of this calibre affect even the distribution network. There is a variety of literature that offers solutions to the issues with the electric traction network. Numerous researchers have attempted to solve those challenges using a variety of methods. In conclusion, sustaining the reliable and secure distribution of electric power to consumers depends on the stability of the power system, which is a fundamental component of power system operation. Steady State stability and dynamic stability are the two main categories of power system stability, and various methods are used to assess and improve stability, including power system modeling, stability analysis, and control design(Li, F., He, J., Li, C., & Qiu, 2018).

However, problems with power quality and dynamic stability can arise in power traction systems, such as power unbalance, harmonics, and reactive power, which can lead to extra line losses, under. Voltage at the terminal of contact wire, and unbalanced utility grid currents. The severity of these issues depends on the railway traction loads, including the movement of trains, tractive profile of electric locomotives, and power supply scheme. To alleviate these power quality problems, Flexible Alternating Current Transmission System (FACTS) controllers are employed. There are four types of FACTS controllers, including series, shunt, combined series. Series, and combined series. Shunt controllers(Zhang, W., Li, L., & Wang, 2019).

Of these, the combined series. Shunt controller, such as the Unified Power Flow Controller (UPFC), is the most versatile, able to perform compensation and control functions for different individual line compensators and controllers.

However, it requires a complex control circuit. The focus of this thesis is on the double track section of the Ethio-Djibouti line from Lebu to Adama, which has experienced problems with reactive power and power factor, resulting in unnecessary additional costs. The aim is to analyze, model, and simulate the traction power supply system and mitigate the power quality problems by introducing a Static Synchronous Compensator (STATCOM) based reactive power mitigation technique. To control the STATCOM device(Amjady, N., & Soroudi, 2010), the system requires a Pulse Width Modulation (PWM) generator based on the feedback controller, with cascade Based PI and PR controllers generating accurate PWM output for power semiconductor device switching. The system is nonlinear and requires an optimization algorithm, such as a Particle Swarm Optimization, to determine the optimal gain for the cascade controller. Finally, the system is simulated using MATLAB/Simulink, and conclusions are drawn based on the results.

1.2. Statement of the Problem

The electric traction system must use electricity cost-effectively, consistently, and efficiently. Although it works efficiently, it is susceptible to problems with the quality of the power, such as reactive power and inadequate power factor, which can cause power imbalance and overload at the loads in the railway feeding system. It is preferable to increase actual power and decrease reactive power consumption while raising the power factor to close to unity in order to optimize traction performance and power supply circumstances. Reactive power can affect voltage regulation, power factor, and transmission efficiency if it is not taken into account, as well as necessitate larger conductors.

Energy meter readings from the Mojjo and Endode substations on the Ethio-Djibouti railway line in August 2018 indicated serious actual and reactive power issues. The total actual and reactive energy at Endode was 520,608 kWh and 490,960 kVar, respectively, with a power factor of 0.67, which is significantly less than the necessary value of 0.95. In order to regulate electric power systems and lower transmission line losses, reactive power compensation is required. It can affect real power, power factor, and system voltage if it is not corrected, resulting in voltage changes, controller's settings. An adequate controller and optimisation methods are needed to reduce these issues. In order to enhance the dynamic performance of the controller's parameters, a STATCOM with traditional PI and PR controllers is applied in the train power supply in this study.

1.3. Objectives

1.3.1. General Objective

The general objective of this study is to model and analyses the traction power supply system and apply appropriate mitigation techniques to improve the quality of power supplied.

1.3.2. Specific Objectives

- To improve the power factor of the railway line's power supply
- To increase the traction power supply system's effectiveness utilizing the STATCOM Controller

- To simulate and analyse the railway line's traction power supply system.
- To use MATLAB to simulate the system with PSO tuned PI controller optimisation and compare the outcomes with and without the added solution.

1.4. Scope of the Research

This thesis examines electricity quality issues and suggests ways to address them while taking the Lebu to Adama railway line into account. There are two types of traction power supply models presented: static and dynamic models. Using PSO-optimized PI and PR controllers for STATCOM converter, the reactive power and power factor problems with respect to power quality were examined. MATLAB/Simulink has been used to simulate the entire model.

1.5. Limitation of the study

This study solely relies on MATLAB simulation and software design to demonstrate parameter improvement. Because of the expense and lack of material accessibility, it is therefore impossible to implement hardware for verifying the precise working of the system

1.6. Significance of the Study

The improvement in power factor on the Ethiopian-Digibuti rail line, notably between Modjo and Adama, is the relevance of this study. Power factor improvement results in increased train active power use and power stability..

1.7. Organization of the Thesis

There are five chapters in this thesis. Chapter one: Describes the context of the investigation, the problem statement, the goals and parameters of the study, the data analysis, and the research technique. The fundamental ideas and theories behind an electrified railway line are described in Chapter 2. The third chapter focuses on the study's modelling. The findings of the simulations and discussions of the study are covered in Chapter 4. In chapter five, general findings are drawn along with suggestions for additional research.

CHAPTER TWO

LITRATURE REVIEW

2.1. Review of Electric Traction Power Supply System

The electrified railway system has a long history that dates back to the 19th century. Throughout its history, it has experienced significant advancements in electrical engineering, mechanical engineering, power electronics, and automation, all of which have led to the development of new technologies. Despite the high investment required for electric traction systems, they offer significant advantages in terms of performance, safety, environmental compatibility, and economy of service. Electrified railways cover over 200,000 km, which is equivalent to 17.2% of the global railway network(Bie, Z., Wang, H., & Li, n.d.).

Electrified railways can be supplied with either AC or DC power. The most common railway systems in the world are 3/1.5 kV DC voltage systems, with a distance of 15.30 km between substations, and 0.6.1.4 kV DC low voltage systems, with a distance of 1.6 km between substations. AC 15kV/16.7Hz or 25kV/50Hz single phase systems, and AC 25kV/50Hz three phase systems are also used(Rendón, A., de Castro, A., & Rodríguez, 2014).

Modern power electronic traction control systems have made DC supply advantageous due to the compact size and weight of chopper and inverter drives. AC power, on the other hand, is more economical for high speed and heavy Haul railways. The high catenary voltage of AC systems means that lower currents and smaller power losses are required, resulting in fewer substations compared to DC traction networks. Low. Frequency, polyphase, and standard frequency AC systems are applicable, with low frequency reducing inductive voltage drop and the required number of substations. The use of polyphase AC systems is limited due to the difficulty of power collection through the pantograph or third rail of the rolling stock. The structure of the 25 kV/50Hz AC railway electrification system is shown in Figure 2.1.

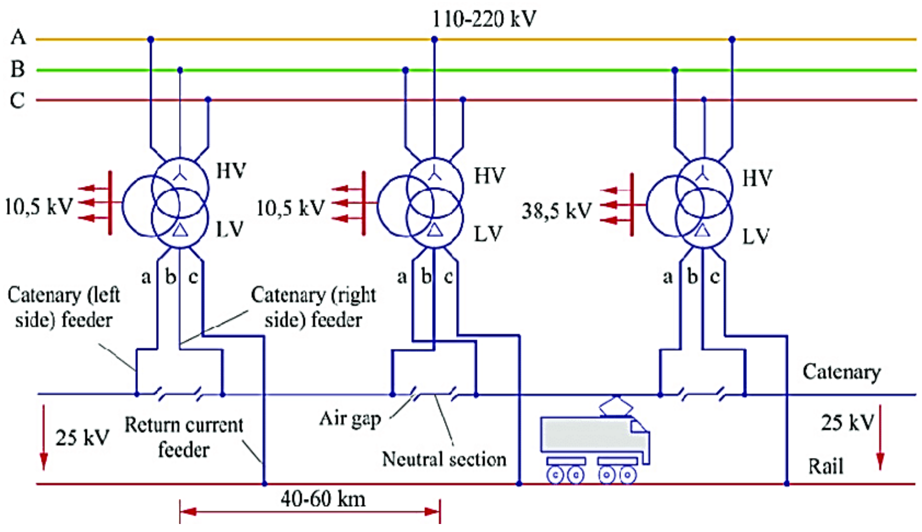

Figure 2. 1.Structure of 25 kV/50Hz AC railways electrification system(Kurdak & B., 2010)

2.2. Feeding Arrangements in AC Traction Power Supply System

There are different feeding mode configurations of the AC traction power supply system. These are direct feeding configurations with and without a return conductor, booster transformer and autotransformer power feeding system.

2.2.1. Direct Feeding Configuration

The direct feeding configuration is the cheapest and simplest way of supplying power. It is performed by the direct connection of the traction feed transformer to the catenary and rails of each substation. This configuration is disadvantageous since it has high feeding impedance with large losses, high rail to earth voltage and the earth currents that can cause interference in the nearby telecommunication circuits(Zargari, N. R., Niroomand, S., & Shahnia, 2018).

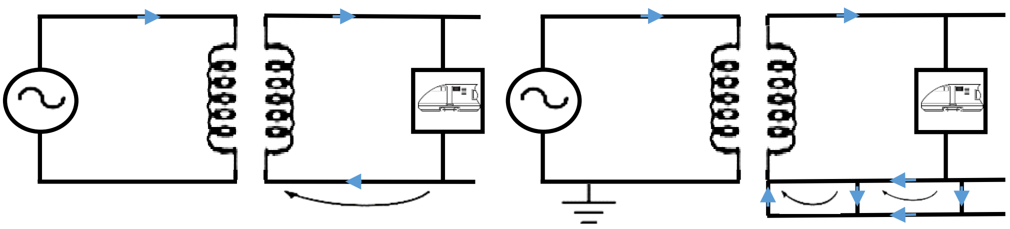

(a) Direct feeding without returns conductor (b) Direct feeding with return conductor

Figure 2. 2.Direct feeding configuration without and with return conductor

A return conductor is added to provide lower impedance traction current return path and reduce the stray current. Figure 2.2 illustrates direct feeding with and without a return conductor.

2.2.2. Booster Transformer Feeding Configuration

To minimize inductive interference on telecommunication lines, a Booster Transformer with a turn ratio of one is installed every 4 km on the contact wire, which boosts the current of the return circuit on the negative line. This is because the current only flows to the rail in certain areas. The primary of the transformer is connected to a gap in the contact wire, while the secondary is connected to an insulated rail section. The transformer forces the traction return current to flow from the rails and earth through its secondary.

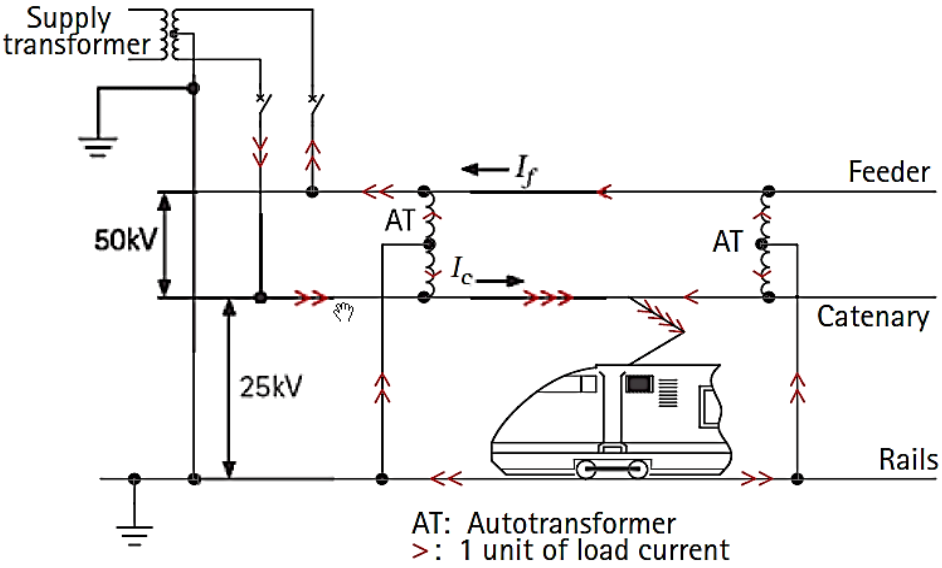

Figure 2. 3.Booster transformer feeding configuration(Nkundineza, 2017)

2.2.3. Autotransformer Feeding Configuration

Unused guidelines for the AC zap system were created and more nations included ATs in their railroad systems after AT was introduced in Japan in 1972, and beginning since 1981. This system was spearheaded within the early 20th century in Philadelphia USA, utilizing 36kV transmission and 12kV supply (Vladu, A., & Andrei, 2015). It combines the advantage of higher voltage power transmission with the good thing about utilizing standard 25 kV/50 kV equipment. The autotransformers along the catenary line are utilized to adjust the voltages between the catenary and the earth, and the negative stage conductor and the soil, and after that disseminate the return current equally between the two stages. As compared to coordinate and Booster transformer bolstering mode arrangement, AT feeding mode has a Lower misfortune since of higher voltage, longer remove between catenary feeder substations additionally way better collection of returning stray streams. Other than, it in addition simpler to preserve since the setup permits isolating a number of substations. Figure 2.4 appears the autotransformer nourishing arrangement.

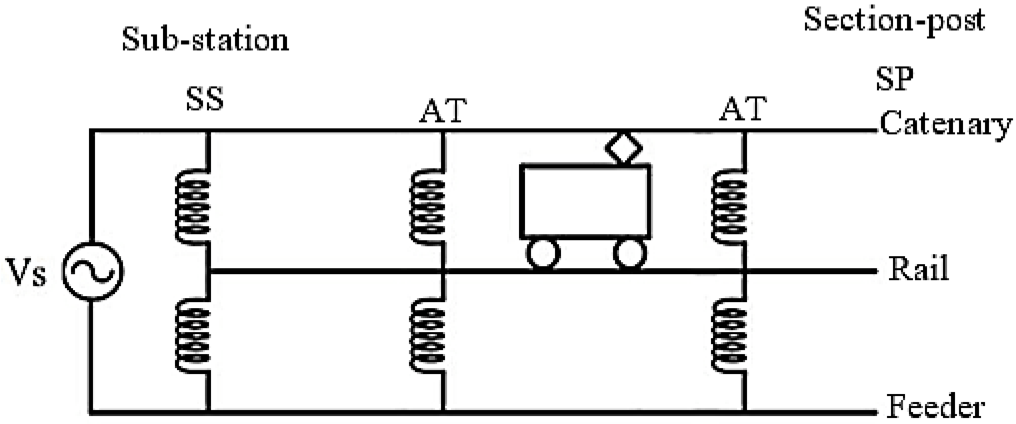

Figure 2. 4.Autotransformer feeding model

2.3. Power Quality in Electrified Railway System

Electrical Control quality can be characterized as the quality of the supply that guarantees legitimate and productive working of gear. IEEE benchmarks express control quality as the concept of controlling and establishing delicate hardware in a way that's appropriate for the operation of that gear and congruous with the preface wiring system and other associated hardware. Control quality, an imperative issue in all fabricating and prepare control situations, can be alluded to as a wide range of parameters, such as voltage changes, voltage and current awkwardness, sounds, responsive control and etc., between which the foremost risky ones in case of railroad industry are system unbalance, voltage/current sounds and responsive control, as has been clarified more within the coming subsections. In railroad systems, control quality has ended up an expanding concern(Zhang, H., Li, L., & Zhang, 2022)(Lou, C., Wei, Z., Lin, Y., & Chen, 2021).

The footing stack is among the most noticeably awful sorts of loads for an electrical utility to supply. It is exceedingly irregular, unpredictable, features a moo stack figure (normal stack separated by the crest stack in a specified period of time) and destitute control figure. That’s, the moving characteristic of association conspire, and the sort of single phase stack associated to the footing system, compound the control quality nourish by the utility. The seriousness of the issue is subordinate on footing stack which changes with the way the prepare voyages, the stacking of prepare and the control supply setup.

The impact of traction loads on the power grid system can be divided into the following characteristics (Al, 2008):(Raju, P. S., Kumar, A. A., & Prasad, 2022)

- Power quality decline
- Produce additional loss, vibrations increase large and the heat increases in the internal of the rotation motors and the transformer and generators
- Increase system power loss, interfere with the normal operation of telecommunications equipment;
- Cause frequent start or lose the lock of the relay protection containing negative sequence components or composite voltage components, may cause the malfunction of phase difference High frequency protection and the protection of generator negative sequence current
- Harmonics may also trigger system inductors, capacitors resonance, and amplified the resonant, threat to the security of power grid.

The major power quality problems in the railway power supply system like harmonics, system unbalance, reactive power, voltage problems, arcing are discussed as follows.

2.3.1. Harmonics

Sounds are sinusoidal voltages or streams having frequencies that are entire products of the recurrence at which the supply system is outlined to function (e.g., 50 Hz or 60 Hz). Sounds are voltage or current waveforms that operate at a recurrence that's a numbers numerous of the elemental recurrence. These are undesirable higher frequencies which superimposed on the basic waveform making a mutilated wave design. Sounds are primarily caused by control supply exchanging circuits such as rectifiers, control converters, and thyristor control controllers, as well as most nonlinear electronic phase controlled loads due to the reality that the controlled current drawn by the stack does not precisely take after the sinusoidal supply waveforms(Mokhtari, H., & Ghazavi, 2021). In this way, twisting makes a complex waveform made up of a number of consonant frequencies, which can have an antagonistic impact on electrical hardware and control lines. Figure 2.5 outlines the impact of 5th consonant.

In common, distorting equipment produces consonant streams that, in turn, cause consonant voltage drops over the impedances of the organize. The most inconvenient impacts of sounds are:

- Malfunction of control devices, main signaling systems, and protective relays
- Extra losses in capacitors, transformers, and rotating machines
- Additional noise from motors and other apparatus.
- Telephone interference.
- The presence of power factor correction capacitors and cable capacitance can cause shunt and series resonances in the network producing voltage amplification even at a remote point from the distorting load.

These days, there have been impressive improvements in mechanical forms which depend on controlled correction for their operation. Railroad systems are one of the imperative clients of the innovation and subsequently, they are a huge source of consonant. As specified some time recently, there are two systems of electrical supply to railroad; AC and DC system. Each system has its claim consonant characteristics, which depend on the organize components utilized within the system. In DC systems, chopper and inverter hardware produces consonant streams and exchanging homeless people. In AC systems, the utilize of converter hardware alters the nature of the footing current range, for the most part expanding the greatness of odd sounds at a few values of prepare speed when compared to what is gotten with tap changer gear(Alipoor, M., Shahabi, M., & Esfahani, 2022).

Electric trains having thyristor or pulls width modulation (PWM).controlled converters infuse consonant streams into the nourishing overhead lines. Consonant streams within the electric prepare are one of the greatest concerns, and the stack current demonstrate to speak to electric trains is proposed. The current sounds infused from an AC electric prepare engender through power feeding circuits. Being a disseminated RLC circuit, the bolstering circuit can encounter parallel reverberation at a particular recurrence. The consonant current is opened up by the reverberation, and the increased consonant current ordinarily actuates different issues, counting obstructions in adjoining communication lines and the railroad signaling system, overheating, and vibration at the control capacitors, and incorrect operation of the defensive gadgets. In this manner, the harmonic current stream must be surveyed precisely within the planning and arranging organizes of the electric traction system. Since the consonant current streams through the catenary system, it ought to be precisely modeled to analyze and evaluate the consonant impact on the power. Feeding system(Chen, X., He, J., Zeng, Z., Yang, H., 2020).

2.3.2. Reactive Power

Responsive Control refers to the surplus control that is created by responsive components, like capacitors or inductors, in an AC circuit or system. In a DC circuit, the power consumed by the circuit can be found by multiplying the volts and amps. However, in AC circuits containing responsive components, this volt.amp product can vary with frequency, making the situation more complex. In AC circuits, the volt.amp product is expressed as volt-amperes (VA) or kilo volt-amperes (kVA), known as Apparent power, symbol S. In purely resistive circuits like heaters, irons, pots, and incandescent bulbs, etc., the reactance is nearly zero, and the impedance of the circuit is composed almost entirely of resistance. In this case, the current and voltage are in.phase, and the power can be found by multiplying the RMS voltage and current values(Kundur, P., & Taylor, 2017). However, if the circuit contains reactive components, the voltage and current waveforms will be "out.of.phase" by some amount determined by the circuit's phase angle. When the phase angle is at its maximum of 90 degrees, the volt.amp product will have equal positive and negative values, and the reactive circuit returns as much power to the supply as it consumes. Therefore, the expression of P = IV (rms) is not valid, and to determine the "real power," also called Active power, symbol P consumed by an AC circuit, we need to account not only for the volt.amp product but also for the phase angle difference between the voltage and current waveforms given by the formula(Glover, J. D., Sarma, M. S., & Overbye, 2018):

$$P = VI\cos\phi \tag{2.1}$$

Then we can write the relationship between the apparent power and active or real power as: Active power, (P) = Apparent power, (S) × power factor

$$Pf = P/S = \cos\emptyset$$

Note that control calculates (PF) is characterized as the proportion between the dynamic control in watts and the clear control in volt amperes and shows how viably electrical control is being utilized. In a no inductive resistive AC circuit, the dynamic control will be rise to to the clear control as the division of P/S gets to be rise to one or solidarity. A circuit's control figure can be communicated either as a decimal esteem or as a rate(Anderson, P. M., & Fouad, 2008).

But as well as the dynamic and clear powers in AC circuits, there's moreover another power component that's display at whatever point there's a stage point. This component is called Receptive Control (some of the time alluded to as fanciful control) and is communicated in a unit called “volt. Amperes reactive”, (Var), image Q and is given by the condition:

$$Q = VI \sin \phi \quad (2.2)$$

Reactive power, or Var, is not really power, at all but represents the product of volts and amperes that are out.of.phase with each other. The amount of reactive power present in an AC circuit will depend upon the phase shift or phase angle between the voltage and the current and just like active power, reactive power is positive when it is “supplied” and negative when it is “consumed”.

The relationship of the three elements of power, active power, (watts) apparent power, (VA) and reactive power, (Var) in an AC circuit can be represented by the three sides of right. Angled triangle. This representation is called a power triangle as shown:

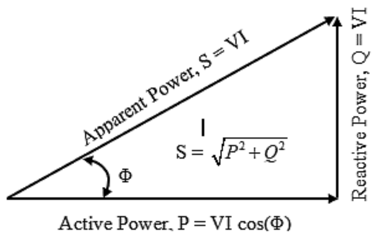

Figure 2. 5.Representation of power triangle

From the over control triangle, ready to see that AC circuits supply or expend two sorts of control: dynamic control and receptive control. Too, dynamic control is never negative, though responsive control can be either positive or negative in esteem, so it is continuously beneficial to diminish responsive control in arrange to move forward system proficiency. But for numerous mechanical control applications, responsive control is regularly valuable for an electrical circuit to have. Whereas the genuine or dynamic control is the vitality provided to run a engine, warm a domestic, or enlighten an electric light bulb, responsive control gives the vital work of controlling the voltage, subsequently making a difference to move control successfully through the utility lattice and transmission lines to where it is required by the stack(Arrillaga, J., Higham, A. D., & Watson, 2012).

Responsive control is both the issue and the arrangement to organization of control systems. The presence of tall receptive control causes voltage drops and warming of the line. It limits the sum of genuine control exchanged within the organization. Energetic responsive control emolument controller can be realized by thyristor exchanging capacitor or other control electronic switches for electric footing control supply system since the inactive ones couldn't receive in understanding with stack changing nature of footing stack in arrange to track emolument naturally.

2.3.3. System Unbalance

In a balanced three phase system, the voltages and currents have the same amplitude and are 120 degree out of phase with each other. However, most traction loads use a single. phase power supply, causing power unbalance. This unbalance can negatively impact both the supply system and connected devices. To limit voltage unbalance from the railway electrification load to one percent (while accounting for one percent ambient unbalance from other sources), passive or active techniques can be used. Passive techniques involve using different transformer connections, such as Leblanc. connected, Scott, or V/V connected transformers. Active load balancing requires controllable high voltage power electronic equipment(Mancilla.David, F., He, Y., Belkhayat, M., & Fathy, 2021). The Scott transformer connection can convert a balanced three phase to a balanced two phase system, but it is expensive and complex. Alternatively, two single phase transformers can be connected in a V/v configuration, which is simpler and cheaper. However, an additional feeding is necessary to balance the three phase system and reduce voltage unbalance.

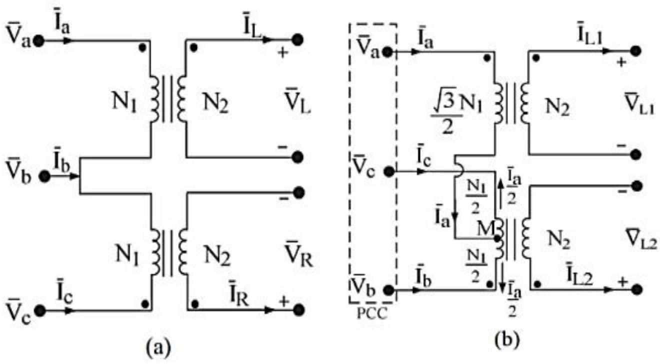

Figure 2. 6.V/v and Scott connection of traction transformers respectively

2.3.4. Voltage Variation

Unsymmetrical electric currents result in asymmetrical electric voltages. When the traction current changes quickly, it causes a sudden change in voltage at the substation connection point and to a lesser extent, on other bus bars. Voltage issues are often related to the magnitude of the voltage. The traction power supply system experiences fluctuations in voltage, including sag or swell, due to significant changes in load. To keep the voltage within a specific range, different controllers based on power electronics can be utilized(Chen, Z., Zhang, Y., Wang, S., & Zhang, 2020).

2.3.5. Arcing

Arcing happens due to the interaction between the pantograph and overhead line or the shoe of the train and third rail. This occurs because of the unavoidable mechanical oscillation, which causes a variation in the air gap. At the overhead systems' section isolators or third rail's ramps, there is a high likelihood of arcing. Arcing can distort voltage and current waveforms and generate unwanted transient DC components in the AC systems(Khan, M. A., Hussain, A., Chen, S., & Shaikh, 2021). This can result in a breakdown of dielectrics.

2.4. Mitigation Techniques

Several technologies and devices have been developed to enhance power quality and ensure efficient operation of electric rail systems. Various techniques for power quality enhancement have been researched and implemented to achieve a system that is more reliable for both AC and DC railway traction systems. The issues faced in railway traction systems are distinct from those encountered in other transmission or distribution systems that work at similar voltage levels. This is primarily due to the continuous movement of the locomotive load, line length variation during operation, and high levels of harmonic distortion. Table 2.1 presents a comparison of different compensation methods, with more asterisks indicating either better capability or higher costs associated with the compensation strategy(Memon, R. A., Khalil, A. M., & Ahmed, 2021).

Table 2. 1.Comparison of different controllers

Compensation strategies	Harmonic Compensation	Imbalance Compensation	Reactive power Compensation	Total cost
Balanced Transformers		*		*
SVC		**	**	**
Passive Filter	*			*
APQC	**	**	**	***
HPQC	***	***	***	***

To effectively control the system voltage and active/reactive power, it's important to understand the relative significance of certain controllable parameters such as the phasor difference between end voltages, line impedance, and phase angle. Below are some important considerations discussed in.

- Controlling line impedance is a powerful way to control current.
- When the phase angle is small, controlling line impedance or phase angle can effectively control active power.
- Injecting a voltage in series with the line perpendicular to current flow can increase or decrease current magnitude. Injecting reactive power in series is effective for controlling line current as it lags the driving voltage by 90 degrees.
- Injecting voltage in series with the line with any phase angle relative to the driving voltage can control both the magnitude and phase of the line current. This requires injection of both active and reactive power in series.
- Controlling the magnitude of one of the line voltages can be a cost effective means to control reactive power flow when the phase angle is small.
- A combination of line impedance control with a series controller and voltage regulation with a shunt controller can provide a cost effective means to control both active and reactive power flow between the two systems.

2.5. Overview of FACTS Devices

The development of Flexible Alternating Current Transmission Systems (FACTS) technology, which utilizes power electronic technology and advanced electronic control methods, has opened up new possibilities for controlling power and increasing the usable capacity of existing and new power transmission lines. This technology allows for the control of currents in a line, which can lead to an increase in capacity without the need for larger conductors(Bhattacharya, S., Ranjan Mahapatra, V., & Mishra, 2018). FACTS Controllers are primarily used to address power quality issues in traction systems by controlling the flow of current through the manipulation of voltage drop, line impedance, and/or angle. These controllers come in different types, including series, shunt, and series. Series, and series. Shunt controllers. Series controllers add voltage in series with the line, while shunt controllers inject current in parallel to the line. Both can provide or consume variable reactive power if the injected voltage/current is in phase quadrature with the line voltage/current. The series controller is suitable for multiline systems, while the combined series. Shunt controllers utilize both series and shunt controllers' operations(Gyugyi, L., & Dugan, 2002).

Table 2. 2.Type of FACTS devices

Types of connection		Controlled Parameters
	Shunt connected (	Q
	Series connected (TSSC, TCSC, and SSSC)	P
Combined series and shunt connected	TCPST and TCPAR	P
	TCVR	Q
	UPFC and IPFC	P and Q

To improve the power transmission system, various types of series controllers are used, such as variable impedance devices like capacitors, reactors, or power electronics. Based sources that provide the required frequency and harmonics. The primary function of these series controllers is to inject voltage in series with the transmission line. They are used to reduce the voltage drop over a power line, limit voltage fluctuations during changing power transmission, improve system damping, and limit short. Circuit currents in networks or substations.

Two common types of series-connected controllers are Static Synchronous Series Compensator (SSSC) and Thyristor Controlled Series Capacitor (TCSC). The SSSC is a static synchronous generator that operates without an external power source. It is used as a series compensator to increase or decrease the overall reactive voltage drop across the line, which helps control the transmitted electric power. The SSSC may also include energy storage or energy absorbing devices to improve the dynamic behavior of the power system by temporarily compensating for real power and increasing or decreasing the overall resistive voltage drop across the line.

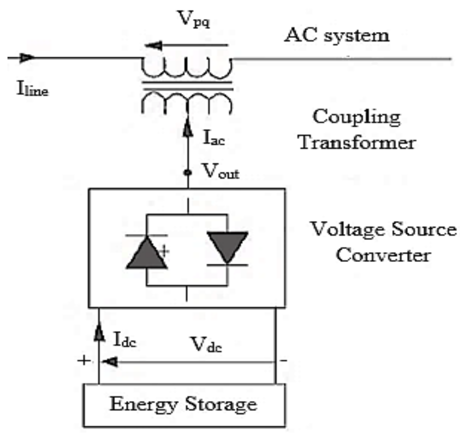

Figure 2. 7.General scheme of SSSC

Thyristor Controlled Series Capacitors (TCSC) are another type of series connected controller that involves a series capacitor bank connected with a Thyristor controlled reactor, allowing for smooth adjustment of the series capacitive reactance. The main purpose of TCSC is to provide electromechanical damping between large electrical systems by altering the reactance of a specific interconnecting power line. With efficient control algorithms, the TCSC can modify the apparent impedance to achieve the desired objectives.

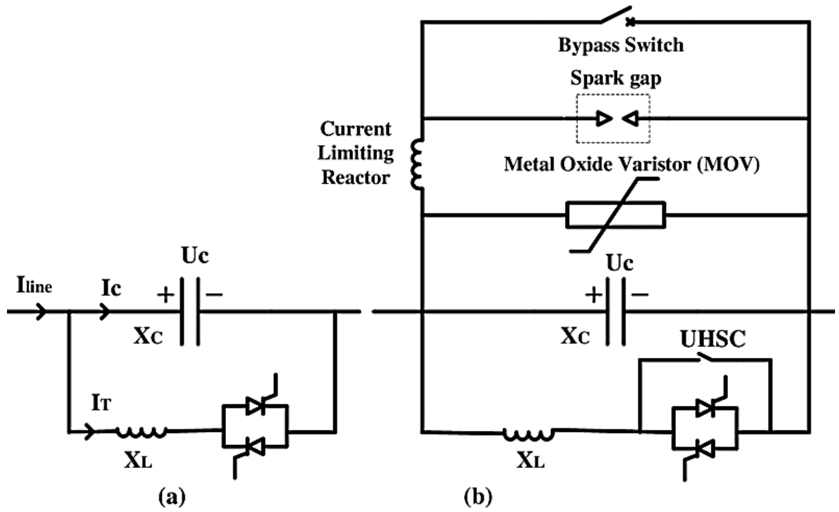

Figure 2. 8.Thyristor controlled series compensation (TCSC)

The Shunt Controllers: in FACTS technology can be variable impedance, variable source, or a combination of both. They inject current into the system at the connection point and are primarily used for controlling the amount of reactive power flowing through the power system. Shunt and series controllers can both be implemented with voltage source or current source converters. Shunt controllers have a variety of applications in power system networks, including reduction of reactive power flows and network losses, improvement of power quality in high load fluctuation demand areas, compensation of Thyristor converters, and improvement of static or transient stability. The most commonly used shunt controllers are the Static Var Compensator (SVC) and STATCOM. SVC is a static Var generator that varies its output to exchange capacitive or inductive current in order to control specific parameters of the electric power system, such as bus voltages. Compared to mechanically switched capacitors or reactors, SVCs have faster reaction times and greater reliability. Fixed capacitor thyristor controlled reactor and thyristor switched capacitor thyristor controlled reactor are the most common configurations for continuously controlled SVCs. The use of power thyristor in static compensators offers several benefits, including high reaction speed, minimal contribution to short circuit power, and low maintenance(Singh, B., & Al.Hinai, 2009).

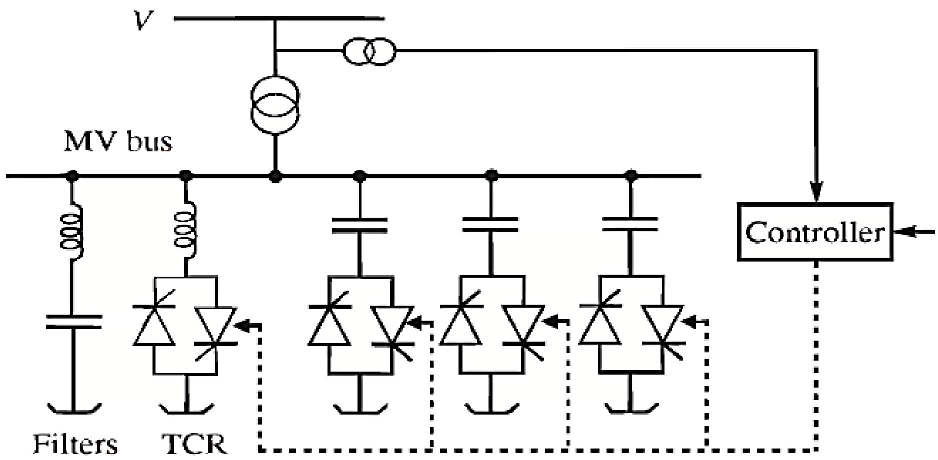

Figure 2. 9.SVC with TCR structure

The Static Synchronous Compensator (STATCOM) is a widely used shunt controller that regulates AC electricity transmission networks. It employs a voltage source converter based on power electronics, which can either supply or absorb reactive AC power from the network. It can also provide active AC power if connected to a power source. Shunt compensation is intended to modify the natural electrical characteristics of the transmission line in order to enhance the steady state power transmission capacity and regulate the voltage profile along the line. All shunt controllers inject extra current into the system at the point of common coupling (PCC) through a voltage source converter(Gyugyi, L., & Luo, 2007).

Compared to Static Var Compensators (SVC), STATCOM can deliver full capacitive output current at any system voltage, even close to zero, while SVC's output current decreases as the system voltage decreases and is limited by the size of the capacitor and the magnitude of the system voltage. Additionally, STATCOM has a higher transient rating in both inductive and capacitive operating regions than conventional SVC. The terms "compensator" and "synchronous" suggest that the device functions as an ideal synchronous generator producing a set of three phase fundamental frequency sinusoidal voltages. "Static" indicates that it is an electronic device without moving parts(Mohan, N., Undeland, T. M., & Robbins, 2002).

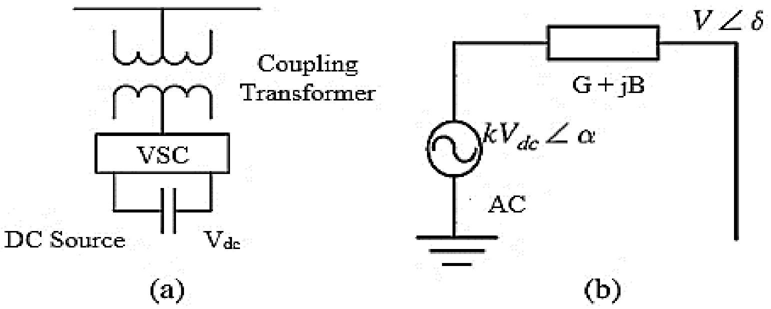

Figure 2. 10.General scheme (a) and equivalent circuit of STATCOM (b)

The current and reactive power transferred can be expressed as:

$$I_t = \frac{V_s - V}{x} \tag{2.3}$$

Where,

$$x = G + jB \text{ And } V_s = kV_{dc}$$

$$Q_t = \frac{V_s^2 - V_s * V\cos(\alpha)}{x} \tag{2.4}$$

where, I_t and Q_t are the current and reactive power transferred to the line from the STATCOM, respectively; α is the angle between the AC side voltage of STATCOM and line voltage; V_s, x, V, and V_{dc} are STATCOM voltage, Reactance, and utility voltage respectively.

In comparison to SVC and other traditional reactive power compensators, STATCOM offers various advantages, as listed below:

- STATCOM has superior dynamic performance compared to other Var compensators.
- The overall response time of the system with STATCOM can be as short as 10 milliseconds or less.
- STATCOM can maintain full capacitive output current at low system voltage.
- The STATCOM configuration requires a smaller capacitor bank, which reduces its size by 30.40% compared to SVC. Additionally, it does not require extensive protection and switching equations.

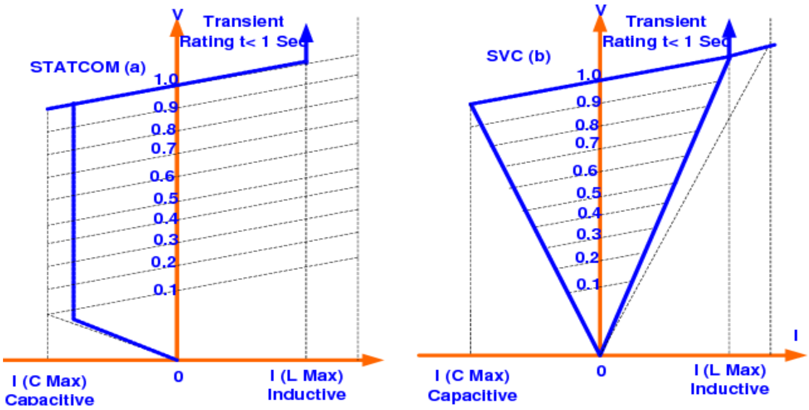

Figure 2. 11.VI curve of STATCOM (a) and SVC (b) (Ángeles.Camacho, 2017)

In Figure 2.12, it is shown that STATCOM has the ability to maintain its full rated reactive current supply to the system even when the voltage value is lower. Unlike SVC, the output current of STATCOM is not dependent on the system voltage, and its compensating current decreases linearly with the system voltage. A typical V.I curve of STATCOM is presented in Figure 2.12, which demonstrates that it can provide both capacitive and inductive compensation, and its output current can be independently controlled over the maximum rated capacitive or inductive range (ICmax and ILmax) without being affected by the AC system voltage. STATCOM can produce full capacitive reactive power at any voltage. This feature makes STATCOM a robust technology that can maintain a constant current output even at lower voltages, which is particularly useful in scenarios where the system voltage needs to be supported during and after faults to avoid voltage collapse(Sadeghi, H., & Reisi, 2017). Figure 2.1 shows that STATCOM has an enhanced transient rating in both the inductive and capacitive operating regions.

2.6. PI with PSO Optimization

Particle Swarm Optimization (PSO) is a nature inspired optimization algorithm that mimics the social behavior of bird flocking or fish schooling. It was originally proposed by Kennedy and Eberhart in 1995. PSO is widely used to solve optimization problems and has gained popularity due to its simplicity and effectiveness. On the other hand, the Proportional Integral (PI) controller is a common type of feedback controller used in control systems. It is designed to regulate a system's output by adjusting its input based on the error between the desired set point and the actual output. The PI controller combines proportional and integral actions to achieve better control performance.

PSO and the PI controller have been extensively studied and applied in various fields, including engineering, robotics, finance, and power systems. The combination of PSO and the PI controller offers a powerful approach for optimizing controller parameters to improve system performance. The main idea behind using PSO to optimize the PI controller is to search for the optimal values of the controller's proportional and integral gains. PSO achieves this by iteratively adjusting a population of potential solutions, represented as particles, in a multidimensional search space. Each particle's position and velocity are updated based on its own best solution and the best solution found by the swarm as a whole(Singh, G. K., & Pant, 2015).

By using PSO to tune the PI controller parameters, the system's control performance can be improved, leading to better stability, faster response times, and reduced steady state errors. The optimization process helps to find an optimal balance between the proportional and integral actions of the controller, considering the specific requirements and dynamics of the controlled system. In summary, the combination of PSO and the PI controller provides a powerful approach for optimizing control parameters in various applications. It allows for automatic tuning of the controller to adapt to system dynamics and achieve desired control objectives.

CHAPTER THREE

METHODOLOGY

3.1. Introduction

In this portion, mathematical analysis and modeling of train dynamics and mainly traction power supply system are presented. Modeling of train dynamics is aimed to show how the variations of the train's speed affect the required power. The longitudinal train dynamics analysis has been done to know the resultant of all forces acting upon the train moving in a leveled track line including force due to acceleration and deceleration. The traction power modeling, which is a great concern, has been performed as explained in the coming sections of this chapter.

3.2. Methodologies

In order to attain the general and specific objectives of this study, the following methods and techniques is followed as shown in Figure 3.1. First the related works are reviewed and then, the necessary data to the research is collected and analyzed. The load demand of the system is determined. The STATCOM device are designed to get the required output voltage and PSO.PI controller is applied to get an optimized power factor for power improvement.

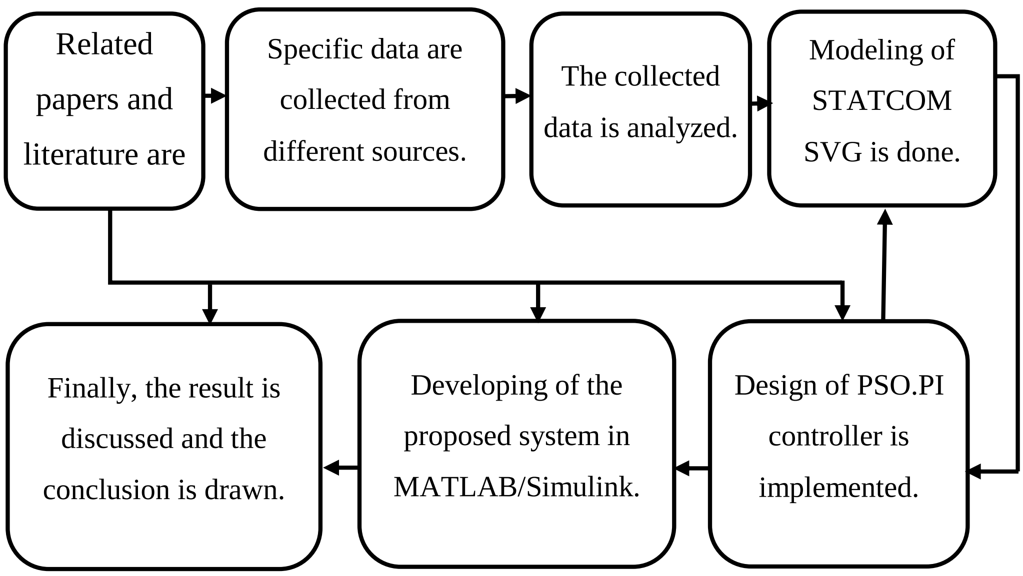

Figure 3. 1.Block diagram of the research methodology

3.3. Materials

For the system design and editing thesis documentation the following computer software's are used.

- Microsoft office 2016,
- Math Type 6.0 equation,
- MATLAB/2021a, and

Microsoft office is used for editing the thesis documentation. Math Type 6.0 is used for writing mathematical equations in Microsoft office word and Power point presentation tools. MATLAB is used for simulation of the system design.

3.4. Data Analysis

The section of the Ethio Djibouti railway line that will be the focus of this research runs from Lebu to Adama, covering a distance of approximately 115 km. currently, this section is operational and is powered by the Endode and Mojjo traction substations. These substations receive power from the Kaliti I, Akaki II, Nazreth II, and Awash II substations of the Ethiopian Electric Utility (EEU). The research team has collected readings of active and reactive energy meters from the Ethio Djibouti Railway Share Company (EDR) for August 2018, and a summary of these readings is presented in Figure 3.1. The raw data collected is included in Appendix A.

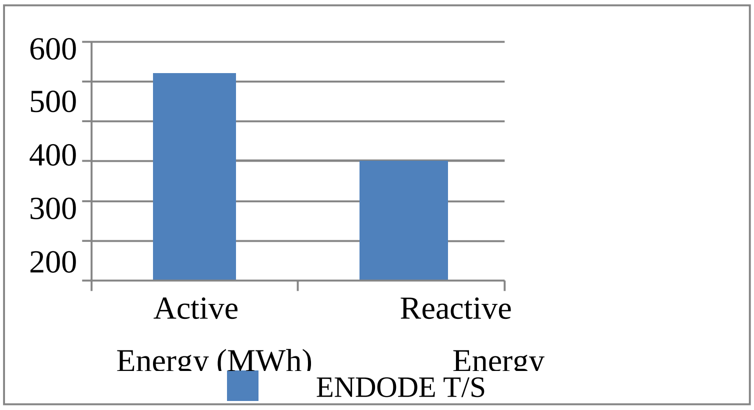

Figure 3. 2.The active and reactive energy meter reading at Endode traction substations in August, 2018

The data presented in Figure 3.1 indicates that there is a significant amount of reactive energy present in the traction substations. This highlights the issue of reactive power generation in traction power supply systems. In this study, the researchers used real time data that includes voltage, current, active power, and reactive power to analyze and create a model. The data presented in Table A in Appendix A was collected during a 15.minute live recording at the Endode traction substation while a train was traveling from Lebu to Bishoftu. The data was measured at 30.second intervals. Figure 3.3 provides a summary of the power factor readings obtained from the data.

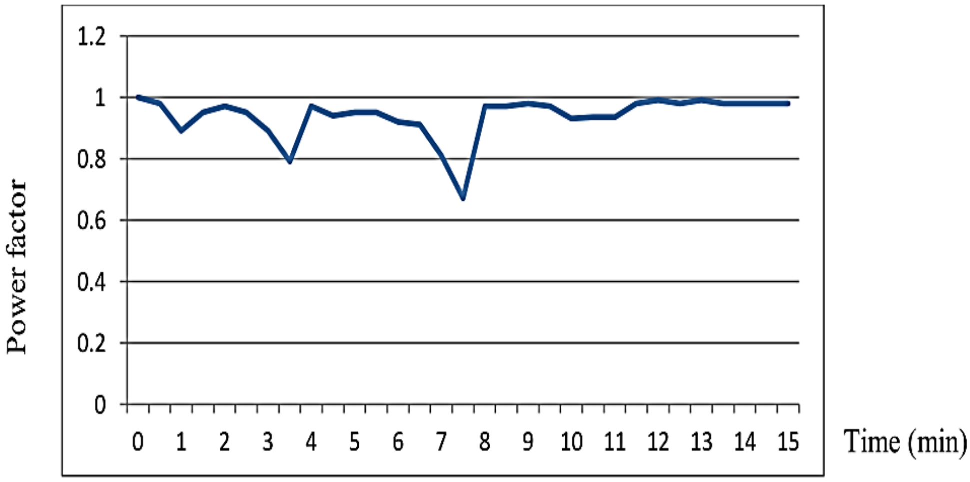

Figure 3. 3.Power factor reading

ERC suggests a power factor of 0.95. Power factor refers to the efficiency of a load in utilizing current drawn from the supply, which comprises two elements: displacement and distortion power factors. The actual power factor is the outcome of multiplying the displacement and distortion factors.

$$P.F_{disp} = \frac{P}{\sqrt{P^2 + Q^2}} \tag{3.1}$$

$$P.F_{dist} = \frac{1}{\sqrt{1 + THD^2}} \tag{3.2}$$

From Equation (3.1) and (3.2)

$$\text{True power factor} = P.F_{disp} * P.F_{dist}$$

Where, P, Q, THD, $P.F_{disp}$ and $P.F_{dist}$ are active power, reactive power, total harmonic distortion, displacement power factor and distortion power factor, respectively.

Figure 3.3 demonstrates the contrast between the directly measured true power factor and the calculated displacement power factor based on the measured active and reactive power.

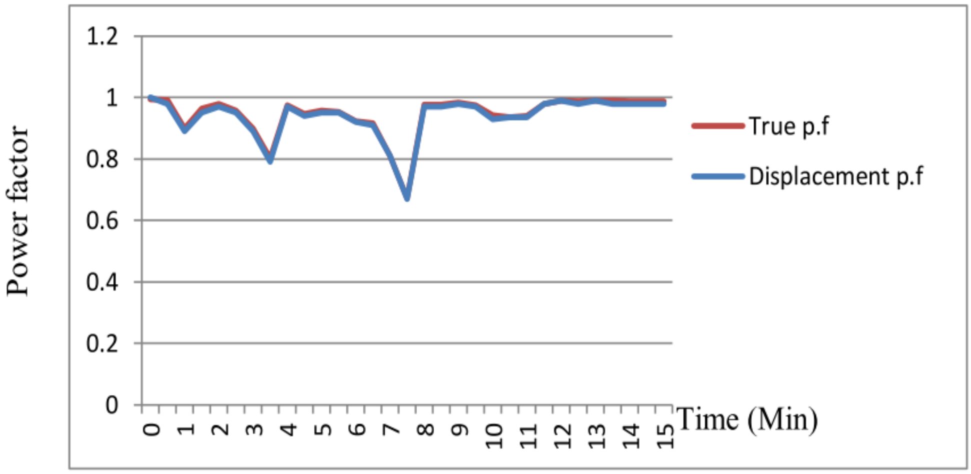

Figure 3. 4.Comparison between true P.F and displacement P.F

When there are few harmonics in the network, the displacement power factor is almost the same as the true power factor. This means that the level of harmonics is low and reactive power is the primary factor causing the reduction of power factor.

3.5. Train dynamics modeling

Figure 3 .5 shows the 3D model of the train. This figure shows the mechanical design for force and friction consideration.

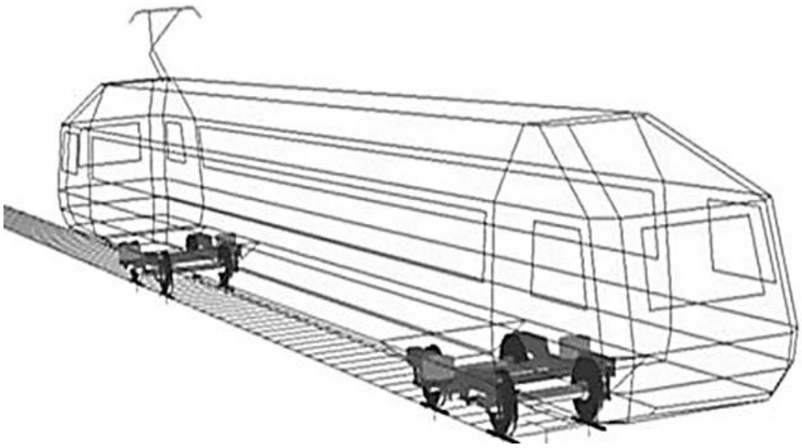

Figure 3. 5.3D model of the train

The first step is driving the mathematical model off the train that governs the physical system. The free body diagram is represented as in Figure 3. 5 below.

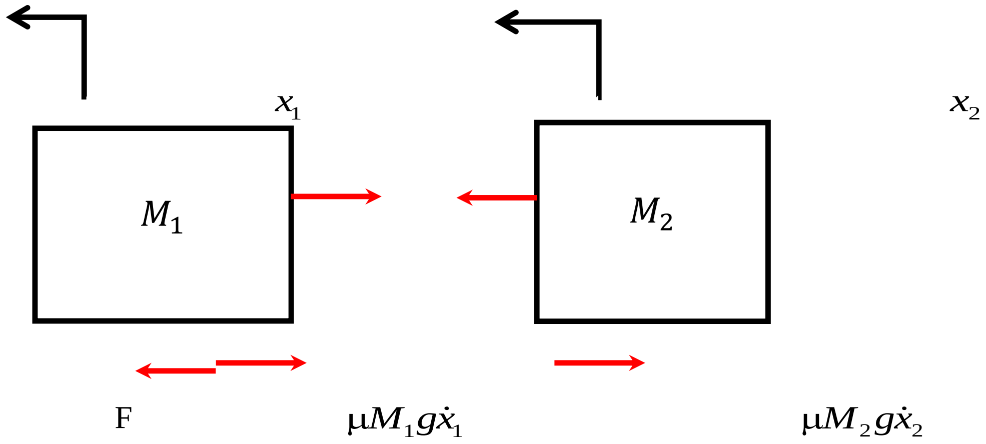

Figure 3. 6.Free body diagram of the train

Based on the above free body diagram apply Newton's second law in the horizontal direction that leads to the following governing equation for the train dynamic system.

$$\sum F_1 = F - k(x_1 - x_2) - \mu M_1 g\dot{x}_1 = M_1\ddot{x}_1 \tag{3.3}$$

$$\sum F_2 = k(x_1 - x_2) - \mu M_2 g\dot{x}_2 = M_2\ddot{x}_2 \tag{3.4}$$

From equation 3.3 and 3.4 above the acceleration of the train that is needed for simulation can be calculated as follows.

$$\ddot{x}_1 = \frac{1}{M_1}(F - k(x_1 - x_2) - \mu M_1 g\dot{x}_1) \tag{3.5}$$

$$\ddot{x}_2 = \frac{1}{M_1}(k(x_1 - x_2) - \mu M_1 g\dot{x}_1) \tag{3.6}$$

From the above equation the Simulink model in mat lab is represented as below in figure

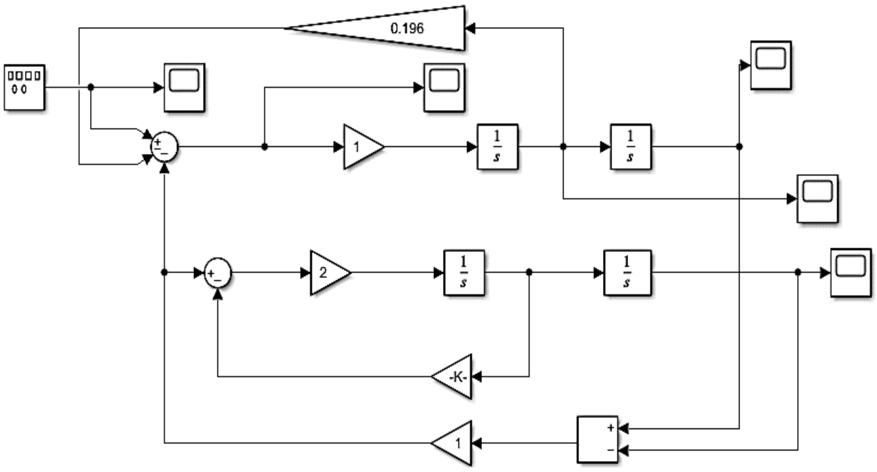

Figure 3. 7.Simulink model of the train

The movement of a train is influenced by different types of forces, including longitudinal forces. These forces comprise

- The rolling resistance force (Fm),
- Aerodynamic resistance force (Fad),
- Acceleration/deceleration force (Fa),
- Force due to the gradient (Fg), and
- Force due to curvature (Fc).

Rolling resistance and aerodynamic can be expressed using the Davis formula as quadratic equation as follows(Profillidis, 2016; Yi, 2017; Z. He, Z. Zheng, 2016):

$$F_R = A + BV + CV^2 \tag{3-7}$$

with constants A, B, and C. A represents the rolling resistance that is independent of the speed of the train, while BV represents the mechanical resistance that depends on both speed and weight of the train, and CV^2 represents the aerodynamic resistance, which is highly dependent on speed. The values of constants A, B, and C vary depending on the type of rolling stock (passenger/freight), wheel rail friction, and atmosphere. Different railways have developed empirical formulas based on the Davis equation to determine the numerical values of these parameters. Instead of generating a new empirical formula for Ethio Djibouti railway, this research work adopts the French railway's formula, which can be used for different train weights and electric passenger trains. The resistive force can be calculated as a result.

$$F_R(N) = (1.3\sqrt{\frac{10}{m}} + 0.01*V)*M + CV^2 \tag{3-8a}$$

$$C = 0.0035*A + 0.0041p*\frac{l}{100} + 0.002*N \tag{3-8b}$$

Where, M is total mass of the train (in tons), m is mass per axle (in tons), V is speed (kilometer per hour), A is front cross sectional area (in meter per second), p is the partial perimeter of the train down to the rail level (in meters), l is train length (in meters) and N is number of raised pantographs.

Based on the document of rolling stock technical specification considering YZ25G hard seat passenger car, the rolling resistance force (in Newton) of the train with 4 axles having 118 passengers is expressed in terms of speed (km/hr.) as:

$$F_R = 74.86 + 0.75V + 0.076V^2 \qquad (3-9)$$

Force because of curvature and gradient

Other forces acting on a moving train are caused by the gradient and curves on the track. The resistance due to curvature depends on the friction between the wheel flange and the rail, the radius of the curve, and the degree of wheel slippage on the rails. This can be mathematically expressed as a function of the mass and radius of curvature.

$$F_C = 0.001\frac{k}{R} * M \qquad (3-10)$$

Where, k can be 500 up to 1200 on average, being 800 and R is a radius of curvature in horizontal plane (meters).

When the radius of curvature is larger than 250 meters, the impact of curve resistance is not significant. Depending on the direction of movement, uphill or downhill, the gradient resistance can be either positive or negative.

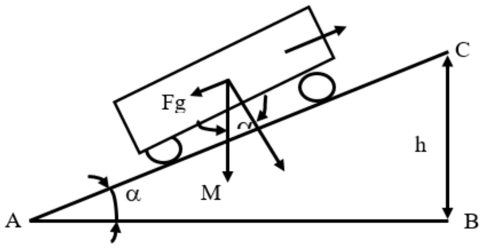

Figure 3. 8.Gradient resistance force representation

The resistance force because of the gradient for the gradient of 1 in X length inclined plane can be calculated as:

$$F_g = Mg\,sin(\alpha) = \frac{Mg}{x} \qquad (3\text{-}11)$$

Force due to Acceleration/deceleration

This force is a result of changes in the speed of the train as it moves. The train undergoes acceleration from the start until it reaches its maximum speed and deceleration when it comes to a stop. Additionally, there are speed variations throughout the journey caused by the alignment of the track line.

$$F_a = M_t * \alpha \qquad (3\text{-}12)$$

Where F_a , a are acceleration force and acceleration respectively and where Mt is the

Summation of rotational and deadweight of the train and usually regarded as 1.1 times dead mass of the train (M).

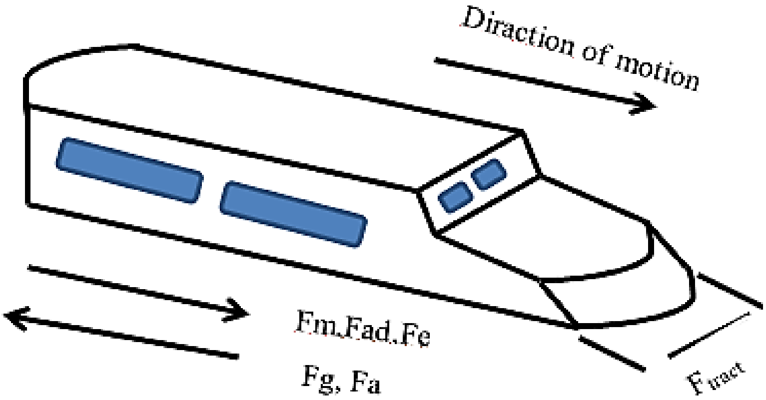

Figure 3. 9.Forces acting on a moving train

When a train moves on a flat track, several forces such as mechanical friction, aerodynamic drag, acceleration/deceleration, and tractive force act on it. To determine the required tractive force as a function of the train's speed, Newton's second law of motion is used. The equation is given below.

$$\sum F = M_t * \alpha \qquad (3-13a)$$

$$F_{tract} - \sum F_{res} = M_t * \alpha \qquad (3-13b)$$

From equation (3.10) and (3.13), the tractive force will be:

$$F_{tract} = 1.1M_a + 74.86 + 0.75V + 0.076V^2 \qquad (3-14)$$

Where, F_{tract} is a tractive force, it is the sum of resistive force and force due to acceleration/ deceleration and acceleration/ deceleration force is the product of total mass and acceleration.

Substituting the total train mass (M) and in terms of speed in m/sec, Equation (3.14) can be rewritten as:

$$F_{tract} = 8.259 * 10^3 \frac{dv}{dt} + 74.86 + 2.7V + 0.99V^2 \qquad (3\text{-}15)$$

Speed –time curve

The train's movement is determined by the net force acting on it. This force can either result in constant velocity, acceleration, or deceleration. To start moving, the tractive force applied must be greater than the total resistive force, causing acceleration until the required speed for free running is achieved. Once the train reaches a constant speed, the tractive force becomes equal to the resistive forces (during time t2 in Figure 3.9). To bring the train to a stop at the desired station, the braking force is applied, taking into account the braking distance. Before applying the braking force, there may be a coasting period where only the resistive forces act on the train. Figure 3.10 displays the estimated speed time curve for a train running from Lebu to Adama, indicating the acceleration, free running, and deceleration periods.

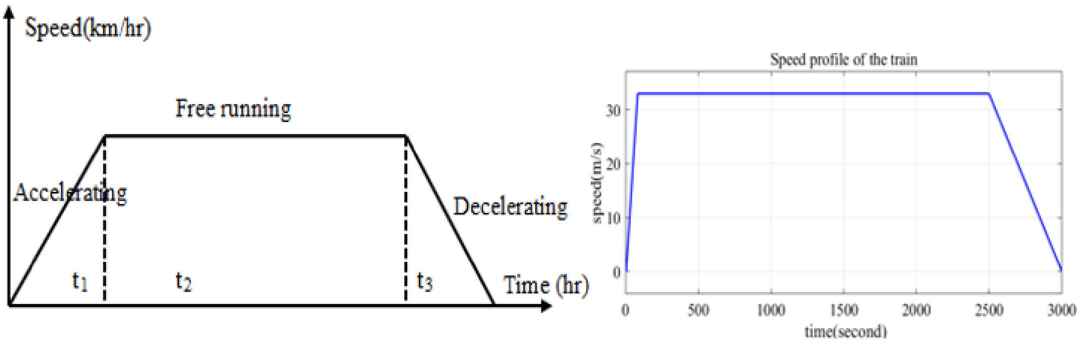

a. From mathematical model

b. From Simulink model

Figure 3. 10.Speed profile (speed – time curve)

The passenger train on the Ethio Djibouti line commences its journey from Lebu Station and makes a temporary stop at Adama station, covering a total distance of 93.55km. The maximum permissible speed for the train is 120 km/hr, which is equivalent to 33.3m/s as indicated in the MATLAB graph. The acceleration and deceleration values for the train have been selected based on the distance within which the train should reach its maximum speed, the braking distance, and the type of rolling stock, which could be either passenger or freight.

To ensure passenger comfort, the maximum acceleration should not go beyond 1.0 m/sec2, as per reference. The acceleration and deceleration values for various rolling stock types are provided in Table 3.1.

Table 3. 1.Values of acceleration and deceleration various rolling stock

Type of train		Acceleration (m/sec²)	Deceleration (m/sec²)
Freight	Conventional	0.2.0.4	0.1
	express		0.25
Passenger	intercity	0.4.0.6	0.4.0.5
	Suburban	0.6.0.8	0.6
	Metros	0.8.1	.

To calculate the total time taken to cover the entire distance, add up the time it takes for the train to accelerate to its maximum speed, the time it spends at a constant speed, and the time it takes for the train to come to a stop. In this particular scenario, the recommended acceleration and deceleration value for intercity passenger trains is 0.4 m/sec2.

$$t_1 = \frac{120-0}{1.44} = 83.33\text{sec}$$

$$t_3 = \frac{0-120}{1.44} = 83.33\text{sec}$$

The distance traveled during acceleration, free running and deceleration time:

$$S_1 = S_3 = 0.5*120*\frac{83.33}{3600} = 1.4\text{km}$$

$$S_2 = 93.55 - 1.4 - 1.4 = 90.75\text{km}$$

Where, S_1, S_2, and S_3 are the distance of the train when they accelerate, free running and deceleration.

Then, the time taken to cover the free running speed (t_2) and the whole distance will be:

$$t_2 = \frac{90.75}{120} = 0.75625 \text{ hr} = 2722.5 \text{ sec}$$

Total time will be the sum of the time taken to cover these three sections which is around 2890 second (0.8hr).

3.6. Traction power supply system modeling

The modeling of an electrified traction system, whether AC or DC, involves various components that are modeled differently depending on the purpose of the study. In the following sections, the mathematical and simulation models of the traction power supply system for the Ethio Djibouti line are explained. This model consists of the key components of the traction power supply system, such as the substation, feeder line, and locomotive(A. Ojo, E. Babalola, 2016).

The role of the traction substation is to oversee the traction power supply system, with the task of converting 132 kV line to 27.5 kV, and equipped with efficient safety and control mechanisms. Additionally, a V/V type traction transformer is incorporated to mitigate any system imbalances that often arise in traction systems.

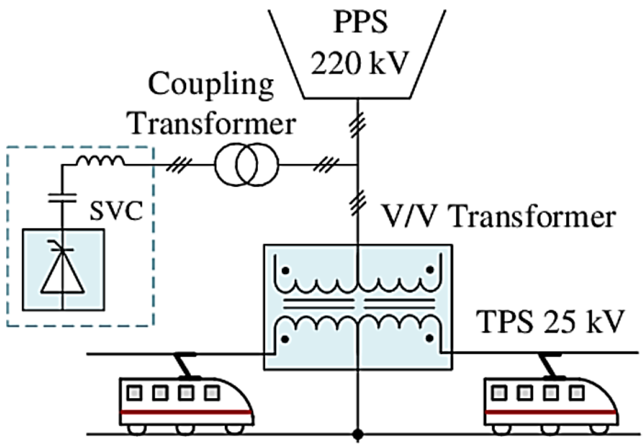

Figure 3. 11.Configuration of V/V transformer

A simplified model of the substation, which involves Thevenin's equivalent circuit with reference to points A and B, can be seen in Figure 3.11. It consists of an ideal voltage source, known as the infinite bus bar, connected in series with the grid impedance and traction transformer.

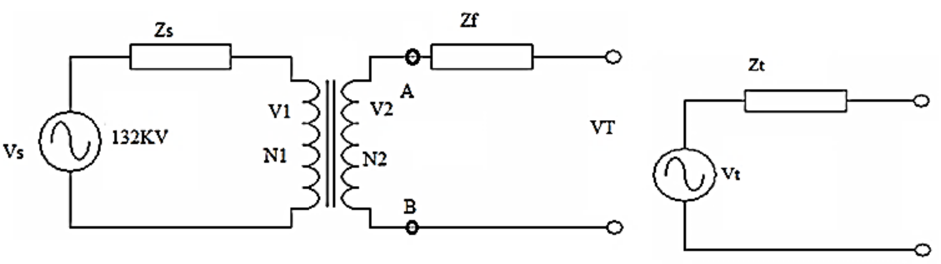

Figure 3. 12.Simplified model of the substation and its Thevenin's equivalent circuit

The parameters of the Thevenin's circuit are computed as follows.

$$I_{sc} = (\frac{N_1}{N_2})^2 \frac{V_t}{Z_s} \tag{3-16}$$

$$Z_t = \frac{V_t}{I_{sc}} = (\frac{N_2}{N_1})^2 Z_s = \frac{Z_s}{a^2} \tag{3-17}$$

where $a = \frac{N_1}{N_2}$, I_{SC} is the short circuit current through point A and B, and Z_S is the summation of the grid and transformer impedance.

Table 3. 2.Transformer specification

Parameter	Values
Rated power	(20,000+20,000) kVA
Rated voltage	132/27.5kV
Rated current	151.5/262.4/151.5A, 727.3/1259.7/727.3
Short circuit impedance	8.33%
No load current	0.1 %
No load loss	26.721 kW
Load loss	158.471 kW
Vector group	Vv0(Vv6)

The per-unit and actual impedance of the traction transformer is calculated based on the information provided on its nameplate at Endode substation, as demonstrated below.

$$R_{pu} = \frac{R_{actual}}{R_{base}}, L(pu) = \frac{L_{actual}}{L_{base}}, L_{base} = \frac{X_{base}}{2\pi f}, Z_{base} = \frac{V_{rated}^2}{S_{rated}} \tag{3-18}$$

The percentage impedance of a transformer refers to the percentage of the rated voltage applied to the primary side needed to circulate the rated current on the secondary winding under short circuit conditions.

Considering S_{base} = 20MVA, which is the rated power of the traction transformer.

V_{base} (high voltage) = 132 kV = V_{rated} (primary side)

V_{base} (low voltage) =27.5kV= V_{rated} (secondary side)

The actual impedance is required on the secondary side (interested on the secondary side). Thus; the secondary side base voltage will be used; to get the base impedance.

$$Z_{base} = \frac{V_{base}^2}{S_{base}} = \frac{(27.5 \times 10^3)^2}{20 \times 10^6} = 37.8125\Omega$$

The actual impedance of the transformer will be calculated using the percent impedance given in the nameplate of the transformer located in Indode Traction Substation.

$$Z_{actual} = \% Z \times \frac{V_{rated}^2}{S_{rated}} = \frac{\% 8.33 \times 27.5^2}{20 \times 10^6} = 3.15\Omega$$

The Per Unit (pu) impedance of the transformer is:

$$Z_{pu} = \frac{Z_{actual}}{Z_{base}} = \frac{3.15}{37.8125} = 0.0833$$

$$R_{pu} = \frac{R_{actual}}{Z_{base}} = \frac{P_{load\ \mathrm{loss}}}{S_{base}} = \frac{158.47}{20 \times 10^6} = 0.007926$$

$$R_{actual} = 0.007926 \times 37.8125 = 0.2997\Omega$$

$$X_{pu} = \sqrt{Z_{pu}^2 - R_{pu}^2} = \sqrt{0.0833^2 - 0.007926^2} = 0.082859$$

$$X_{actual} = \sqrt{Z_{actual}^2 - R_{actual}^2} = \sqrt{3.15^2 - 0.2997^2} = 3.134$$

Therefore, $X_{actual} = 3.134\Omega$ and $\mathrm{L} = \frac{3.134}{2\pi \times 50} = 0.01H$

Therefore, the equivalent impedance of transformer referred to secondary will be:

$$Z_{transformer} = 0.2997 + j3.134.$$

Considering only inside the substation and thus grid impedance is not considered in this substation model.

3.6.1. Modeling of Overhead Line System (Catenary System)

The pantograph is used to transfer power from the contact wire to the electric train. In this thesis, the design is focused on a single phase train supply system, which differs from a three phase supply. The overhead line system serves as a power distribution system for electric trains and has varying types of geometries depending on factors such as train speed, environmental conditions, voltage level, substation distance, voltage drop, and impedance. The overhead line system behaves like a transmission line and has specific values of capacitance, inductance, and resistance per unit length, determined by physical characteristics such as the copper conductor's diameter and height above the ground. Consequently, the overhead line system has characteristic impedance, which follows a hyperbolic curve and alternates between capacitive and inductive values. The system has resonant conditions between the supply and the overhead, resulting in a set of characteristic resonant frequencies(A. Costabeber, R. Gerin.Lajoie, 2008). The supply from the grid to the feeder station is essentially inductive.

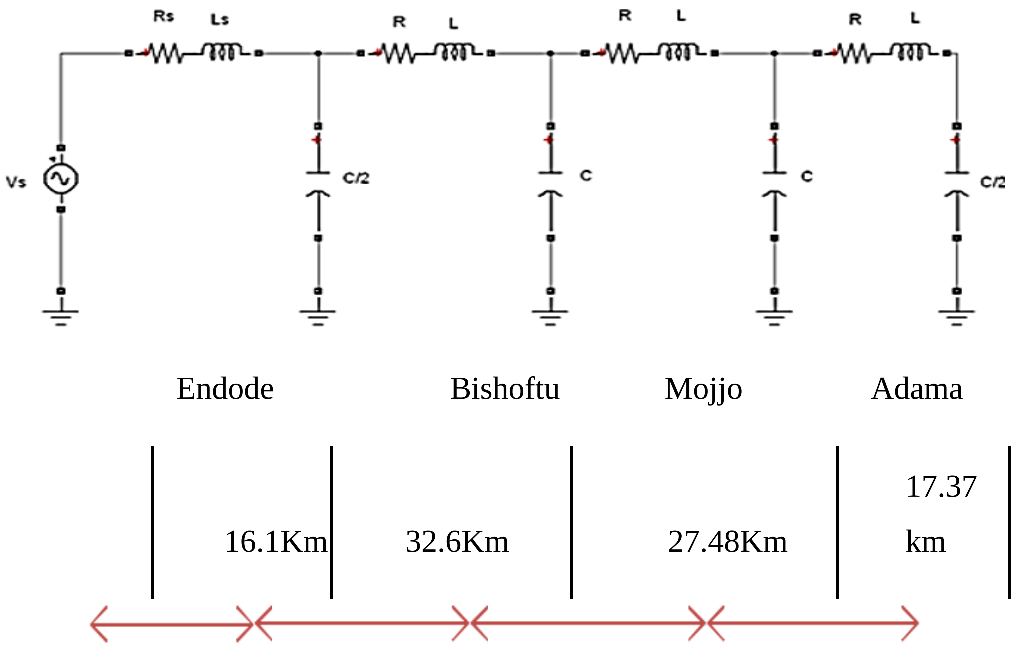

Figure 3. 13.Modeling of the AC electrified railways system feeder line

The electrified railway system studied in this thesis is a 25kV AC single phase system. The distribution circuit associated with this system is considered to consist of lumped circuits. The feeder line, which runs from Lebu to Adama, is modeled using three pi sections, each of which consists of a resistance, R, in series with an inductance, L, and a parallel capacitance, C. The feeder line is represented by a circuit having a longitudinal impedance of 0.130081+j0.39238 Ω/km at 50 Hz and shunt capacitance of 0.011 μF/km. Figure 3.12 illustrates the modeling of the feeder line.

The transmission line is characterized by its series resistance, series inductance, and shunt capacitance parameters, which vary depending on its length. Generally, transmission lines can be classified into three categories: short lines for lengths less than 80 km, medium lines for lengths between 80 km and 250 km, and long lines for lengths greater than 250 km In the case of a short transmission line, the series impedance is considered to be concentrated while the shunt capacitance is minimal. Hence, the total lumped impedance is calculated by multiplying the impedance network per kilometer with the length of the line in kilometers.

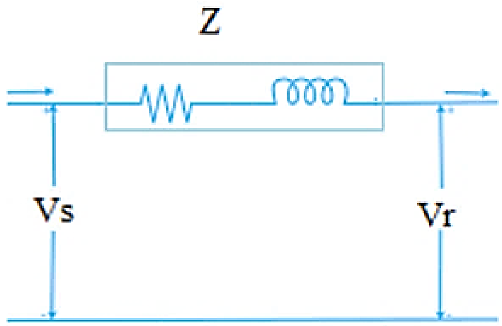

Figure 3. 14.Short line transmission model

3.6.2. Locomotive Load Modeling

The amount of power used by the train depends on various factors such as the speed of the train, the operation mode, the weight of the train, track geometry, and train control strategies. These factors can cause a significant variation in power demand during an inter station run, especially since the train is in motion. This complexity makes the load flow calculation for railway power supply different from that of conventional power systems. The calculation also needs to consider the number of trains in a feeding section, which can run at different speeds and draw varying amounts of power, impacting the supply system differently. Additionally, the nominal separation between trains is important and should follow the train services' timetables or dispatching schedules(S. Paudyal, R. Rajamani, 2019).

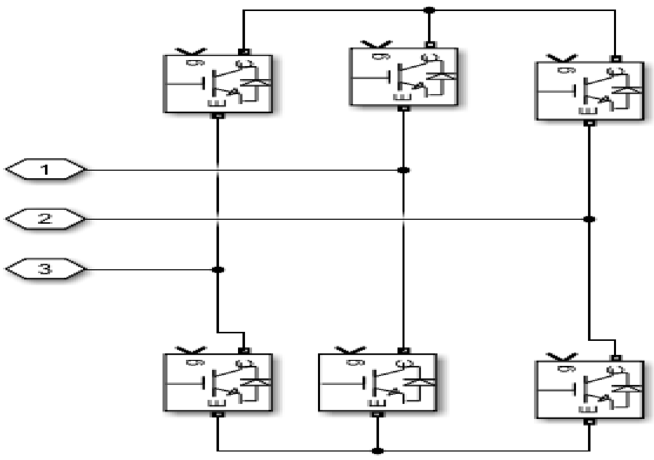

Figure 3. 15.The AC locomotive load model representation

Determining the load that draws power from the catenary system is a complex task and involves consideration of various factors, such as

- the number and size of loads,
- changing speeds of vehicles due to driver behavior and scheduling, and
- Load differences in various sections of the catenary system.

Many 25.kV electrified AC railway systems operate with ac-dc phase controlled thyristor converters that power DC motor drives in locomotives. These older locomotives are expected to coexist with newer GTO or IGBT locomotives for many years to come. However, thyristor based locomotives have a low displacement power factor and generate rich harmonic content in their load current. This causes significant reactive voltage drop along the feeder line and a distorted pantograph voltage waveform. This can limit the number of locomotives the system can support, and IEC specification 349 requires a minimum pantograph voltage of above 19 kV continuously and 17.5 kV for short periods. In this study, a single phase bridge rectifier with RL load is used to represent the load block, which generates harmonic currents and reactive power demand. The simulation will be performed under different load conditions and locomotive positions.

Table 3. 3.Load parameters(Schmid, n.d.)

Parameter	Values
Resistance (R)	30Ω
Inductance (L)	10mh

3.6.3. Train Model

Both freight and passenger trains run on the railway line, and there are different ways to model a train, such as using impedance, current, or power model. To use the impedance model, it is necessary to interpret the power factor phase angle at the train, while the effective current model requires determining the phase angle. However, for this thesis, the power model is used, which can be achieved by measuring the active and reactive power. This approach is preferred because it is based on the measured parameters(G. Chicco, M. Mancarella, 2020).

Table 3.4 displays the recorded data of current, active power, and reactive power of the line during a 15.minute period when a specific passenger train travels from Lebu to Endode. This section of the line does not have regular freight train traffic, so only the passenger train is taken into account. The table also shows the average values of these parameters.

Table 3. 4.I, P and Q Measurement

Time(Minute)	I(A)	P(kW)	Q(kVar)
0	58.6	1591.23	161.1
0.5	119.62	3263.04	443.13
1	56.15	1369.67	664.69
1.5	68.31	1812..8	503.56
2	176.4	4753.56	986.97
2.5	92.78	2437.21	245.28
3	56.15	1369.67	664.69
3.5	40.28	866.11	664.56
4	184.33	4914.7	1148.1
4.5	53.71	1369.67	1463.27
5	64.7	1671.8	1503.56
5.5	98.37	2558.66	805.7
6	67.75	1691.95	704.98
6.5	61.64	1571.09	684.84
7	44.56	946.68	684.84
7.5	39.67	604.27	664.69
8	59.21	1591.24	342.41
8.5	95.31	1722.37	382.7

9	73.85	2014.22	382.7
9.5	62.87	1671.9	382.7
10	43.95	1127.96	402.84
10.5	45.78	1118.39	422.99
11	45.17	1168.25	422.99
11.5	70.8	1913.5	402.844
12	89.11	2437.2	362.56
12.5	92.17	2517.18	382.7
13	93.39	2558.06	362.56
13.5	93.39	2558.06	382.7
14	94	2558.06	402.84
14.5	94	2558.06	402.84
15	91.56	2497.6	382.7
Average	78.30903	2025.941	590.1624

The data presented in Table 3.4 represents the active and reactive power consumption of the train at the substation. The average values of these measurements have been calculated and the active and reactive power loss along half of the line between Lebu and Indode has been subtracted. It is assumed that the remaining power consumed is used by the train. Since the train is traveling from one end to the other, an average distance equal to half of the total distance from Lebu to Indode is used.

$$\text{Total distance} = 16.1\text{km}, \text{ half of the distance} = 8.05 \text{ km}$$

The average current during the whole recorded travel was 78.309A.

$$\text{The line impedance } (Z) = 8.05*(0.130081 + j0.392381) = 1.04715205 + j3.15866705$$

$$\text{The power drop in the line } (S_L) = I^2 * Z = 6421.45 + j19369.58 \text{ kVAR.}$$

$$\text{Active power} = 6.42145 \text{ kW.}$$

$$\text{Reactive power} = 19.36958 \text{ kVar.}$$

Therefore, the passenger train operating at Ethio Djibouti line can be modeled as constant power of the value:

$$\textit{Active power} = 2025.94 - 6.42145 = 2019.52 \; kW$$

$$\textit{Reactive power} = 590.162 - 19.36958 = 570.79242 \; kVar$$

Therefore, in this thesis, the locomotive's constant power model can be represented by using the average values of 2.02 MW active power and 0.570 MVar reactive power. On the other hand, the dynamic power model is created based on the actual variable power readings, which better simulates the real behavior of a train during its operation using actual measurements of active and reactive power.

3.7. SVG Modeling

SVG is a type of FACTS (Flexible AC Transmission System) device that offers exceptional performance for dynamic reactive power compensation. It is capable of compensating for reactive power by controlling the amplitude and phase of its output voltage at the AC side or by directly controlling the output current. This technology has become a hot topic in the field of research related to reactive compensation and electric power quality control. SVG is selected as a method due to its numerous advantages such as continuous reactive power throughput, a wide range of regulation for reactive power, fast response, high precision control, and reliable operation. In a scenario where two sources are connected with a series reactance of value X in between and the voltage of source V1 is at an angle of zero degrees and V2 at an angle δ, as shown in Figure 3.15 below(A. Padilha.Feltrin, J. S. da Costa, 2007).

Suppose having two sources connecting with a series reactance of value X in between and suppose the voltage of sources V1 at an angle of zero degree and V2 at an angle δ. as showed Figure 3. 15. Below.

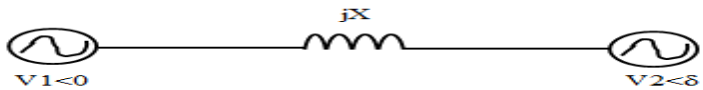

Figure 3. 16.Voltage source for two reactance’s with delta phase difference

$$Q = \frac{(V_1 - V_2)V_2}{X} \qquad (3-19)$$

From the Equation $(3-19)$ reactive power is directily proportional to the magnitude of the difference of two voltages, $(V_1 - V_2)$, When $V_1 > V_2$ reactive power flows from V_1 to V_2 and if $V_1 < V_2$ reactive power flows from V_2 to V_1.

3.7.1. The Basic Working Principle of the SVG

To use the SVG in the system, it is connected in parallel with the load. Initially, a power transformer is employed to reduce the voltage from the high voltage bus bar and then supply it to the medium voltage bus bar. Subsequently, the medium voltage bus bar feeds the thyristor controlled reactors and the thyristor switched capacitor. The thyristor firing rate is regulated by an external controller which is responsible for managing the thyristor firing rate. This firing rate controls the reactive power injection into the system through inductors or the absorption of reactive power from the system via capacitors.

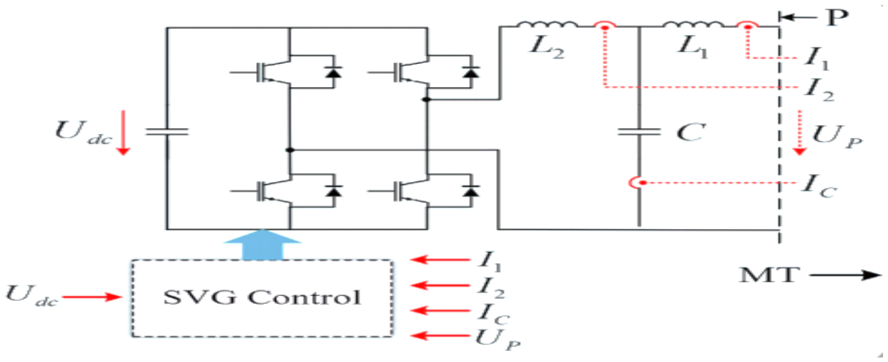

Figure 3. 17.Basic block diagram of SVG with LCL filter

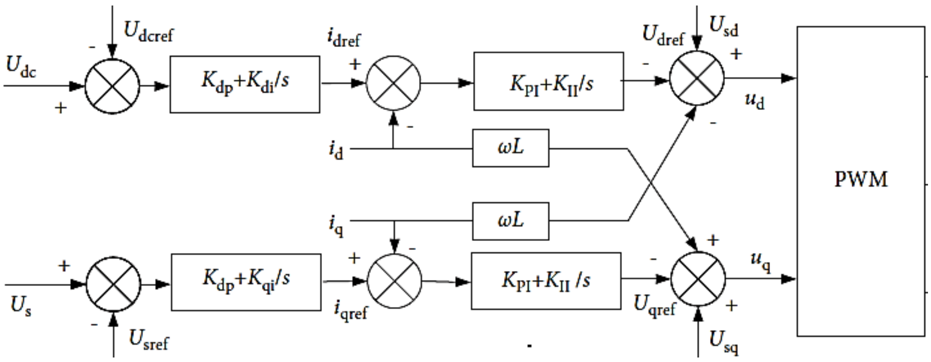

Figure 3. 18.Control Bloch diagram of SVG STATCOM with PWM

SVG usually adopts a double closed loop control with an outer voltage control loop and an inner current control loop, as shown in Figure 3.17. DC voltage control compares the DC voltage U_{dc} with the reference voltage and generates a d-axis reference current i_{dref} through an outer loop proportional Integral (PI) DC voltage controller. The grid connected voltage control compares the grid connected voltage U_s with the reference voltage U_{ref} and generates a q-axis reference current i_{qref} through an outer loop PI grid connected voltage controller.

SVG feedback currents i_d and i_q are compared with reference values i_{dref} and i_{qref}, respectively, and the SVG voltage control targets, U_{dref} and U_{qref}, are generated through the PI controller of the inner current control loop. The voltage control signal U_d is generated after comparing U_{dref} with the voltage generated by the grid connected voltage d-axis component, U_{sd}, and feedback current i_q through line inductance L. Similarly, a control signal U_q is generated. Pulse-width modulation based on U_d and U_q is used to generate insulated gate bipolar transistor (IGBT) break pulse signals, *S* from the four gates(Y. Xu, L. M. Tolbert, F. Z. Peng, J. N. Chiasson, 2007). ,

The PI control model of the outer DC voltage control loop is given by

$$\begin{cases} \frac{dx_1}{dt} = U_{dc} - U_{dref} \\ i_{dref} = K_{dp}(U_{dc} - U_{dref}) + K_{di}x_1 \end{cases} \tag{3-20}$$

Where x_1 is the intervening variable K_{dp} and K_{di} are the proportional and integral control gains, respectively. The PI control model of the outer grid connected voltage control loop is given by

$$\begin{cases} \frac{dx_2}{dt} = U_s - U_{sref} \\ i_{qref} = K_{qp}(U_s - U_{sref}) + K_{qi}x_2 \end{cases} \tag{3-21}$$

where x_2 is the intervening variable K_{dp} and K_{di} are the proportional and integral control gains, respectively. The PI controller model of the inner current control loop is given by

$$\begin{cases} \frac{dx_3}{dt} = i_{dref} - i_d \\ u_d = u_{sd} - \omega L i_q - K_{PI}(i_{dref} - i_d) - K_{II}x_3 \end{cases} \tag{3-22}$$

$$\begin{cases} \frac{dx_4}{dt} = i_{qref} - i_q \\ u_q = u_{sq} - \omega L i_d - K_{PI}(i_{qref} - i_q) - K_{II}x_4 \end{cases} \tag{3-23}$$

where x_3 and x_4 are intervening variables K_{PI} and K_{II} are the proportional and integral control gains, respectively. Overall, the wind farm SVG model parameters for estimation were K_{dp}, K_{di}, K_{qp}, K_{qi}, K_{PI}, K_{II}, and L.

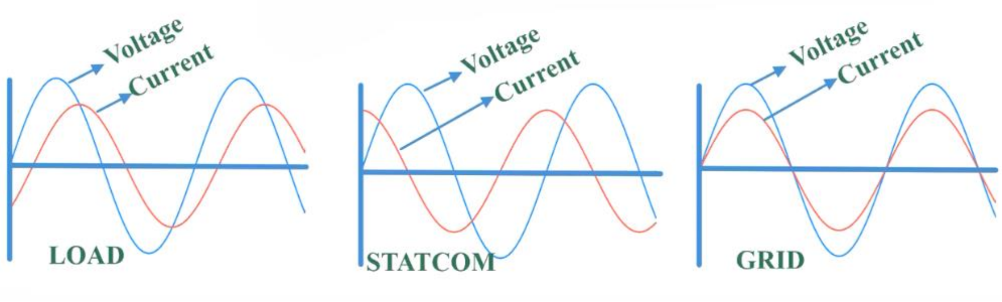

Figure 3. 19.Basic block diagram of SVG

3.8. Unipolar PWM

Figure 3.28 illustrates the generation of PWM using the unipolar PWM technique. In this method, the reference voltage is compared with a triangular current wave. Since unipolar PWM uses both positive and negative references, the output of each comparator is inverted and connected to each IGBT(Al.Haddad, 2002).

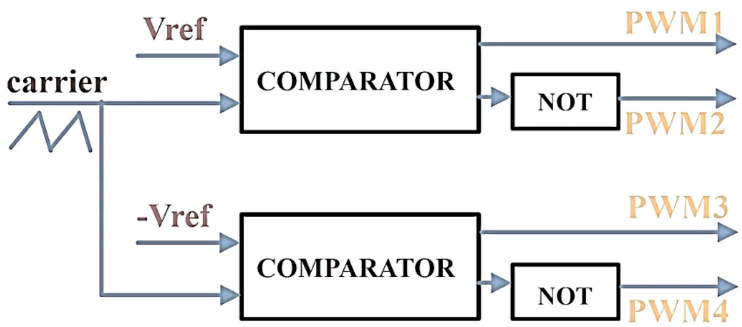

Figure 3. 20.Unipolar PWM

3.8.1. Reactive Component Estimation

The process of determining the reactive component of the load current can be illustrated by considering a load that consumes reactive current and is connected to the grid. This load can be represented as an RC load, as depicted in Figure 3.20.

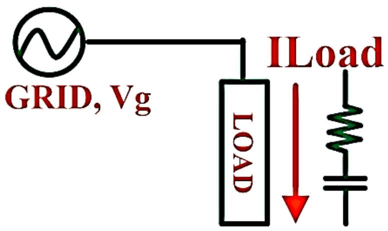

Figure 3. 21. RC load

Now the grid voltage Vg can be written as

$$Vg=Vm\sin(\omega t) \qquad (3-25)$$

$$I_{load}=I_m\sin(\omega t+\phi) \qquad (3-26)$$

$$React = Im\sin(\omega t+\phi)+\cos(\omega t) \qquad (3-27)$$

To understand the phaser diagram for this scenario, we need to first represent the desired voltage as a phaser with amplitude Vm, and then draw the current phaser with amplitude Im, which leads the voltage by an angle ϕ.

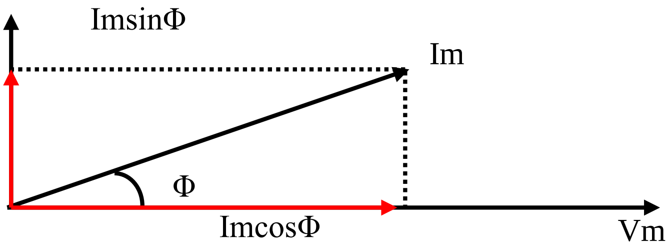

Figure 3. 22.Phaser diagram of voltage and current

The phaser diagram helps us to determine that the load current $Im\cos\phi$ has an active component that is in phase with the grid voltage and a reactive component $Im\sin\phi$ that leads the voltage by an angle of 90 degrees.

However, the goal here is to determine the reactive component of $Im\sin\phi$ given the voltage and current information. To accomplish this, we must first multiply the current by coswt. Then we gate reactive component is equal to $Im\sin(\omega t+\phi)$ in to $\cos\omega t$. Now we will be wondering from where I gate this cosωt term, this term I have obtained from PLL. From PLL we gate one active component and one reactive component. This $\cos\omega t$ is basically the reactive component(V. S. Tejwani, H. B. Kapadiya, A. S. Pandya, 2015).

Now the equation can be solved using trigonometric identity that is: .

SinAcosB = $\frac{1}{2}$ [sin (A+B) + sin (A.B)], so we will gate reactive component

$$React = \frac{Im}{2} = [\sin(\phi)+\sin(2\omega t-\phi)] \qquad (3-28)$$

The first $\frac{Im}{2}\sin(\phi)$ is the DC term and the second $\sin(2\omega t-\phi)$ high frequency term. Now use the low pass filter to complete filter out the high frequency term.

Then reactive component: . $\text{Re act} = \frac{\text{Im}}{2}\sin(\phi)$, multiplied this component by 2,

$$Re\,act = \text{Im}\,sin(\phi) \qquad (3-29)$$

Positive=Imcosflux (3_30)

This is how to estimate the reactive component.

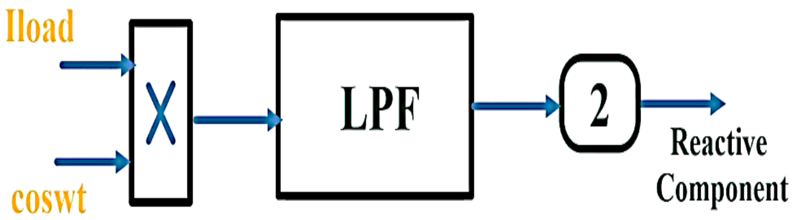

Figure 3. 23.Low pass filter

3.9. Overall Compensation Operational Principle

The purpose of the aforementioned modeling is to prevent the source from providing reactive power and to enhance the power factor of the system. This is achieved when the source can perceive only the resistive impedance of the load (train) and the transmission line (catenary). This implies that the waveform of the source current only contributes to the active power load.

Vs=RI (3__31)

React=Imsin(ωt+φ)+cos(ωt) (3__32)

$P(t) = R(t)i^2_{(t)}$ (3__33)

$$P(t) = \sum_{1}^{n} V_n(t)\, i_n(t) \qquad (3-34)$$

Considering the single phase circuit,

$$P(t) = v(t)\,i(t) \qquad (3-35)$$

The power that is not useful and causes line current losses and increases generation requirements for utilities is called non active power. This power circulates among phases and between sources and loads, and its average value is zero. The active power is the average value of instantaneous power over the interval (t.Tav, t).

$$P = \frac{1}{Tav}\int_{t-Tav}^{t} P(\gamma)\,d\gamma \qquad (3-36)$$

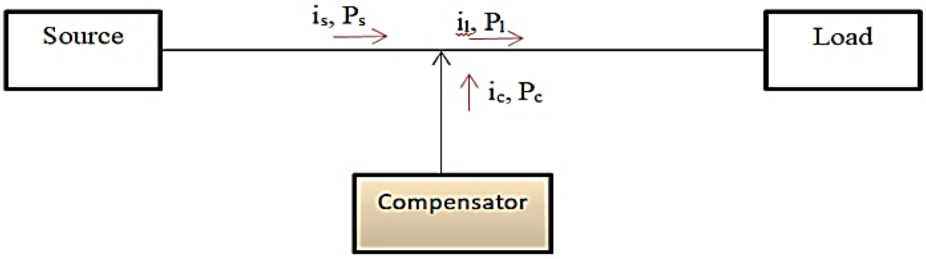

Figure 3. 24.Scheme of compensation

Considering Figure 3.24: $p_s + p_c = p_l$ (3−37)

$Ps = Pl$, since Pc is zero as time goes to infinity.

Then, the instantaneous active current and non-active current are calculated using the following equations [39] – [41]:

$$i_a(t) = \frac{P}{V_r^{\,2}} v_r(t) \qquad (3-38)$$

$$i_n(t) = i_l(t) - i_a(t) \qquad (3-39)$$

Where, P is the average active power load over the averaging interval, $Vr\ (t)$ is the RMS value of the reference voltage, $v_r\ (t)$ is the instantaneous reference voltage; $ia\ (t)$ is the instantaneous active component of load current, $i_n\ (t)$ is the instantaneous non-native component of load current

The selection of the averaging interval (Tav) and reference voltage $vr\ (t)$ depends on the compensation strategy. Tav can have a value between zero and infinity. If Tav is zero, the average power will be the same as the instantaneous power, and the instantaneous non-active power will be zero. This is not suitable for generating the non-active current. Conversely, the averaging interval should not be set to infinity because it is impractical for any power system.

The selection of the averaging interval (T_av) and reference voltage (v_r) is crucial in determining the source current behavior in the compensation strategy. The value of T_av can range from zero to infinity, but neither extreme is practical. It has been proven in that setting Tav = n (T/2), where T is the system period and n is an integer, will result in the source current following the reference voltage. Additionally, the reference voltage chosen can affect the waveform of the active component of the current.

To make the source current in phase with the sinusoidal source voltage, v_r is set as the reference voltage. Therefore, an averaging interval of half the period is used to obtain average and RMS values of power and voltage, respectively. Using Equation (3.38) and (3.39), non-active current is generated, and this is considered as the reference current input to the controller. The Simulink model of this reference current is illustrated in Figure 3.25

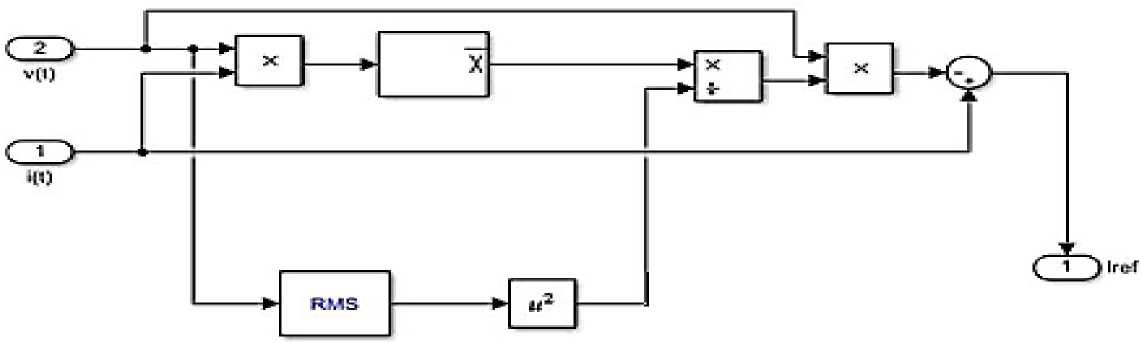

Figure 3. 25.Reference current model

The instantaneous power is the product of instantaneous voltage and current. The average value of this instantaneous power over a period of averaging interval (T_{av}) is the active power.

$$i_n(t) = i_l(t) - i_a(t) \qquad (3-40)$$

$$P = \frac{1}{T_{av}} \int_{t-T_{av}}^{t} P(\gamma)\,\mathrm{d}\gamma = \frac{1}{T_{av}} \int_{t-T_{av}}^{t} v(\gamma)\, i(\gamma)\,\mathrm{d}\gamma \qquad (3-41)$$

The reference (source) voltage and load current, respectively, are:

$$\mathrm{v_s}(t) = \mathrm{V_m} \sin\omega t = \sqrt{2}\mathrm{V_s} \sin\omega t \qquad (3-42)$$

$$\mathrm{i}_l(t)=\sqrt{2}\sum_{n=1}^{\infty}\mathrm{I}_n\sin\left(\mathrm{n}\omega\mathrm{t}-\phi_{\mathrm{n}}\right) \qquad (3-43)$$

Substituting the above two equations, equation (3.42) and (3.43) into equation (3.35):

$$\mathrm{P}(t)=2\mathrm{V}_{\mathrm{s}}I_1cos\phi_1\left(1-cos2\omega t\right)+2\mathrm{V}_{\mathrm{s}}I_1sin\omega t\; cos\omega t\; sin\phi_1$$
$$+\sum_{n=2}^{\infty}\mathrm{I}_n\sin\,\omega\mathrm{t}\,\sin\left(\mathrm{n}\omega\mathrm{t}-\phi_{\mathrm{n}}\right) \qquad (3-44)$$

From Equation (3. 41) and (3. 44),

$$\mathrm{P}=\frac{1}{T_{av}}\int_{t-T_{av}}^{t}P(t)=\mathrm{V}_{\mathrm{s}}I_1cos\phi_1=\mathrm{P}_{\mathrm{a}} \qquad (3-45)$$

$$\mathrm{P}_{\mathrm{na}}=\ \mathrm{P}(t)-\mathrm{P}_{\mathrm{a}} \qquad (3-46)$$

Where, P_a and P_{na} are active and non.active power.

Thus, from Equation (3.38), (3.42) and (3.45), the active current component will be:

$$\mathrm{i}_{\mathrm{a}}(t)=\sqrt{2}\mathrm{I}_1cos\phi_1\sin\,\omega\mathrm{t} \qquad (3-47)$$

Here, this current ia (t) is in phase with source voltage. The remaining unwanted component of current (non-active current) which regarded as reference current will then be:

$$\mathrm{i}_{\mathrm{R}}(t)=i(t)-\mathrm{i}_{\mathrm{a}}(t)$$

$$\mathrm{i}_{\mathrm{R}}(t)=-\sqrt{2}\mathrm{I}_1cos\omega\mathrm{t}\sin\,\phi_1+\sqrt{2}\sum_{n=2}^{\infty}\mathrm{I}_n\sin\left(\mathrm{n}\omega\mathrm{t}-\phi_{\mathrm{n}}\right) \qquad (3-48)$$

The reference current, generated by the reference current block model in Figure 3.33, will serve as the input to the PR controller which will regulate the output current of the voltage source converter. As a result, as illustrated in Figure 3.32, the source current will solely contribute to the active component of the load current, while the compensator will supply the remaining parts. This approach significantly enhances the power factor.

3.10. Rating and Cost Estimation

The components of the STATCOM system will be chosen appropriately so that it can compensate for all the reactive power, resulting in a power factor of one throughout the train's operation. STATCOM consists of a voltage source converter, a capacitor that serves as a DC voltage supply, and a coupling inductor to prevent rapid discharge of the capacitor and short circuiting. The specific value and type of these components depend mainly on the power and current transfer requirements, as well as the control method, which is based on Fryze's non-active current concept(Akagi, H., Kanazawa, Y., & Nabae, 2000).

To ensure effective transfer of reactive power, the DC voltage source must have a minimum voltage of 27.5 kV in the AC side of the converter. In order to calculate the appropriate capacitor value, the highest reactive power that needs to be compensated, which is 1148.1 kVAr, should be taken into account.

For the 25kV application, the converter switches should have the ability to handle medium voltage. Power electronic switches, such as IGBTs, that can handle high voltage and current can be utilized. Research has shown that the cost of FACTS equipment is only half of the overall expenses, with the remainder being made up of civil works, installation, commissioning, insurance, engineering, and project management. Operating costs are frequently overlooked. Despite providing good control to improve electric power quality, power electronic based controllers have a significant drawback: their cost is higher than that of comparable conventional equipment.

The total cost of implementing a FACTS device depends on the individual costs of the coupling inductor, capacitor, power electronic switches, and associated protection and control circuit. The cost of the device is determined based on its rated electrical capacity. There are different options available for designing and implementing a FACTS device, and thus, determining the exact cost for this type of controller configuration is challenging. However, some reports have provided approximate prices for FACTS devices, indicating that the price range for these devices is considerable.

Based on the information presented, as well as the cost of the Static Synchronous Compensator (STATCOM) for medium voltage and the dynamic reactive power compensation products from Shandong Hoteam Electric Co. Ltd, an estimate of the installation cost for this mitigation technique has been made. It is estimated that the cost for a 1.5 MVar capacity will be around $60,000 based on a rate of $40/kVar. To effectively generate reference current that accurately tracks the sinusoidal source voltage, it is recommended to install the mitigation technique at each traction substation. However, it is also possible to install it on each rolling stock. Therefore, approximately $600,000 should be invested to include this kind of mitigation technique on the 10 trains currently operating on the Ethio Djibouti line.

3.11. Controller Design

The phase locked loop produces two components, one active and one reactive. The active component, illustrated in figure 3.21, is synchronized with the grid in phase, while the reactive component, shown in figure 3.22, is aligned 90 degrees out of phase with the grid.

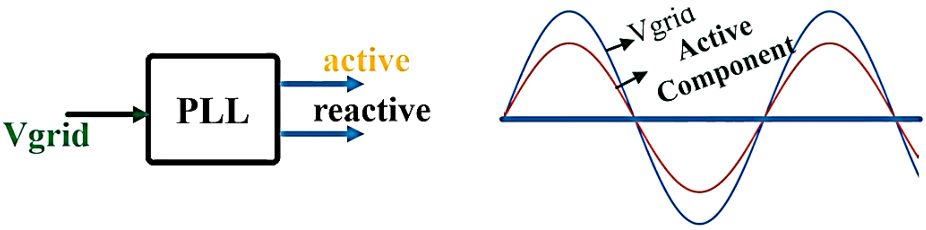

Figure 3 . 1: Active component of PLL

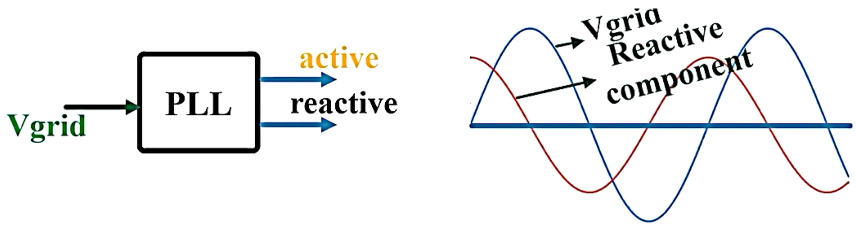

Figure 3. 26.Reactive component of PLL

To deliver an active current to the grid, it's crucial to synchronize the voltage and current phases. To achieve this, a reference signal is required, which should be synchronized with the actual voltage and have a magnitude ranging from 1 to .1. A grid connected inverter uses a phase locked loop (PLL) to generate this reference signal, which is then utilized as a basis for the current controller's operation. In a similar manner, a PLL is utilized to produce signals that are 90 degrees out of phase with the actual voltage when reactive electric power needs to be delivered to the grid.

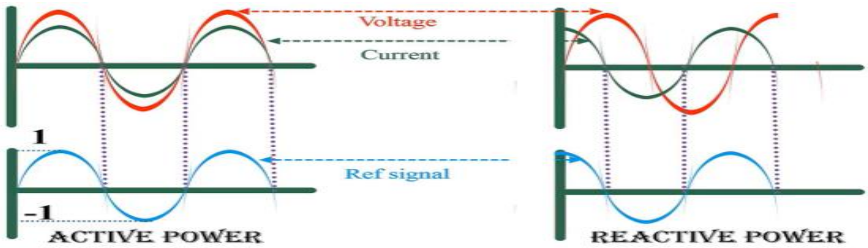

Figure 3. 27.PLL single phase connected inverter

Next, let's explain the procedure for generating alpha beta voltage in a single phase system. The initial step involves feeding the voltage into a low pass filter, allowing us to identify its transfer function.

$$TF = \frac{\omega c}{S+\omega c},\ \omega c = \text{corner frequency, Suppose } S = j\omega$$

$$TF = \frac{\omega c}{j\omega+\omega c}$$

The approach listed below can be used to determine the low pass filter's magnitude and phase:

$$TF = \frac{\omega c}{\sqrt{\omega^2+\omega c^2}} < \tan^{-1}\frac{\omega}{\omega c} \quad \text{Suppose } \omega = \omega c$$

$$TF = \frac{1}{\sqrt{2}} < .45$$

The magnitude will increase if added one more LPF.

$$TF = \frac{1}{\sqrt{2}} * \frac{1}{\sqrt{2}} < .45 - 45$$

$$TF = \frac{1}{2} < .90$$

By multiplying the second low pass filter output by 2, we obtain a signal that is comparable to the input signal. Due to the fact that the Beta signal always leads the Alpha signal by 90 degrees, a phase shift of 90 degrees occurs. This method allows us to produce alpha beta voltage in a single phase system, with the input signal referred to as Beta and the resulting output signal referred to as Alpha.

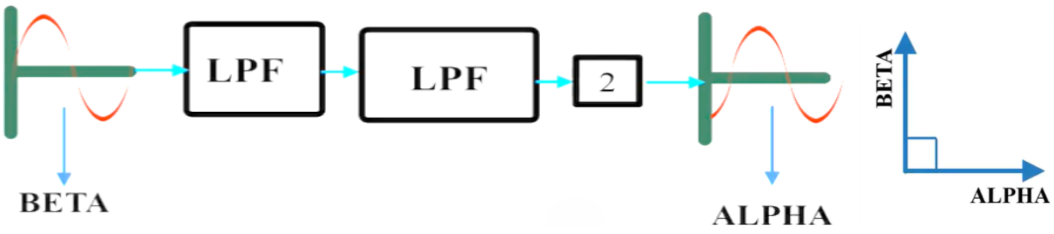

Figure 3. 28.Low pass filter operation

Initially, convert the alpha beta signal into DQ signals, and the control system produces DQ output. Then calculate the difference between the Q and Q reference values and set Q reference to zero. Then, sending this error to a proportional integral (PI) controller. The output of the PI controller provides angle information, which can be integrated to determine ωt. This ωt value is then transmitted to the block that transforms alpha, beta, and DQ signals. The PI controller is always active, and its output angle ωt serves as an input signal to the alpha beta to DQ transformation block. Using this ωt value, it can generate both active and reactive current reference signals. This approach is employed for implementing PLL in a single phase system.

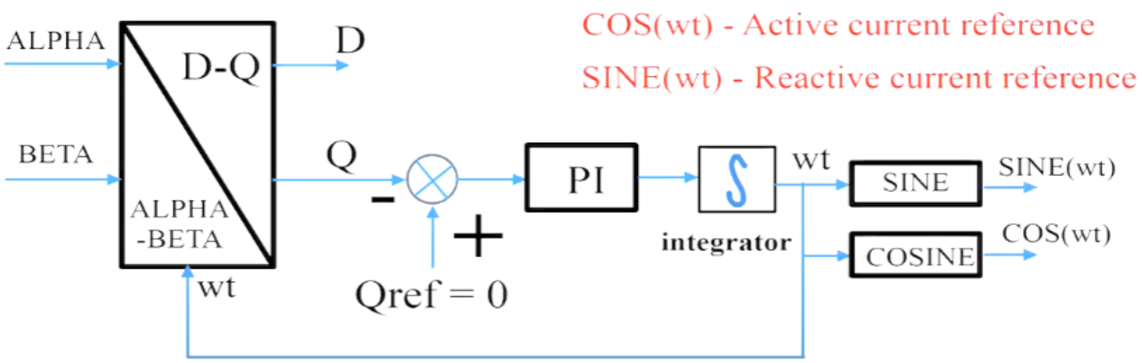

Figure 3. 29.PLL block diagram

3.11.1.Design the PI controller

The value that takes from the name-plate of data recorded from substation is listed in below tables.

Table 3. 5.Design specification of PI controller

Parameters	Value
Input Voltage (Vin)	27.5kV
Output voltage (Vo)	25kV
Output power (Po)	2MW

Output frequency (f)	50Hz
Switching frequency(fsw)	10kHz
Total Harmonic (THD)	<5%
Current Ripple (ΔI)	20%
Capacitor ESR	0.0042Ω

Table 3.5 displays the parameters of the proportional integral (PI) controller, which plays a vital role in regulating the traction supply system. These parameters are solely employed during the controller's design phase.

Design the LC filter parameters

$$\text{Output current (Io)} = \frac{\text{Po}}{Vo} = 80 \text{ A}$$

$$\text{Maximum curent Riple} = \Delta\text{Ippmax} = 0.2 * \text{Io} * \sqrt{2} = 22.6 \text{ A}$$

$$\text{Inductor} = \text{L1} = \frac{Vdc}{4 * Fsw * \Delta\text{Ippmax}} = 0.\ 030\text{H}$$

$$\text{Inductor} = \text{L2} = \frac{0.1 * Vo}{S * 2 * Pi * f} .\text{L1} = 3.98 * 10^{-3} \text{ mH}$$

$$\text{Capacitor} = \text{C} = \frac{0.05 * S}{(Vo)^2 * 2 * Pi * f} = 5\mu F \text{Control time constant, T} = 150\ \mu s$$

$$\text{Inductance, L} = 0.\ 030\text{H}$$

$$\text{Inductance internal resistance, RL} = 1\text{m}\Omega$$

$$\text{Kp} = \frac{L}{T} = 200$$

$$\text{Ki} = \frac{RL}{T} = 6.67$$

When using PI controller, never gate zero steady state error to avoid this issue use a PR controller.

Table 3. 6.PI Vs PR controller

PI	PR

$Y(s) = E(s) * (Kp + \frac{Ki}{s})$ 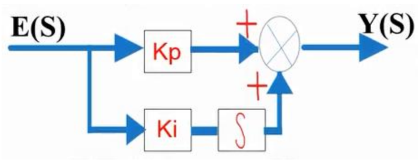	$Y(s) = E(s) * \left(Kp + \frac{KrS}{S^2 + w^2}\right)$ 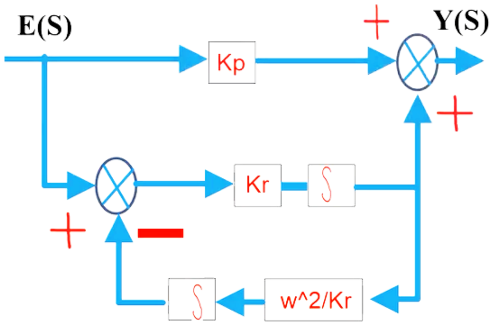

The first step involves calculating the error between the reference voltage and the actual voltage, which is known as a proportional integral (PI) controller. The controller's output generates the capacitor current, which is then added to the load current. According to Kirchhoff's law, the total current yields the inverter reference current, as depicted in Figure 3.26 below. Next, compare this current with the actual inverter current to produce the error signal, which is also considered a PI controller. The output of this controller provides the voltage across the inductor. Adding this voltage to the load voltage yields the inverter reference voltage, which is utilized as the reference voltage for the pulse width modulation (PWM) generation block. Figure 3.26 illustrates this process.

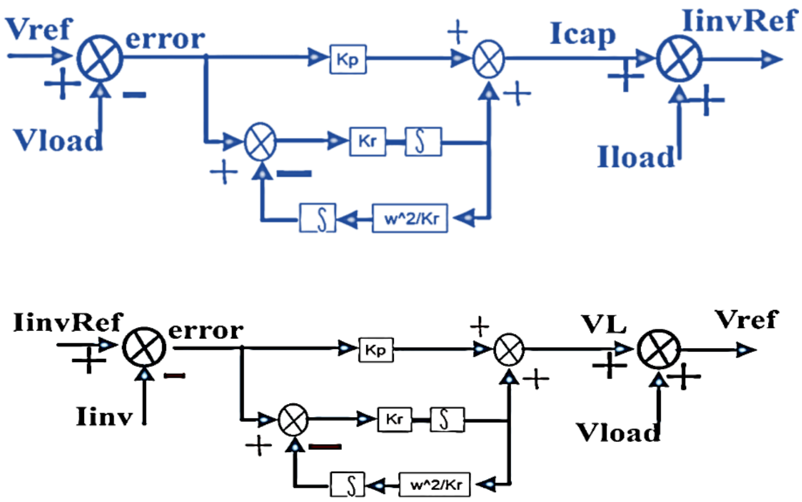

Figure 3. 30.PR Controller block diagram

Voltage controller	Current Controller

Controller Time Constants = 200μs Filter capacitance = 6.23μ F Capacitor ESR = 0.0042ohm Value of Kp = capacitance / Time constant $= \frac{6.23\mu F}{200\ \mu S} = 0.03115$ $G_n = \frac{Kr\,\omega n}{\omega n^2 - \omega^2}, \omega_n = \frac{1}{\sqrt{LC}}$, w = 2*pi * 50, G_n = 0.1, Kr value for voltage controller = 400 $\frac{\omega^2}{Kr} = \frac{(2*pi*50)^2}{400} = 246.7$	Controller Time Constants = 150μs Filter inductor = 4.06 mH Inductor series resistance = 0.001 Value of Kp = Inductance / Time constant $= \frac{4.06\text{ mH}}{150\ \mu S} == 27.066$ $G_n = \frac{Kr\,\omega n}{\omega n^2 - \omega^2}, \omega_n = \frac{1}{\sqrt{LC}}, \omega = 2*pi * 50,$ G_n = 0.1, Kr value for voltage controller = 100 $\frac{\omega^2}{Kr} = \frac{(2*pi*50)^2}{100} = 986.83$

The subsequent step entails determining the reactive current present in the load, which governs the amount of current the Static Var Generator (SVG) must generate.

- To begin, compute the error between the actual sensed VDC and the reference VDC, which is the discrepancy between the desired signal and the current being injected by the Voltage Source Converter (VSC).
- Next, apply a PI controller to the error signal, and the output of this controller is multiplied by the active component generated by the Phase Locked Loop (PLL).
- Subsequently, multiply the estimated reactive component in the load current by the reactive component produced by the PLL.
- Then add the resulting products in a multiplier to obtain the current reference.
- The current reference is compared with the actual inverter current to determine the error, which is then fed to a proportional resonant (PR) controller.
- The output of the PR controller is added to the grid voltage to obtain the final reference voltage, which is used for pulse width modulation (PWM) generation.

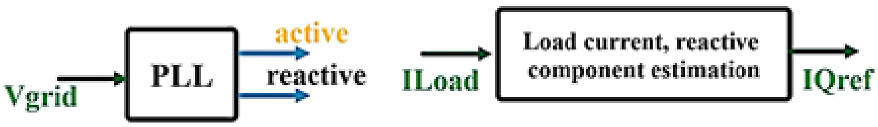

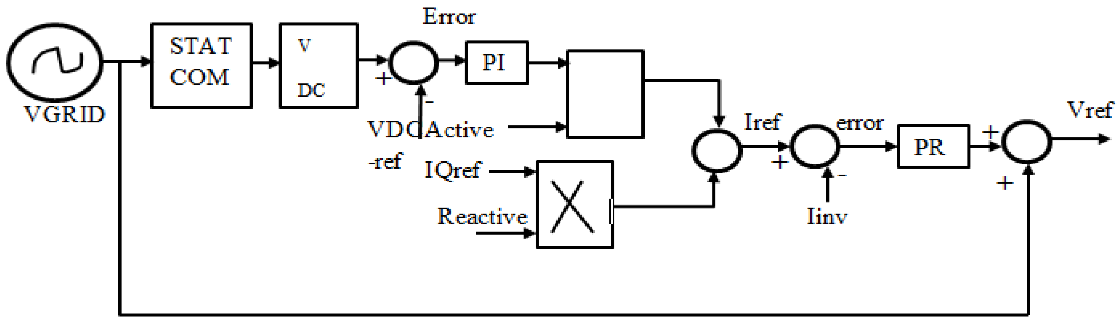

Figure 3. 31.Controller block diagram

3.11.2. PI controller optimization using PSO

The PSO optimized PI controller algorithm is a method of tuning the proportional integral (PI) controller parameters using Particle Swarm Optimization (PSO) algorithm. The PI controller is a widely used control algorithm in various control applications, including power electronics, process control, and robotics. The PSO algorithm is a stochastic optimization technique inspired by the behavior of birds flocking and is commonly used to find the optimal solution for various optimization problems.

In this algorithm, the PI controller parameters (proportional gain, integral gain) are considered as the variables to be optimized. The objective function is defined as the integral of the squared error between the reference signal and the output signal over a certain time period. The PSO algorithm then optimizes the PI controller parameters by adjusting them iteratively, using the objective function as the fitness function.

The PSO algorithm uses a swarm of particles, each representing a possible solution, to search for the optimal solution. Each particle has a position and a velocity, which are updated based on its own best position and the best position of its neighbors in the swarm. The position of each particle corresponds to a set of PI controller parameters, and the velocity represents the change in those parameters. The PSO algorithm iteratively updates the position and velocity of each particle until the optimal solution is found. The optimized PI controller parameters are then used to control the system.

The PSO optimized PI controller algorithm has shown to be effective in various control applications, including voltage regulation, current control, and speed control. It offers a fast and efficient method of tuning the PI controller parameters without requiring extensive knowledge of the system dynamics.

3.11.3. Particle Swarm Optimization (PSO)

PSO is one of the most powerful methods for solving the nonlinear optimization problems. It is basically developed through the simulation of bird flocking. In two Dimensions space [18.25]. Flocking of birds optimizes a definite objective function. Each.one of. Agent knows the best value so far (pbest) and its best XY position. In addition, it knows the best value so far in the group (gbest) among pbest. Each agent do its best to modify its position using this information(Kennedy, J., & Eberhart, 1995):

1. its current position $x.y$,
2. its current velocities $(v_x.v_y)$,
3. The distance between the current position, and pbest and gbest.

The commencement of modification for a searching point in PSO algorithm can be illustrated as in Figure 3.32

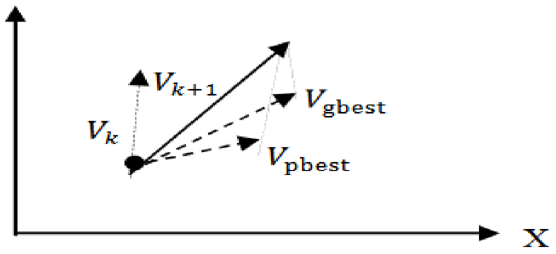

Figure 3. 32.Conception for modifying a point of searching

where s^k : current searching point.

s_i^{k+1} Modified searching point.

v_k : Current velocity.

v_i^{k+1}Modified velocity.

Vgbest: velocity based on Vgbest

Vpbest: velocity based onVpbest

Objective Function with Problem Formulation

In this paper, the PSO is used for obtaining the coefficients of PI controller K P and K i. The main object of the optimal PI controller design is eliminating the harmonic currents generated by the nonlinear load in the electric grid. The integral of squared error (ISE) is considered as the cost function to be minimized. The objective function is given as:

The total cost of implementing a FACTS device depends on the individual costs of the coupling inductor, capacitor, power electronic switches, and associated protection and control circuit. The cost of the device is determined based on its rated electrical capacity. There are different options available for designing and implementing a FACTS device, and thus, determining the exact cost for this type of controller configuration is challenging. However, some reports have provided approximate prices for FACTS devices, indicating that the price range for these devices is considerable.

Based on the information presented, as well as the cost of the Static Synchronous Compensator (STATCOM) for medium voltage and the dynamic reactive power compensation products from Shandong Hoteam Electric Co. Ltd, an estimate of the installation cost for this mitigation technique has been made. It is estimated that the cost for a 1.5 MVar capacity will be around $60,000 based on a rate of $40/kVar. To effectively generate reference current that accurately tracks the sinusoidal source voltage, it is recommended to install the mitigation technique at each traction substation. However, it is also possible to install it on each rolling stock. Therefore, approximately $600,000 should be invested to include this kind of mitigation technique on the 10 trains currently operating on the Ethio Djibouti line.

CHAPTER FOUR

SIMULATION RESULTS AND DISCUSSIONS

The results of the simulations performed on the five models covered in the previous chapter are presented in this chapter along with a thorough analysis of the findings. One of these models examines the longitudinal train dynamics, particularly the relationship between speed fluctuation and the accompanying mechanical power needed. The four remaining simulation models are made to simulate the traction power supply system, including static and dynamic power models, with and without the application of the outlined mitigation strategy. Tables 4.1, 4.2, and 4.3 provide an overview of the parameters used in this thesis before moving on to the analysis of the results. Table 4.4 also displays the results of the Particle Swarm Optimisation method, particularly the PID parameter values.

Table 4. 1.Catenary parameters

Parameter	Values
Impedance (Z)	0.130081+j0.39238 Ω/km
Shunt capacitance (C)	0.011 μF/km
Frequency (F)	50 HZ
Series resistance (R)	0.130081 Ω/km
Series inductance (L)	1.25mH/km

Table 4. 2.Substation and SVG parameters

Parameter	Values
Substation supply voltage(V)	25kV
Dc bus capacitor (C)	$4.25*10^{-5}\ F$
Resistance (R)	0.001 Ω
Inductance (L)	4.2 mH

Table 4. 3.Train parameter values(Ethiopian Railways Corporation, n.d.)

Parameter		Value
G	Gravity constant	$9.8 m/s^2$
m	Mass per axle	17t
K	Friction constant	600
A	Front sectional area	$4m^2$

P	Partial perimeter of the train	57m
N	Number of raised pantographs	2
F	Input force	60N
R	Radius of curvature in horizontal plane	800m
V	Construction speed	140km/h
V	Maximum speed in operation	120km/h
M	Weight	75.081t
Railway gauge		1435mm
Car dimension	Length	25500mm
	Width	3105mm
	Height	4433mm
	Vehicle center distance	18000mm
Rated seat	118 persons	

Tabel 4. 4.Controller parameter output

(M.cheng, n.d.)

Parameter value in manual tuning				Parameter value in PSO tuning			
PI controller		PR controller		PI controller		PR controller	
Kp	Ki	Kpr	Kir	Kp	Ki	Kpr	Kir
10	500	0.5	100	0.537667	1.833885	0.0001	0.86217

4.1. Simulation result of train dynamic model

The speed-time curve and the accompanying mechanical power needed to produce the train's acceleration are shown on the graph in Figure 4.1, which illustrates the link between speed and time. To provide real-time representation based on the mathematically computed total duration of 2890 seconds, the simulation for this model is run over 3000 seconds. The derivative block can be used to generate acceleration and deceleration because the primary sampling time is set at 0.01 seconds.

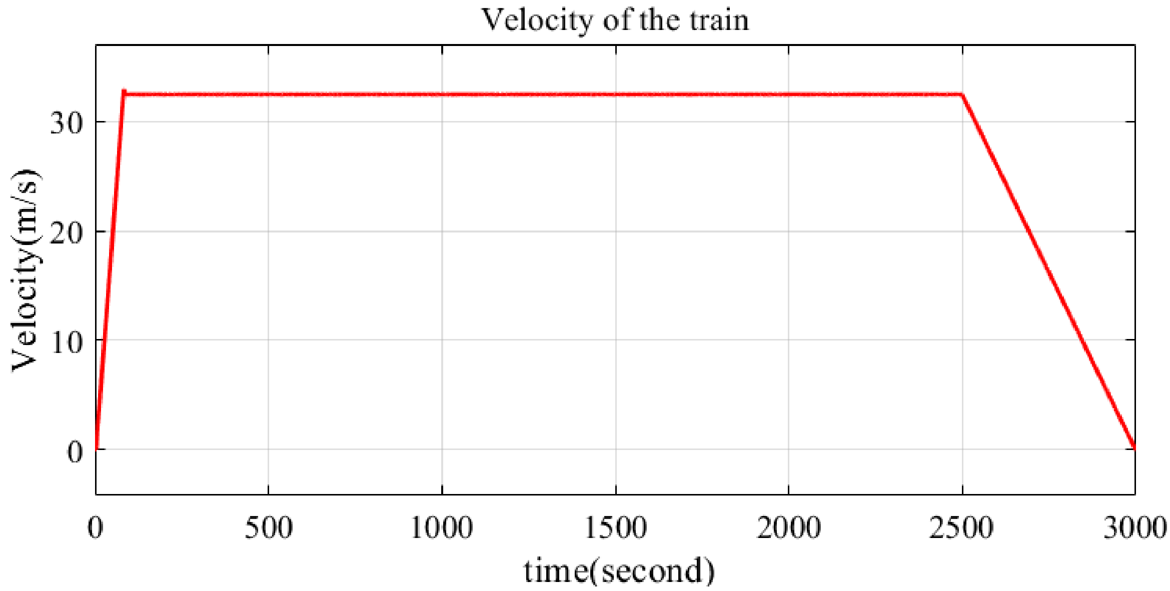

Figure 4. 1.Velocity of the train

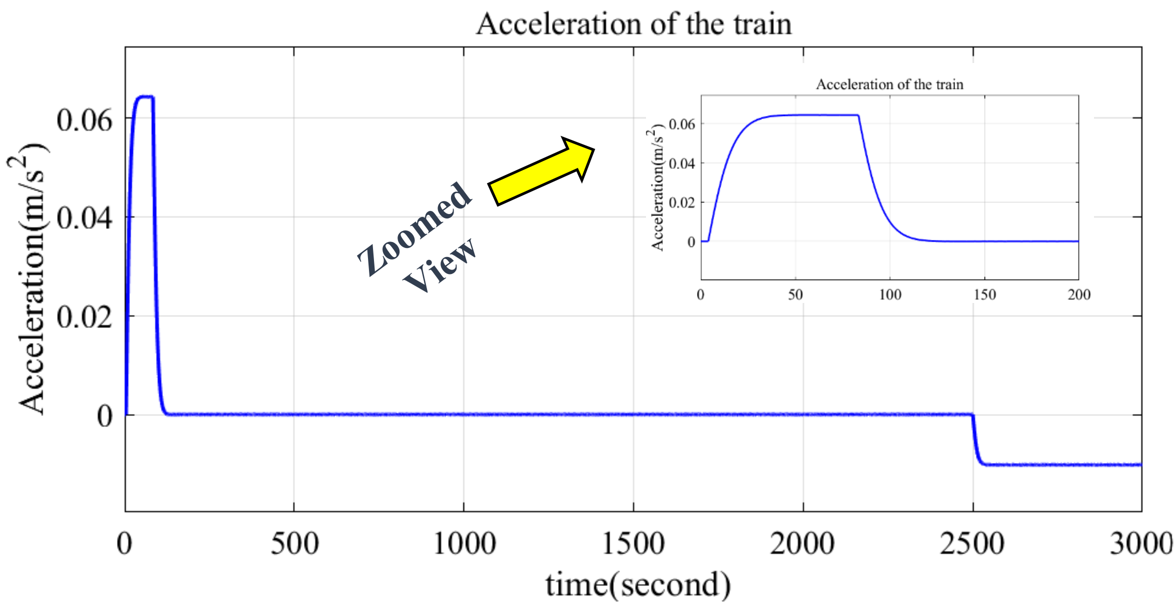

Figure 4. 2.Acceleration of the train

As the train's speed increases between 0 and 83 seconds, it can be seen in Figure 4.2 that the train starts to accelerate. The train travels at a constant pace for a while, and then, as described in Chapter 3, it begins to slow down for the final 83 seconds of the trip, beginning at 2722 seconds. The increased time gap in Figure 4.2 is meant to show how the train moves over a longer period of time.

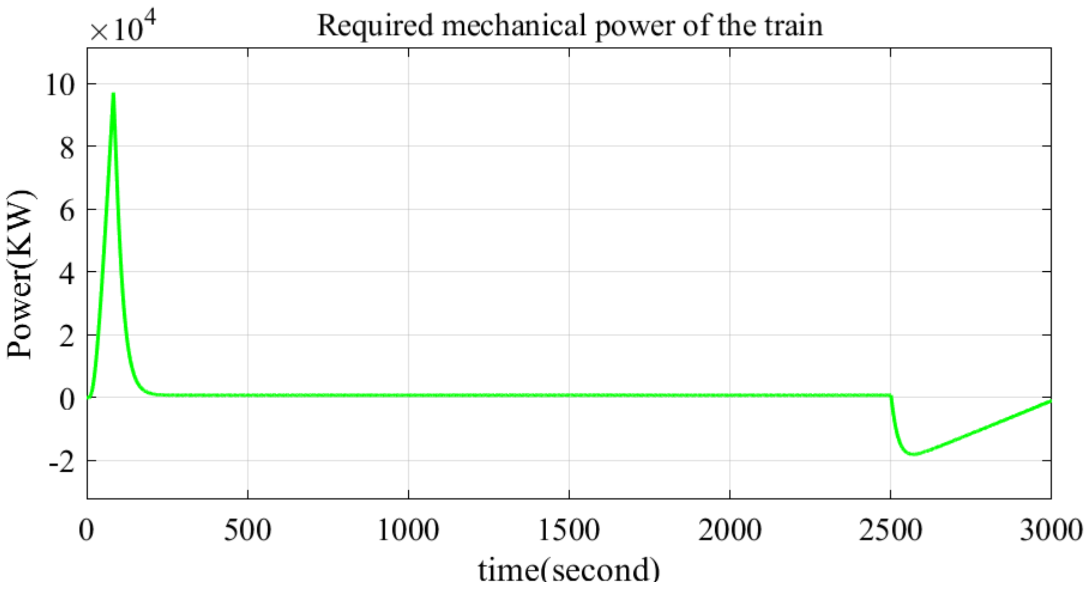

Figure 4. 3.Required mechanical power

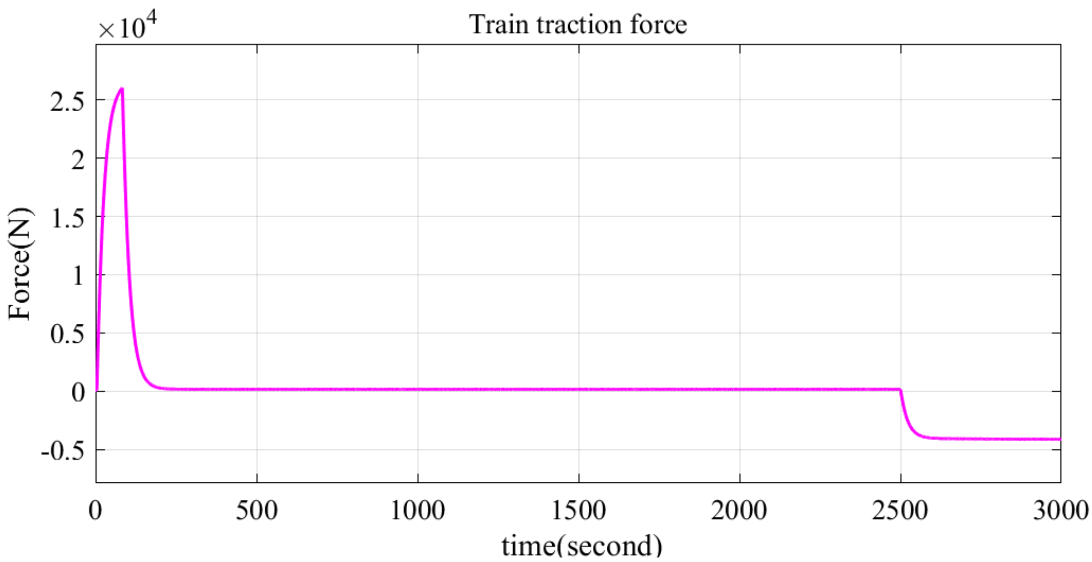

Figure4. 4. Traction force of the train before connected with the supply.

The power required by a moving train and the traction force it generates are substantially influenced by how quickly the speed varies and the actual speed value, as shown in Figures 4.3 and 4.4. Both the necessary mechanical power and traction force alter in accordance with fast changes in speed. Furthermore, Figure 4.2 demonstrates that the load varies as the speed changes. From this, it can be seen that the variations in mechanical power and traction force, as well as the rate at which the speed changes and the train's velocity, are all exactly related to one another. Additionally, the traction force and power levels are within acceptable limits.

4.2. Simulation result of static model

With the use of Particle Swarm Optimisation, the static train model is emulated using a PI controller. The static model's figures use the identical PI settings as those presented there.

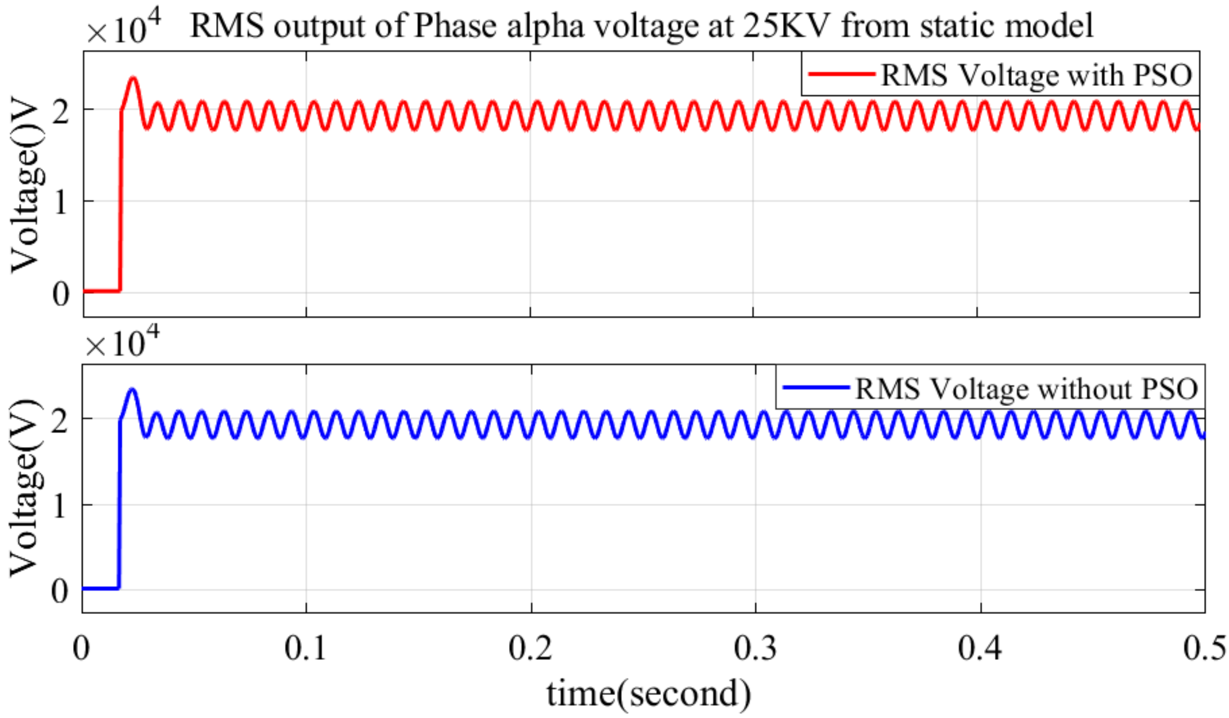

Figure 4. 5.RMS of Phase α Voltage at 25 kV

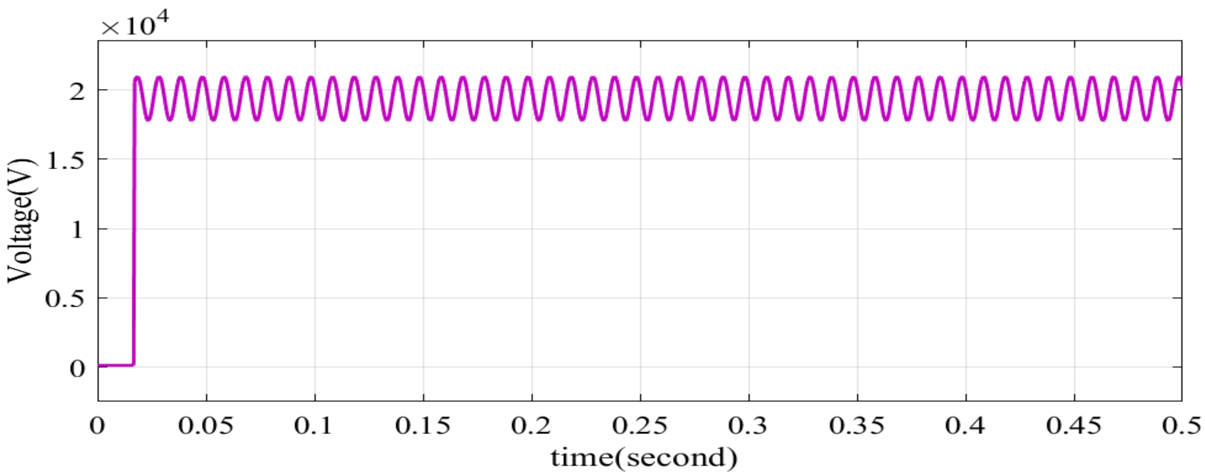

Figure 4. 6.RMS of Phase β Voltage at 25 kV side

It is clear from looking at Figures 4.5 and 4.6 that there is a substantial difference in the alpha phase voltage when contrasting the outcomes with and without PSO (Particle Swarm Optimisation). The voltage is optimised using Particle Swarm Optimisations in a wave sequence that is similar to that seen in Figure 4.5. The presence of a red wave indicates that all sinusoidal waves have the same amplitude and exhibit stable values over the course of the experiment. The blue wave, on the other hand, does not show consistent values over the course of the simulation. This generalisation leads to the observation that the voltage overshoot, in the absence of PSO optimisation, reaches a value of 2.023%. The overshoot is significantly reduced to 0.235% when optimised with Particle Swarm Optimisation, indicating that the PSO optimisation technique reduces the system's dynamic performance. It should also be noted that the voltage's root mean square (RMS) value complies with international standards in real-world applications. Figure 4.7 below shows the static model output of alpha phase voltage with and without Particle Swarm Optimisation.

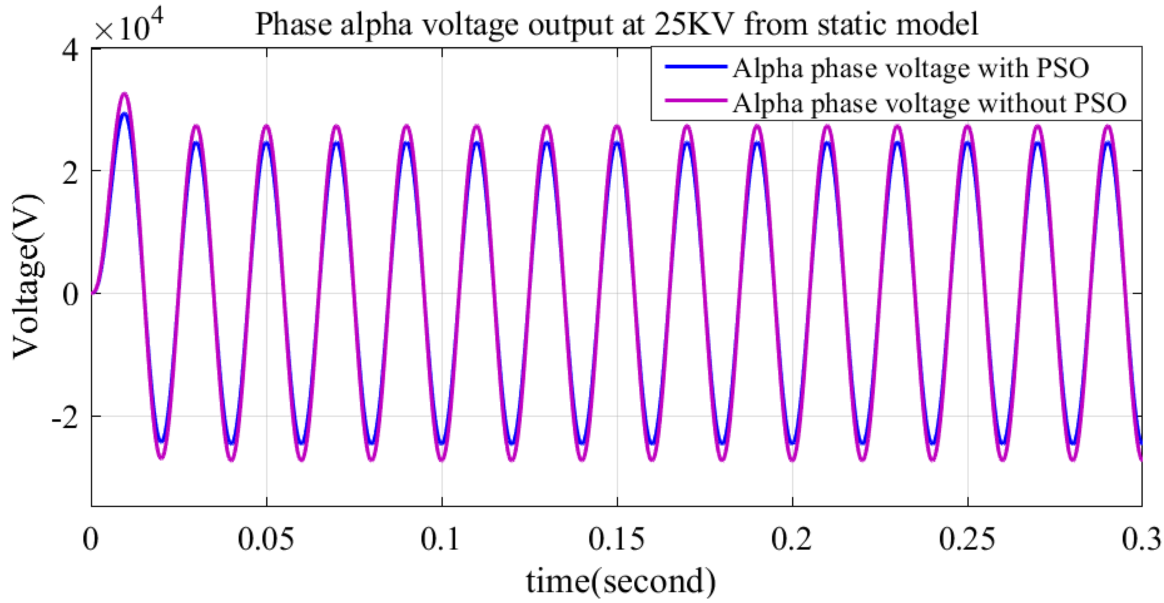

Figure 4. 7.Static model phase α voltage at 25 kV reading

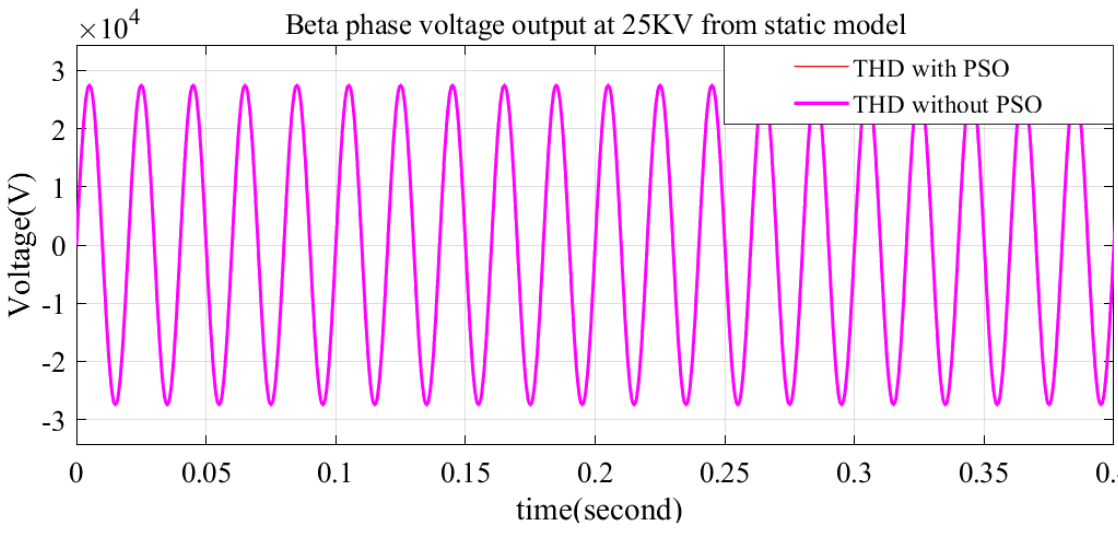

Figure 4. 8.Static model phase β voltage at 25 kV reading

As shown in Figure 4.8 the output voltage from β phase at static model is line with the supply voltage of the source. This phase voltage has no change when the controller is optimized with Particle Swarm Optimization. Similarly, phase α voltage in Figure 4.7 has no change in controller optimization.

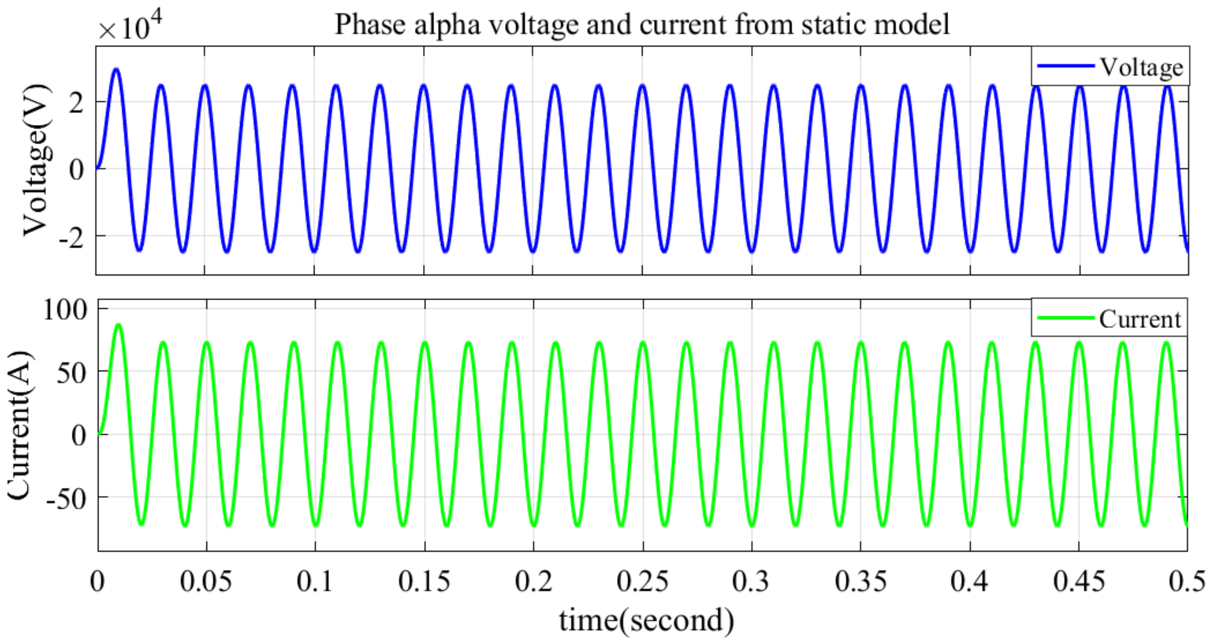

Figure 4. 9.Phase α Voltage and Current at 25 kV reading in static model

Figure 4.9 is the phase alpha phase voltage and current from the static model. Similarly figure 4.10 is the beta phase voltage and current in the same model. From the two figures signal the voltage almost similar in the two phase signal. But the current is different. The alpha phase current is approximately 71A and the beta phase current is approximately 95A and averagely there will be 83A.this shows the signal current generated is satisfies the design current in chapter 3.

Figure 4.9 and 4.10 has almost the same oscillatory motion and has smaller difference in magnitude with the supply voltage 25KV. Similarly the current output in the same phase has similar output in both phases. And also there is no variation in voltage and current with controller optimization with PSO. In both cases the signal has no any chatter this makes the system to reduce the THD.

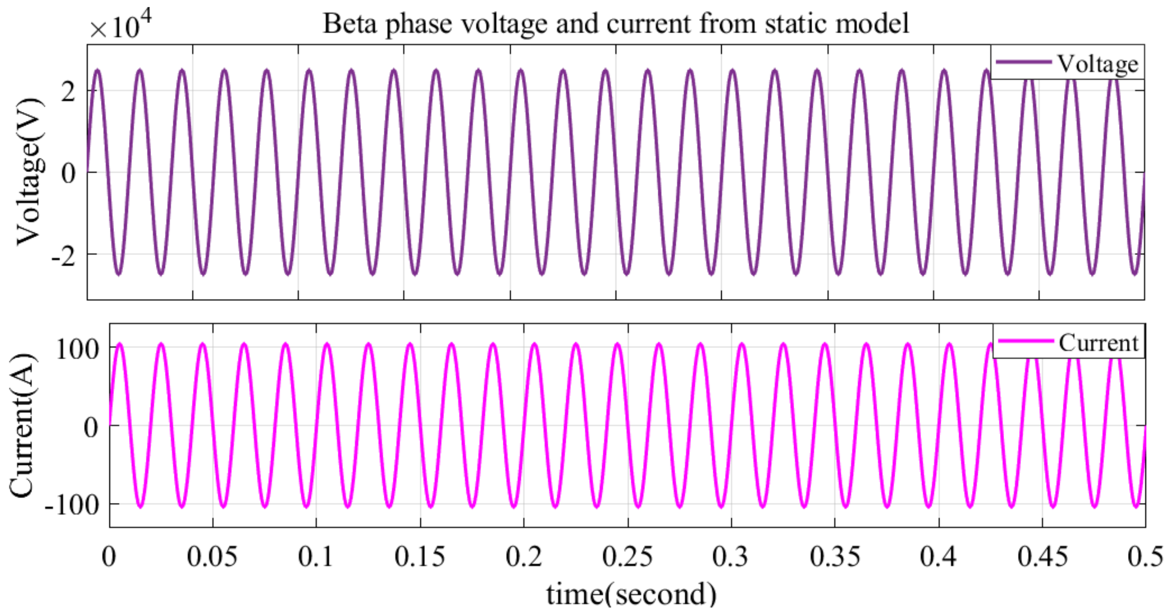

Figure 4. 10.Phase β Voltage and Current at 25 kV reading from static model

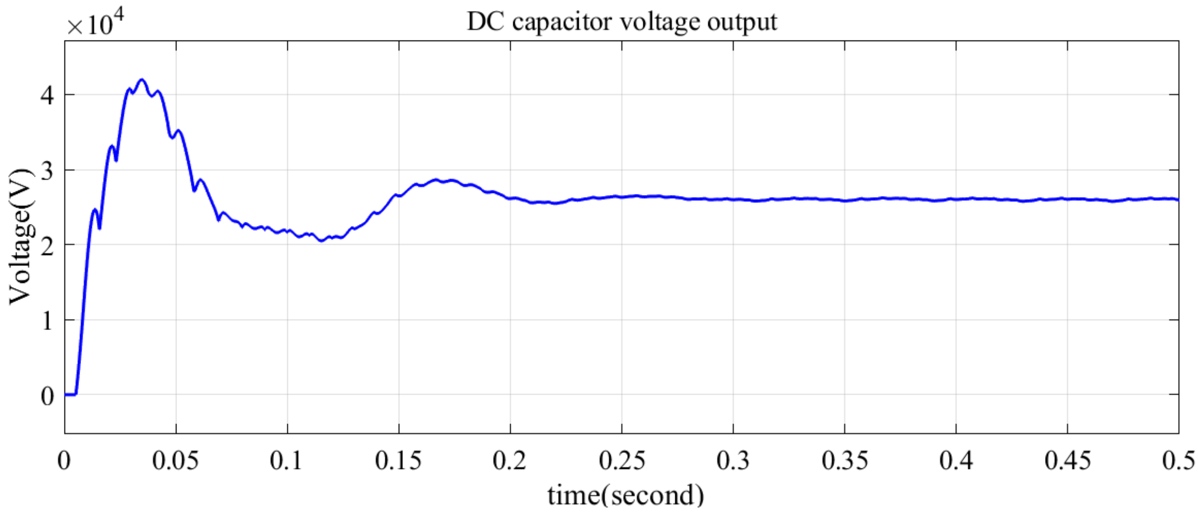

Figure4. 11.Output of DC side Voltage of STATCOM

The graph presented in Figure 4.11 displays the DC capacitor voltage output of the supply system, and it demonstrates that the selected system operates satisfactorily.

When examining Figure 4.12, it becomes apparent that the optimization of the controller parameter impacts both the load current and the inverter current. This is because the load current and inverter current serve as inputs to the PR controller and as outputs from the optimized STATCOM (Static Synchronous Compensator) in the Simulink model. Consequently, any changes in the controller parameter optimization directly affect the controller's output.

However, it should be noted that the grid voltage, grid current, load current, and inverter current are not that much influenced by the optimization of the controller parameter. These is because they serve as inputs to the system and as outputs from the SVG (Static Var Generator) optimized STATCOM, and thus remain unaffected by the controller parameter optimization.

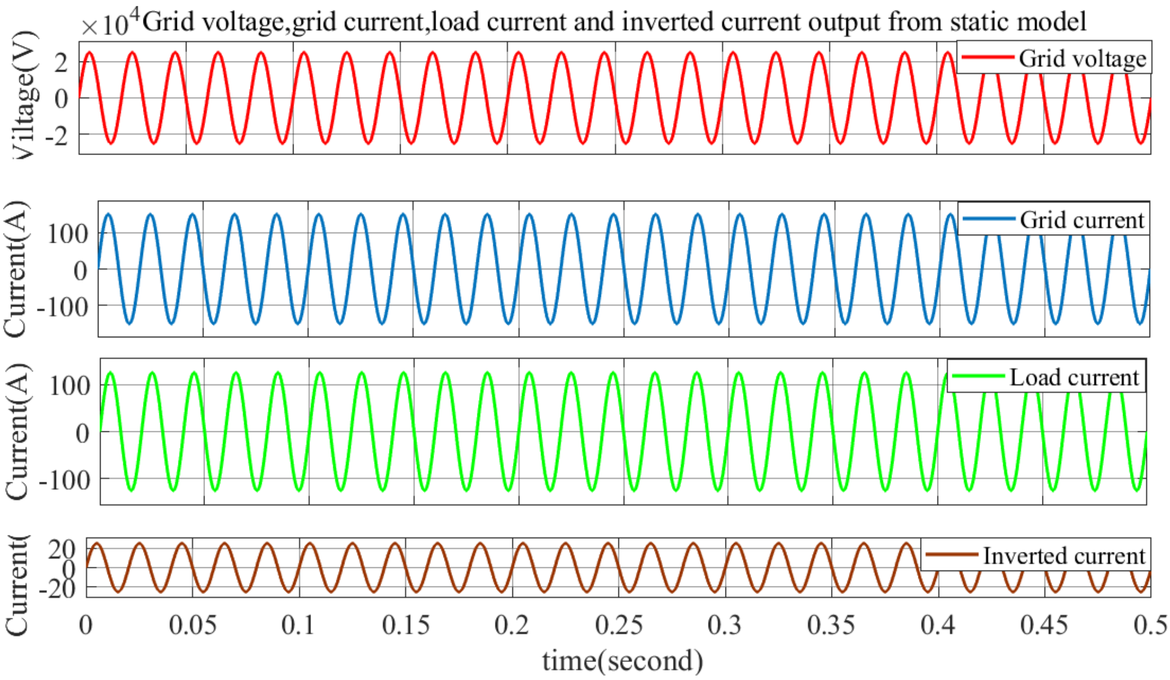

Figure 4. 12.Grid voltage, Grid current, Load current and Inverter output

Figure 4.13 below show the active and reactive power output of the static model after optimization of the controller. The result shows that the active power output shows around 2.0MW and above which is approximate with the calculated result. Compared to the active power, the reactive power output is very small. This shows that the system designed in Ethio-dijibuti is effective since there is no more unused power in the railway line.

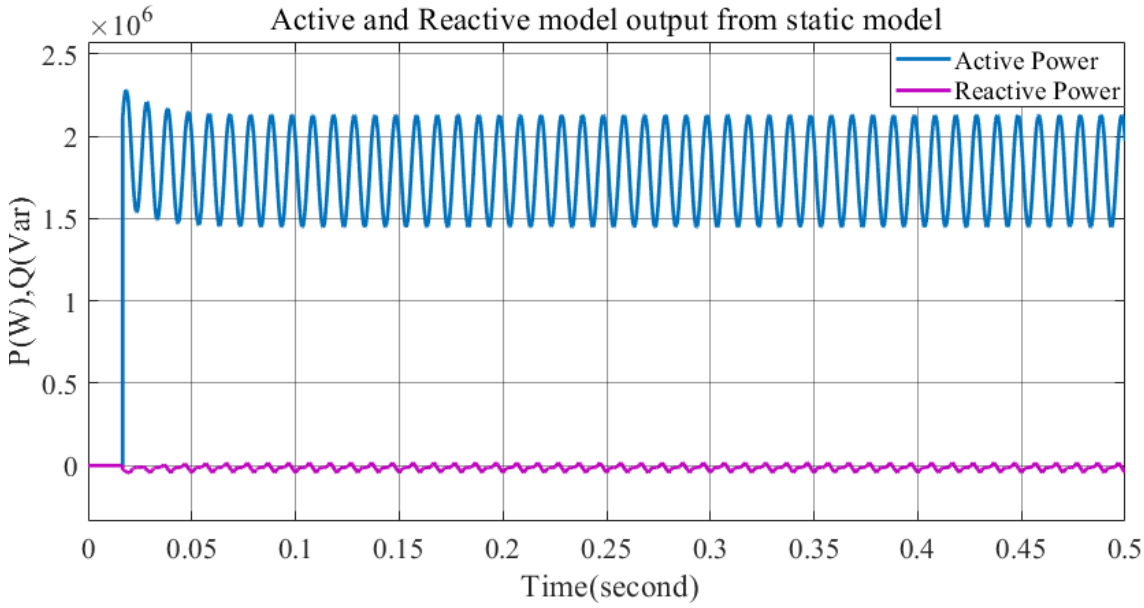

Figure 4. 13.Active and Reactive power output from static model

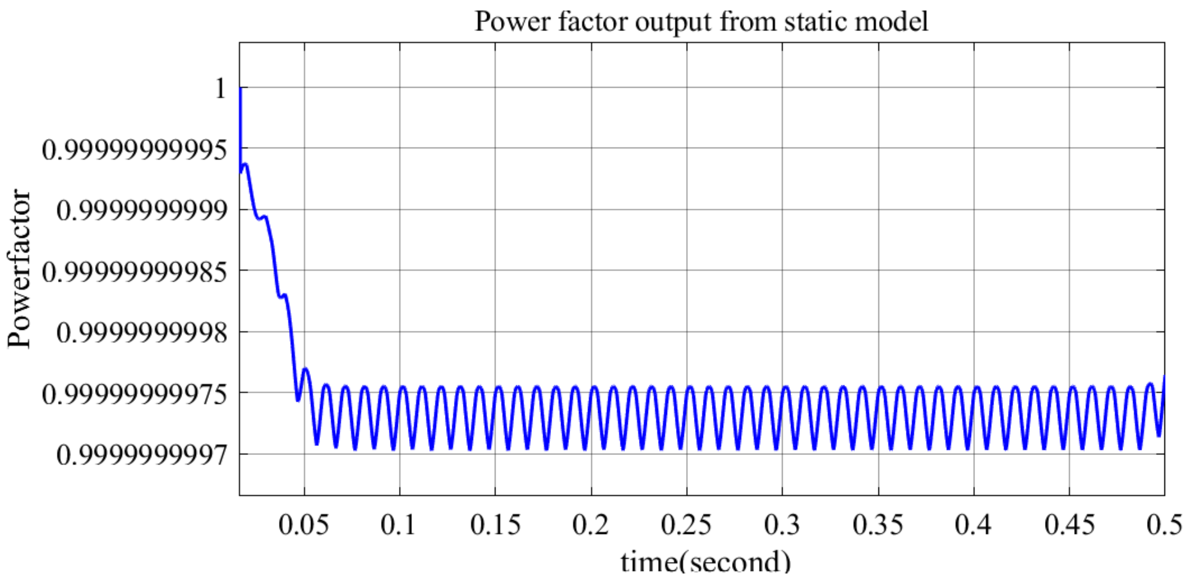

Figure 4. 14.Power factor output from static model

The power factor derived by the static model is shown in Figure 4.14. The efficiency of the system in utilising power is referred to in this context as the power factor. A lower power waste or unused power within the system is indicated by a greater power factor. The decrease in reactive power has an impact on the power factor in this system as planned. As a result, the supply line's power factor declines, suggesting a more effective use of electricity.

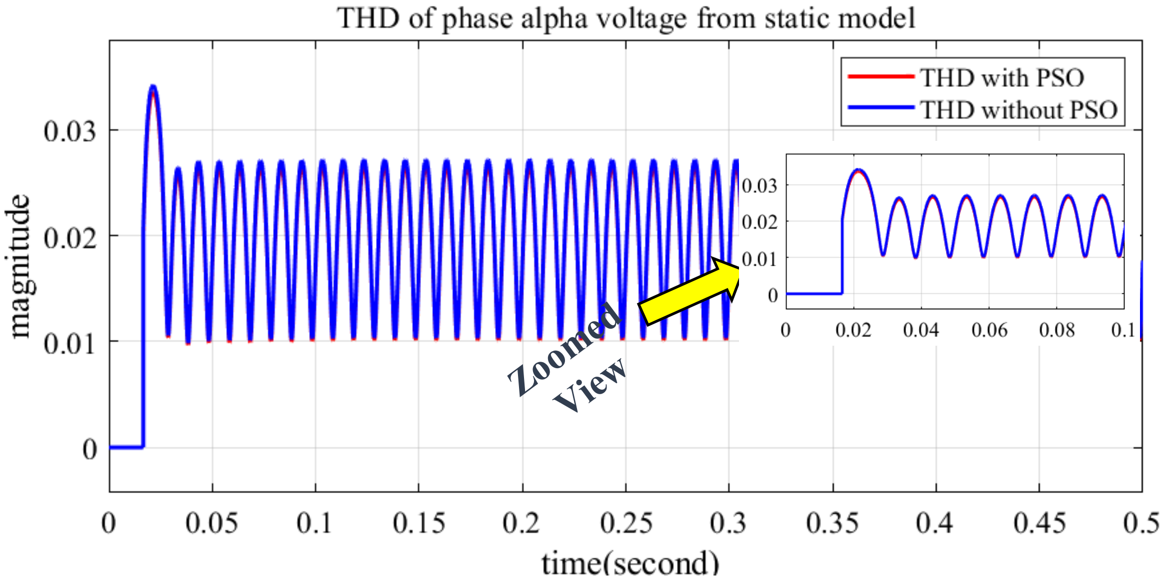

Figure 4. 15.THD of Phase α Voltage at 25 kV supply in static model

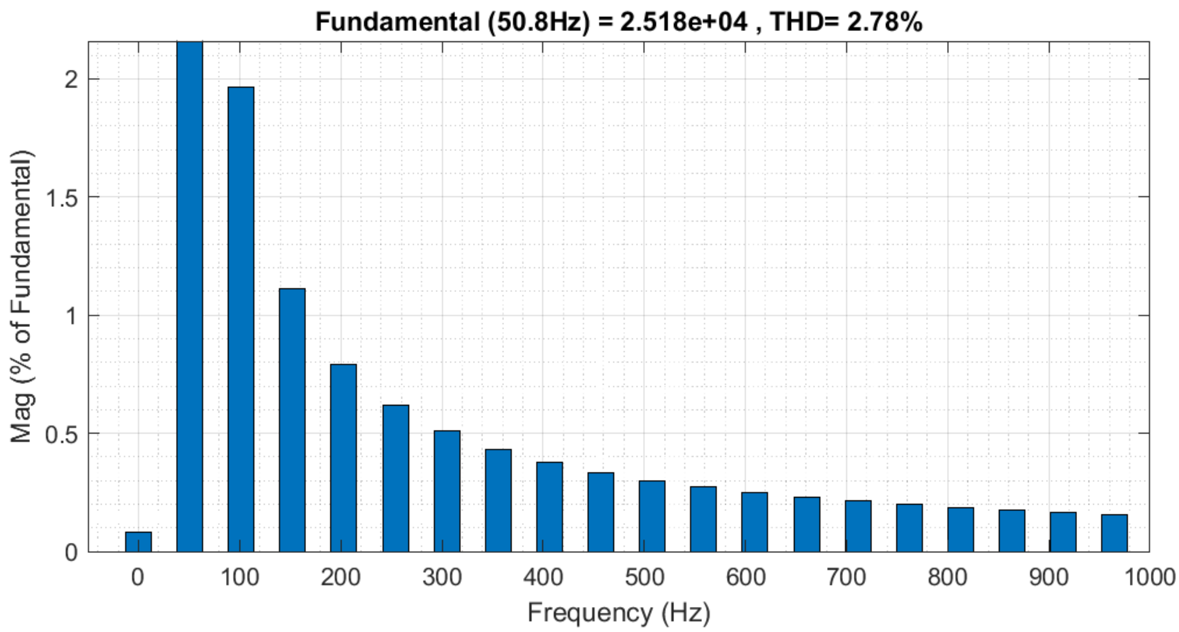

Figure 4. 16.FFT of Static Model THD at Phase α Voltage at 25 kV supply

Figures 4.15 to 4.18 describes the total harmonic distortion (THD) of the alpha and beta voltage in signal form. These figures indicate that both voltage signals exhibit similar THD values in the static model. The harmonic percentage for both phases is 0.14% or 0.0014 at 50Hz. As time progresses in the figures, the amplitude of the harmonic order decreases. The THD value obtained in these results is desirable when compared to the designed system. The reduction in total harmonic distortion signifies a decrease in reactive power, which was also described in Figure 4.13. This reduction in harmonic distortion is indicative of improved system performance and a more efficient utilization of power.

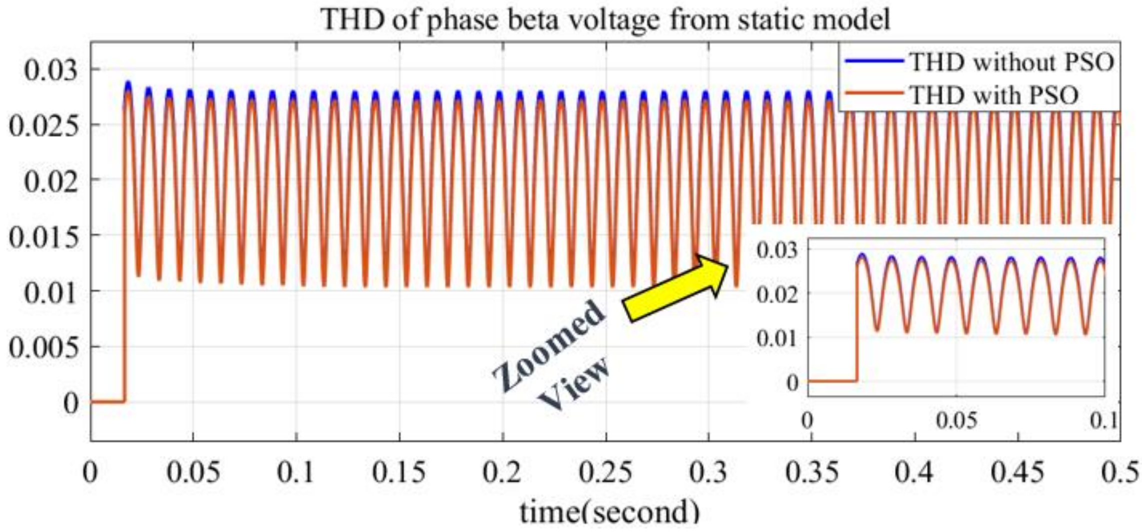

Figure 4. 17.THD of Phase β Voltage at 25 kV supply in static model

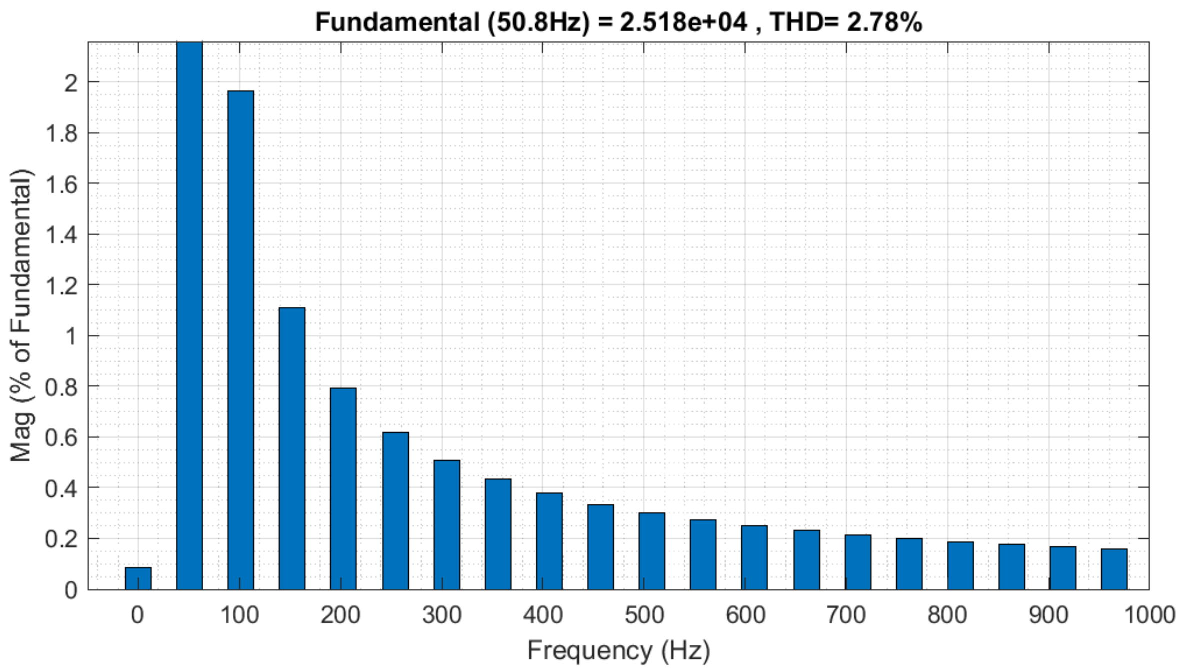

Figure 4. 18.FFT of Static Model THD at Phase β Voltage at 25 kV supply

Table 4. 1: THD (%) of Phase α and Phase β Voltage at 25 kV side of Lebu Adama railway line for static model

Lebu to Adama line	THD	GB/T 14549.1993	IEC TR.61000.3.6.2008

		3%	6.5%
Phase α	2.78%	Satisfied	Satisfied
Phase β	2.78%	Satisfied	Satisfied

4.3 Simulation result of dynamic model

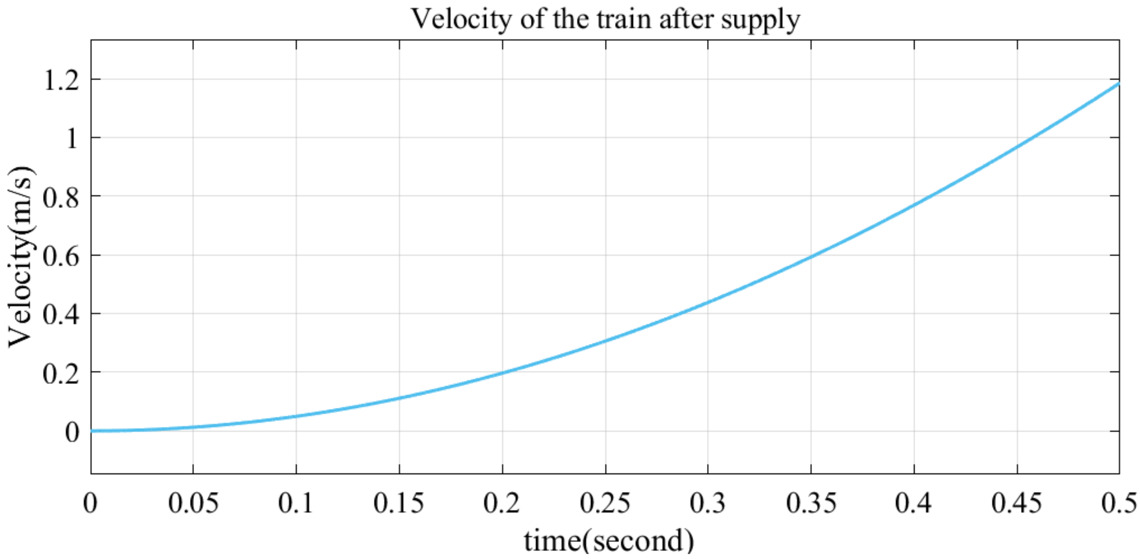

Figure 4. 19.Speed time curve (speed profile) after supply voltage

Figure 4.19 illustrates the velocity of the train when it is connected to the supply voltage. This graph displays a steady and consistent increase in the train's velocity, ensuring a safer experience for the passengers. On the other hand, Figure 4.20 represents the acceleration of the train in the dynamic model when it receives power from the supply. The acceleration signal demonstrates that the train maintains a constant acceleration during certain time intervals, ensuring a smooth and safe journey for the passengers. However, during speed variations, there are instances in the harmonic signal where the train's movement may become less safe for passengers. It is important to note that the acceleration signal in Figure 4.20 exhibits a very small parabolic shape, indicating minimal speed variations and slight instability in the train's movement.

Figure 4.21 and 4.22 described below are the required mechanical power of the train, Required Traction force of the train after connected with the supply respectively. The mechanical power is increasing with increasing the run time of the train. Since there is a similar load change in the run time of the train the required mechanical power increases in constant value as shown in figure 4.21.but the traction force of the train is constant throughout its movement.

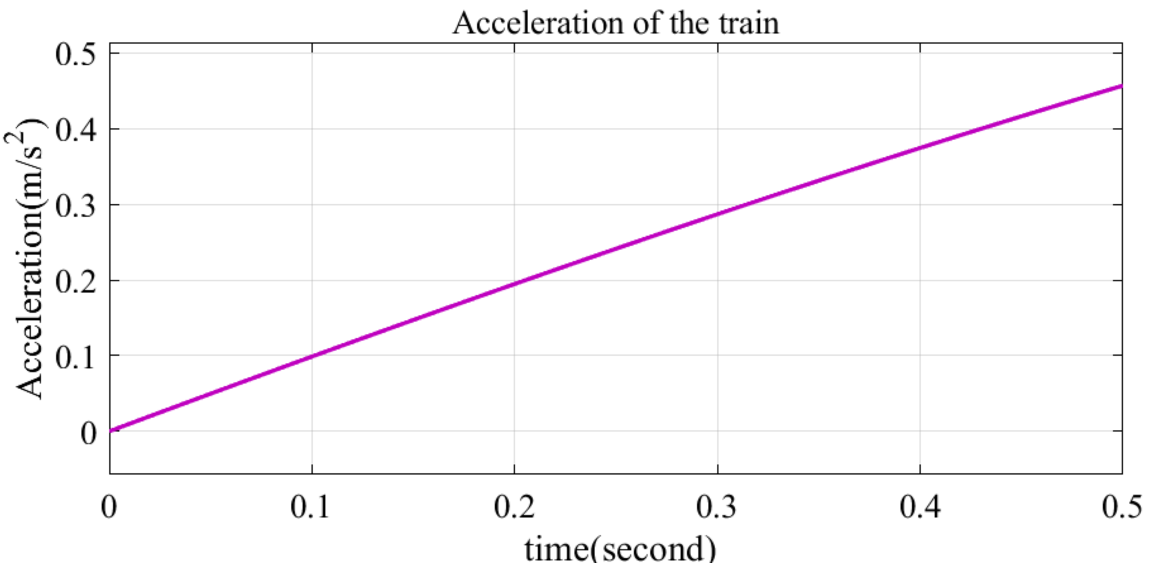

Figure 4. 20.Acceleration of the train after the supply voltage

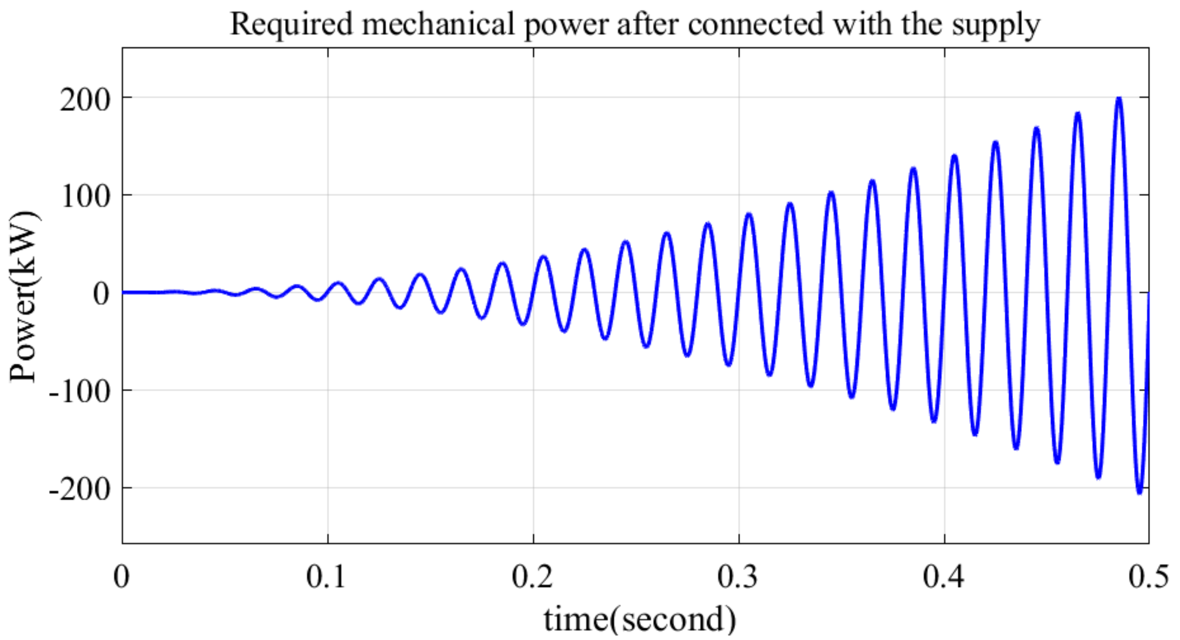

Figure 4. 21.Required mechanical power of the train after connected with the supply

Figure 4.23 below displays the alpha phase voltage and current, while Figure 4.24 below represents the beta phase voltage and current. By examining these outputs, we can observe that the alpha and beta phase voltages remain unchanged when the train dynamics are applied to the static system. This means that the dynamic and static models have the same phase voltage. However, there is a noticeable difference in the two phase currents between the dynamic and static models. This difference arises because the train is introduced as a load in the system, resulting in varying current flow in the alpha and beta phases. Each train operates with a different pantograph on the same feeder and supply line, which contributes to the differences in traction force and the corresponding pantograph, as explained in Chapter 3.

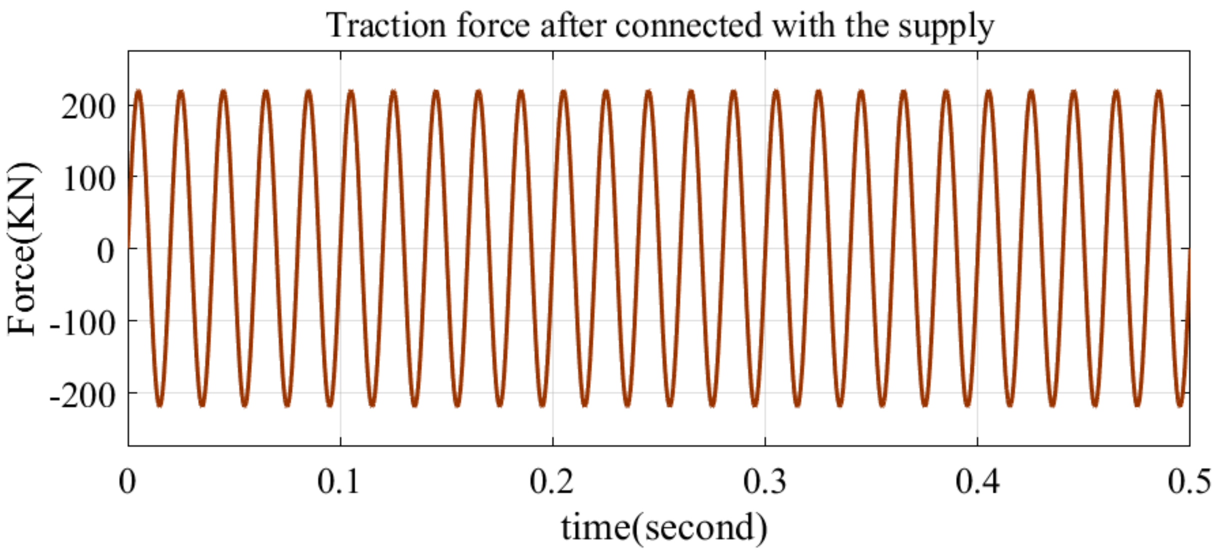

Figure 4. 22.Required Traction force of the train after connected with the supply

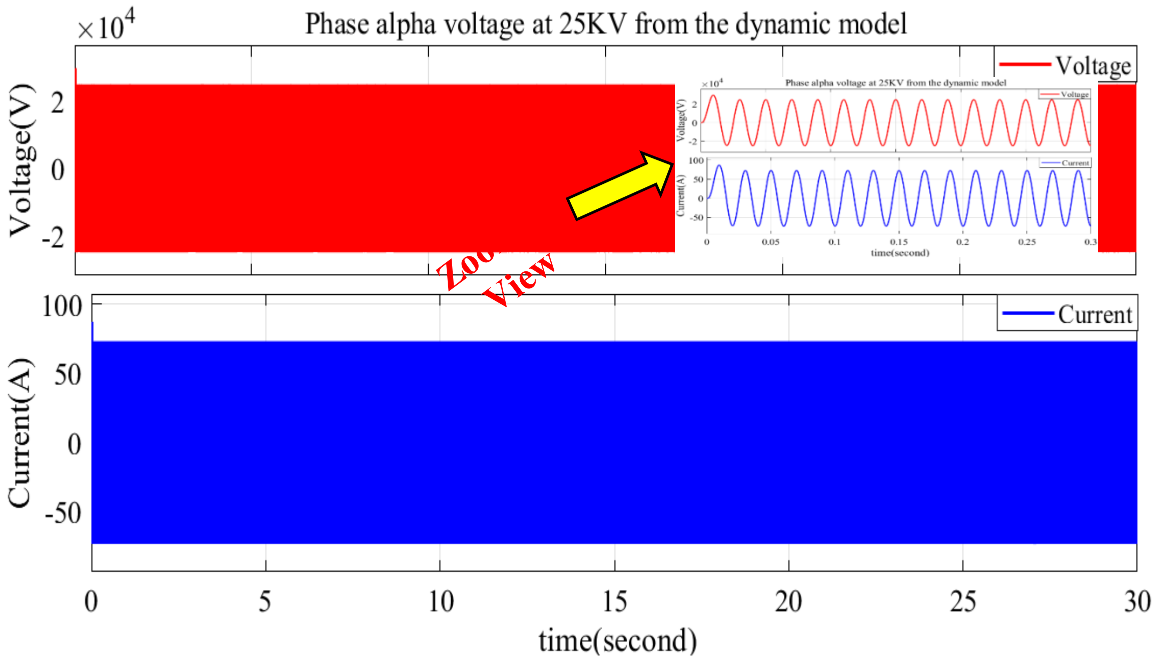

Figure 4. 23.Phase α Voltage and Current at 25 kV supply from dynamic model

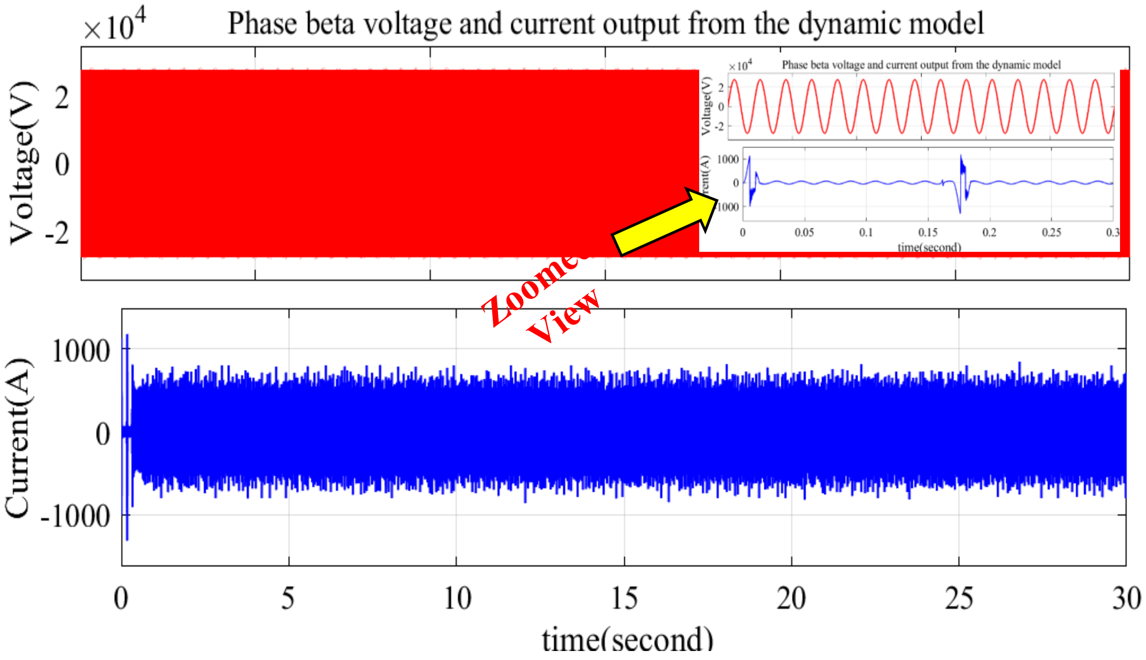

Figure 4. 24.Phase β Voltage and Current output at 25 kV supply from the Dynamic model

The dynamic model's active and reactive power are shown in Figure 4.25 below when the train is connected to the supply line. In this concept, the signal that represents the active and reactive power fluctuates in amplitude as it runs. This is because the power values are influenced by the train load, which might change as the train travels. It can be seen that the reactive power is quite low when the active power and reactive power are compared. This is supported by the Simulink display, which indicates that the active power is roughly 1885 kW and the reactive power is 33 kVar. We determine a value of roughly 0.00176 for the reactive power to active power ratio. Subtracting this value from one gives us 0.99998 or 99.99%, which indicates a power factor close to unity.

Compared to the previous power factor in Ethiopia, which was 0.67, this research has significantly improved the power factor by 0.33 or 33%. This demonstrates that the system in the dynamic model is well. Designed, and the compensator and mitigation techniques have been effectively implemented.

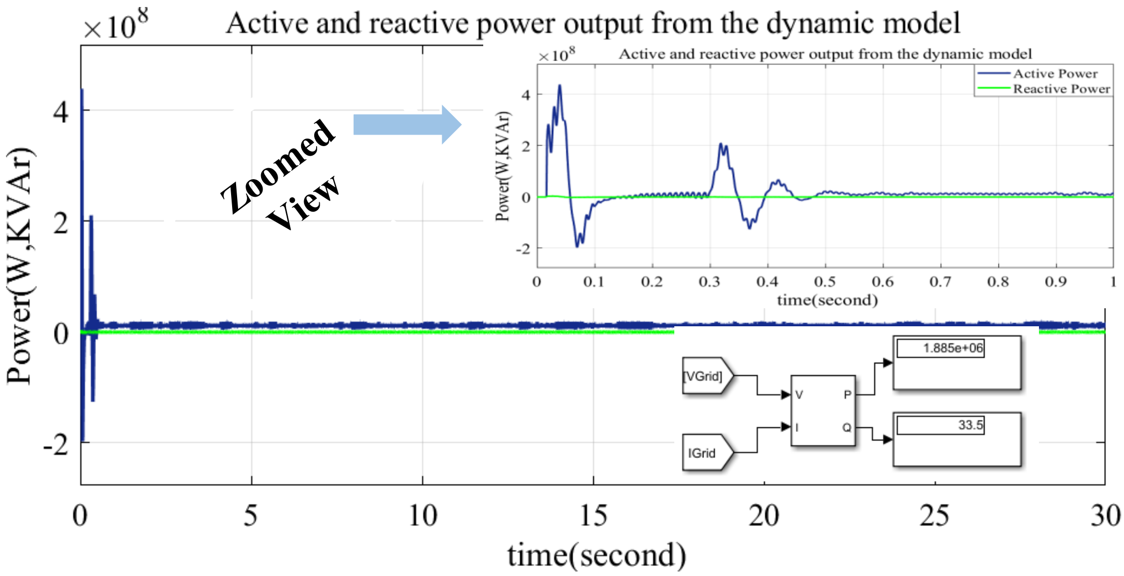

Figure 4. 25.Active and reactive power output from the dynamic model

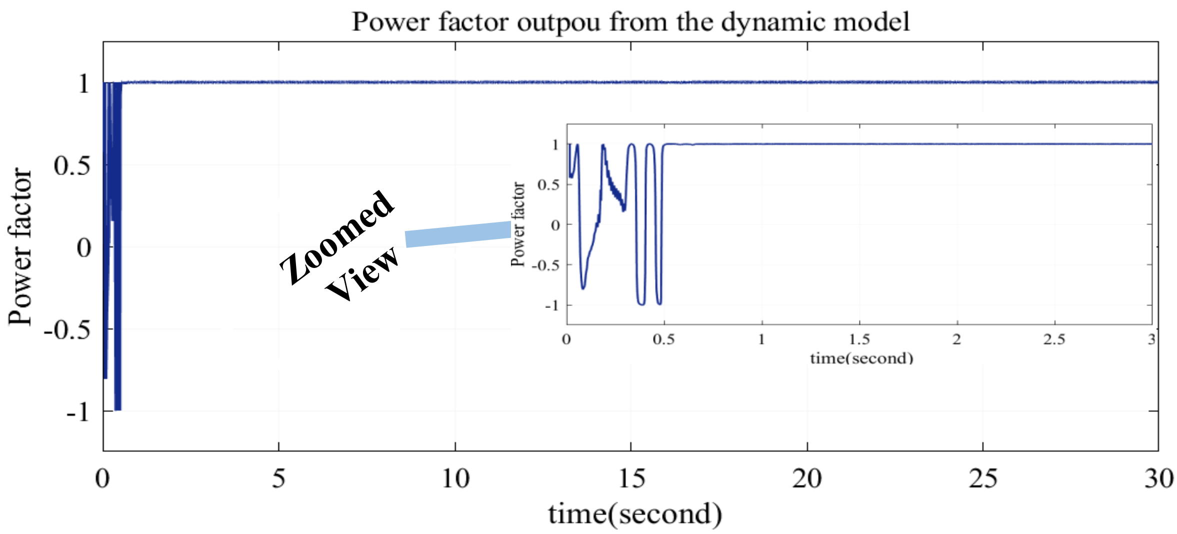

Figure 4. 26.Dynamic model power factor

Figure 4.26 is the power factor of the dynamic model of the Ethio-dijibuti railway line. This power factor is more effective than the static model. This is why the reactive is highly reduced or there is no more unused power in the railway line. This fulfills the objective of the research.

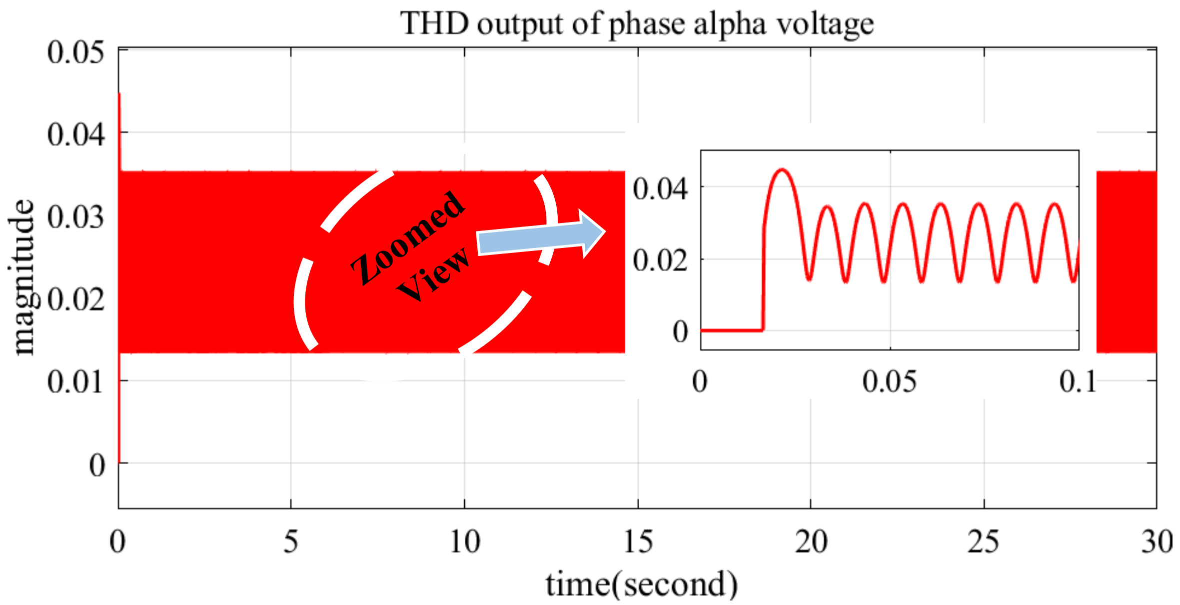

Figure 4. 27.Dynamic Model THD of Phase α Voltage at 25 kV reading

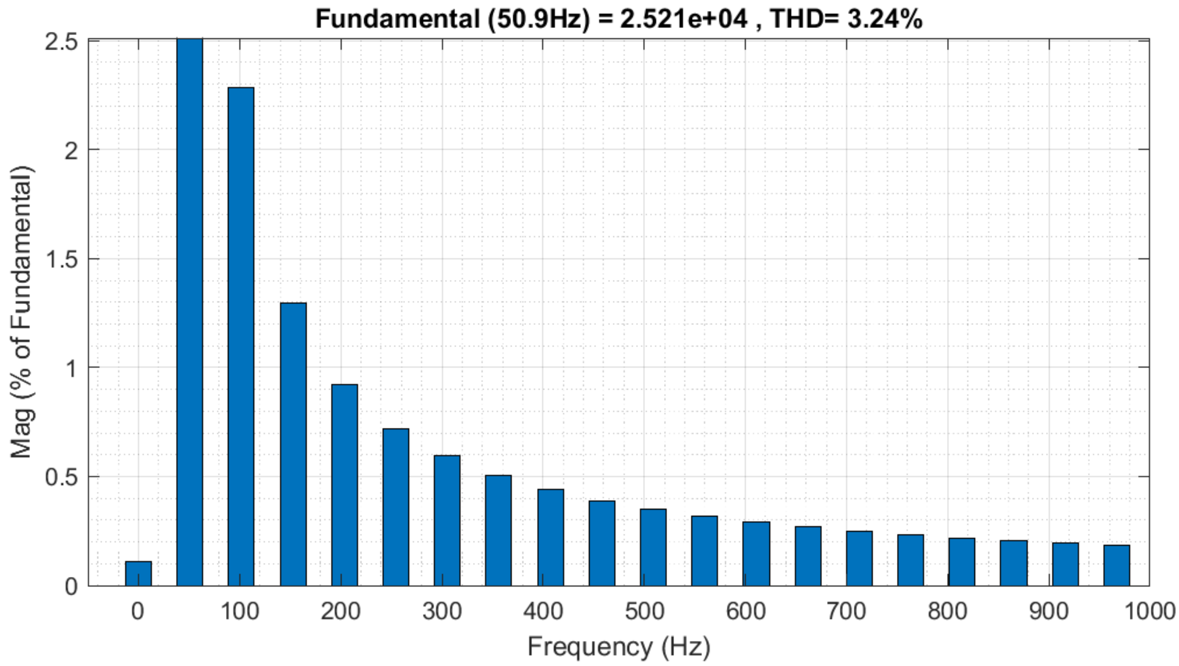

Figure 4. 28.FFT of Dynamic Model THD at Phase α Voltage at 25 kV reading

In general, the previous results from the Figure 4.13 up to Figure 4.30 reveal that the introduced model flexibility towards variable power load experienced in traction power systems. In the other figure also, the RMS and phase voltage are in their range and this indicates the mitigation technique and controller optimization is effective.

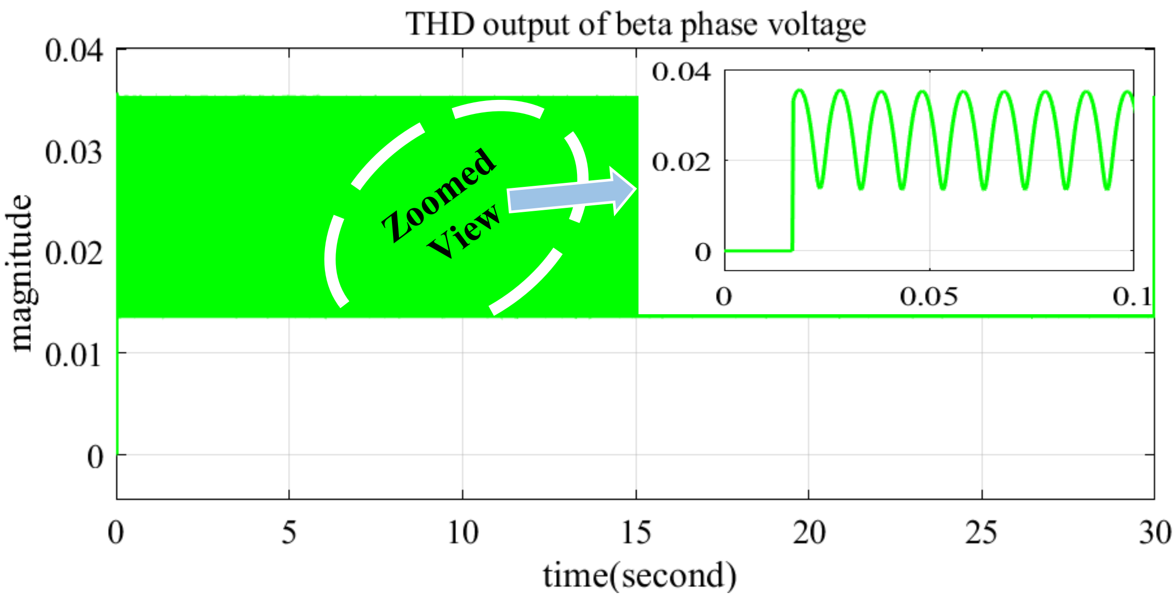

Figure 4. 29.Dynamic Model THD of Phase β Voltage at 25 kV reading

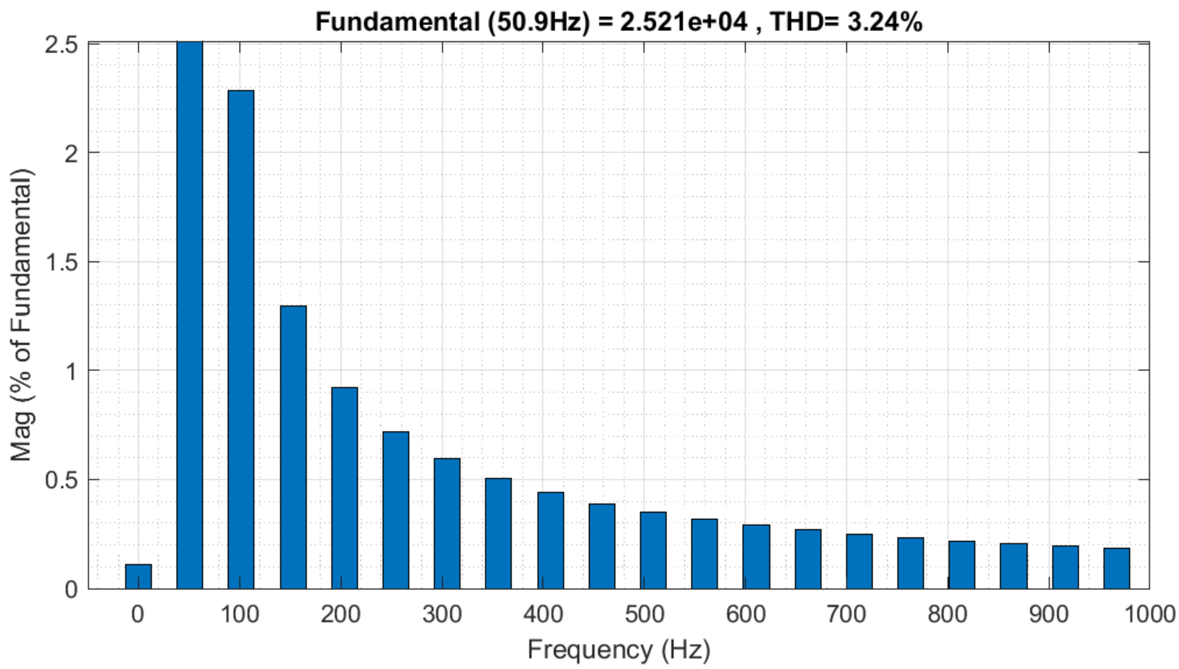

Figure 4. 30.FFT of Dynamic Model THD at Phase β Voltage at 25 kV reading

When the train model employs a variable power model based on the real power supplied for the passenger train in the Ethio-Djibouti line, active and reactive power from the source is delivered. Before employing the mitigation strategy, the power factor reading of the relevant model varies as low as 0.67 over the course of the entire movement. After the controller/compensator was introduced, the active and reactive power readings showed that the reactive power values had almost completely decreased to zero. It's significant that the power factor is almost constant throughout the entire running time. The harmonic content of the voltage is shown in Figures 4.27 through 4.30 to be within the parameters of both the GB/T 14549.1993 and the IEC TR.61000.3.6.2008 standards.

Table 4. 2: THD (%) of Phase α and Phase β Voltage at 25 kV side of Lebu Adama railway line for dynamic model and static model

Lebu to Adama line	THD	IEC TR.61000.3.6.2008
		6.5%
Phase α	3.24%	Satisfied
Phase β	3.24%	Satisfied

In order to properly handle the high reactive power reading and improve the low power factor in the traction power supply system, the introduced compensator model, SVG optimised STATCOM running based on nonnative theory control algorithm, is guaranteed.

CONCLUSIONS AND RECOMMENDATIONS

5.1. Conclusion

Modelling of the traction power supply system and efficient mitigation approaches have been used to improve the power quality, notably in terms of addressing reactive power and boosting weak power factor. The goal of this thesis was to model the system and develop a successful mitigation plan to improve the line's power quality, particularly between Lebu and the Adama line, on the Ethiopia-Djibouti route.

There has been a detailed analysis of many types of literature on AC traction power supply systems, power quality problems in TPSS, and their remediation methods for problems with high reactive power reading and poor power factor. In the literature, there is also information on modelling traction power supply components like traction substations, transmission lines (catenary systems) and/or trains (load).

Mathematical study and modelling have been done on the system for supplying traction electricity while taking into account the Lebu to Endode line. Both static and dynamic power models are employed. The model can faithfully represent the phenomenon of running the train in terms of power changes because it is based on actual measured operating data obtained from the Endode traction substation.

The research is able to show how SVG-optimized STATCOM can operate using active and non-active current theory and implement to traction power supply system in order to address the issues of high reactive power and poor power factor, which the research work primarily investigated as a problem and was focused to address.

In line with both GB/T 14549.1993 and IEC TR.61000.3.6.2008 international standards, the study shows how well the STATCOM control technique reduces THD.

The non-active current theory-controlled STATCOM is used to introduce and simulate both constant and variable power models of traction power supply systems in MATLAB/SIMULINK 2021a. According to the results, the amount of reactive power decreased by 99.9% after the controller was installed when compared to the reactive power data from before, and the power factor remained largely stable during the operation.

Particle Swarm Optimization (PSO) has an impact on the dynamic performance of the controller parameter, changing the overshoot from 2.356% to 0.352%, the rising time from 2.5% to 0.2356%, and the settling time. Additionally, the dynamic model's total harmonic distortion is 3.24%, whereas the static model's total harmonic distortion is roughly 2.78%, describing the b-spline difference between the two models

This thesis develops a flexible model of the AC traction power supply system in general. Additionally, a strong mitigation technique that can address the concerns with reactive power and weak power factor has been implemented and its engaging operation has been guaranteed. The simulation results shown in Figures 4.5 through 4.31 demonstrate the achievement of better power quality.

5.2. Recommendations

The works below are worthwhile additions.

- A thorough assessment of the line's power quality issues, including a look at their underlying causes.
- A thorough examination of the costs and benefits of implementation.
- Research the main causes as well as the accuracy of the energy readings in the traction substations.
- Create a model and evaluate the entire line in terms of the efficacy of the mitigation strategy employed in this thesis.

Once more, it is advised that Ethio-Djibouti Railway Share Company take the created model for its traction power supply system into consideration.

The author of this thesis recommends the future researcher in this area to develop a hardware model to test better accuracy and efficiency of the line from Lebu to Adama case study. And also it is better to use latest future control technology of the recent day.

REFERENCES

A. Costabeber, R. Gerin.Lajoie, and S. R. (2008). Modeling of the catenary/locomotive interaction in electrified railway networks. *In 2008 IEEE Power Electronics Specialists Conference, pp. 3304.3*.

A. Ojo, E. Babalola, and S. I. (2016). Modeling and simulation of the traction power supply system for electric railway networks. *In 2016 International Conference on Computational Science and Computational Intelligence, (CSCI),*.

A. Padilha.Feltrin, J. S. da Costa, and E. R. C. da S. (2007). Modeling and control of a static Var generator for power quality improvement. *IEEE Transactions on Power Delivery, 22, n*.

Akagi, H., Kanazawa, Y., & Nabae, A. (2000). Instantaneous Reactive Power Compensators Comprising Switching Devices without Energy Storage Components. *IEEE Transactions on Industry Applications*.

Al.Haddad, B. S. and K. (2002). Power Electronics: Converters, Applications, and Design. *John Wiley & Sons*.

Al, J. W. et. (2008). The interaction research between public grid and traction power supply system. *China Int. Conf. Electr. Distrib. CICED*, 1–8.

Alipoor, M., Shahabi, M., & Esfahani, M. R. (2022). Harmonic modeling and analysis of railway power supply systems. *IEEE Transactions on Power Delivery, 37(1)*.

Amjady, N., & Soroudi, A. (2010). *Optimal planning of FACTS devices in power systems using multi.objective particle swarm optimization*. *IEEE Trans*.

Anderson, P. M., & Fouad, A. A. (2008). (2008). *Power system control and stability. John*

Ángeles.Camacho, E. B. and C. (2017). Technical comparison of FACTS controllers in parallel connection. *J. Appl. Res. Technol, 15, n*, 36–44.

Arrillaga, J., & Watson, N. R. (2008). *Power System Harmonics*.

Arrillaga, J., Higham, A. D., & Watson, N. R. (2012). *Power system harmonics. John Wiley & Sons*.

Bhattacharya, S., Ranjan Mahapatra, V., & Mishra, S. (2018). Power Quality Improvement in Railway Traction System Using FACTS Controller. *In Proceedings of the International Conference on Power, Energy and Control (ICPEC) (Pp. 1.6). IEEE.*

Bie, Z., Wang, H., & Li, Y. (2016). (n.d.). Development of railway electrification systems: A review. Electric Power Components and Systems,. *2016, 44(1), 91..*

Chen, X., He, J., Zeng, Z., Yang, H., & C. (2020). Study on harmonic current characteristics and control strategy of high.speed train power.feeding system. *Journal of Modern Power Systems and Clean Energy, 8(4).*

Chen, Z., Zhang, Y., Wang, S., & Zhang, X. (2020). Voltage stability control strategy for railway power supply system based on multiple FACTS devices. *IET Electrical Systems in Transportation, 10(3),.*

Corporation, [37] Ethiopian Railways. (n.d.). *Rolling stock technical specification in Ethio. Djibouti railway line.*

Corporation, E. R. (2021). *About the Addis Ababa.Djibouti Railway. Retrieved from https://www.erc.gov.et/new/ethiopian.railways.corporation/155.about.the.addis.ababa.djibouti.railway.*

G. Chicco, M. Mancarella, and A. N. (2020). Impedance models for train.induced voltage disturbances in electrified railways. *IEEE Transactions on Power Delivery, 23, n.*

Glover, J. D., Sarma, M. S., & Overbye, T. J. (2018). *Power system analysis and design. Cengage Learning.*

Gyugyi, L., & Dugan, R. C. (2002). FACTS Controllers in Power Transmission and Distribution. *IEEE Transactions on Power Delivery, 17(3).*

Gyugyi, L., & Luo, A. (2007). STATCOMs: A Smart Grid Technology for Reactive Power and Voltage Control. *IEEE Power and Energy Magazine, 15(3),.*

Kennedy, J., & Eberhart, R. (1995). Particle Swarm Optimization. *Proceedings of IEEE International Conference on Neural Networks.*

Khan, M. A., Hussain, A., Chen, S., & Shaikh, F. K. (2021). (2021). Impact of Arcing Faults on the Reliability of Electrical Power Systems. *A Review. IEEE Access, 9.*

Kundur, P., & Taylor, C. W. (2017). *Power system stability and control. McGraw Hill*

Kurdak, & B. (2010). A Single Phase PLL Based Active Power Filter Solution for Power

Quality Problems in Railway Electrification Systems Using Scott Transformer. *Çukurova University*.

Li, F., He, J., Li, C., & Qiu, F. (2018). *Power quality analysis and improvement of electric railway system considering regenerative braking. Electric Power Components and Systems,. 46(13.14),.*

Lou, C., Wei, Z., Lin, Y., & Chen, W. (2021). *Analysis of power quality problems in electric railway systems and corresponding measures*.

M.cheng, G. kuma. (n.d.). Particle swarm optimization optimization of reactive power compensation. *2005*.

Mancilla.David, F., He, Y., Belkhayat, M., & Fathy, H. K. (2021). Mitigation of voltage unbalance in railway electrification systems. *A Comprehensive Review. IET Electrical Systems in Transportation, 11(1)*.

Memon, R. A., Khalil, A. M., & Ahmed, M. U. (2021). ower Quality Enhancement Techniques for AC Railway Traction Systems: *A Comprehensive Review. IET Electrical Systems in Transportation, 11(3)*.

Mohan, N., Undeland, T. M., & Robbins, W. P. (2002). *Power Electronics: Converters, Applications, and Design. Wiley*.

Mokhtari, H., & Ghazavi, M. (2021). Analysis and mitigation of harmonics caused by non.linear loads in railway electrification systems. *International Journal of Electrical Power & Energy Systems*, *125*, *10708*.

Nkundineza, C.(2017). Rail Motive power Lecture Note. *Addis Ababa Institute OT.*

Profillidis, V. (2016). Railway management and engineering. *4th Ed. Routledge*.

Raju, P. S., Kumar, A. A., & Prasad, A. N. (2022). Power quality improvement in electrified railway traction systems using a unified power quality conditioner. *International Journal of Electrical Power & Energy Systems*, *135*, *10707*.

Rendón, A., de Castro, A., & Rodríguez, J. (2014). (2014). *Power supply systems for electrified railways: A review.*

S. Paudyal, R. Rajamani, and D. G. (2019). Electric locomotive dynamic load modeling for railway traction power systems. *IEEE Transactions on Power Systems*, *32*, *n*.

Sadeghi, H., & Reisi, A. H. (2017). Comparison between SVC and STATCOM controllers for dynamic voltage stability enhancement. *2017 10th International Symposium on Telecommunications (IST), 522.527*.

Schmid, B. P. R. and F. (n.d.). A review of methods to measure and calculate train resistances. *Proc. Inst. Mech. Eng. Part F J. Rail Rapid Transit*, *214*, 185–199.

Shoman, W., Karlsson, S., & Yeh, S. (2022). Benefits of an Electric Road System for Battery Electric Vehicles. *World Electric Vehicle Journal*, *13*(11). https://doi.org/10.3390/wevj13110197

Singh, B., & Al.Hinai, M. (2009). *Applications of FACTS Controllers in Power Systems. Springer*.

Singh, G. K., & Pant, M. (2015). Particle Swarm Optimization.Based Proportional.Integral Controller Design for Load Frequency Control of Interconnected Power Systems. *IEEE Systems Journal, 9(3)*.

V. S. Tejwani, H. B. Kapadiya, A. S. Pandya, and J. B. B. (2015). Power quality improvement in power distribution system using D.STATCOM. *2013 Nirma Univ. Int. Conf. Eng. NUiCONE 2013*, *4*, *no*, 75–80.

Vladu, A., & Andrei, V. (2015). (2015). *Considerations regarding the autotransformer feeding mode in railway systems. 2015 Inter*.

Y. Xu, L. M. Tolbert, F. Z. Peng, J. N. Chiasson, and J. C. (2007). Compensation. based non.active power definition. *IEEE Power Electron. Lett*, *1*, *no*, 45–50.

Yi, S. (2017). Traction Calculation," in Principles of Railway Location and Design. *Academic Press*, 73–157.

Z. He, Z. Zheng, and H. H. (2016). Power quality in high.speed railway systems.

Zargari, N. R., Niroomand, S., & Shahnia, F. (2018). *Investigation of direct feeding and autotransformer feeding methods in the electrified railway system. IET Electr*.

Zhang, H., Li, L., & Zhang, L. (2022). ower quality analysis and improvement for railway traction systems. *Electric Power Systems Research, 203, 107570.*

Zhang, W., Li, L., & Wang, H. (2019). *Power quality analysis of high.speed railway traction system based on unbalanced power flow*. *IEEE Acces*.

Appendix

A. Total Energy Reading for One Month

The total sum of active and reactive energy reading measured in railway energy meter reading at the Ethio-Djibouti railway line in August 2018.

No.	Line Name	Total Active Energy in kWh	Total Reactive Energy in kVarh
3	Kaliti-I C10 to Endode T/S (Control Room)	520,608.00	490,960.00
4	Akaki-II E02 to Encode T/S		
5	Nazareth II E07 to Mojo T/S	427,680.00	2,954,160.00
6	Awash II Hepp E12 to Wulunchiti T/S		
7	Meteora E03 To MELKA Jilo T/S	683,484.00	5,317,648.00
8	Awash 7-KILOE05 to Awash T/S		
9	Awash 7-KILO E06 to Sirba Kunkur T/S	490,788.00	4,379,008.00
10	Asebe Teferi E05 to Miesso T/S		
11	Asebe Teferi E04 to Afdem T/S (existing line)	426,880.00	7,219,840.00
12	Hurso D10 to Hurso T/S (new one) 230KV		
13	Hurso E01 to Gota T/S (existing line) 132 KV	422,400.00	2,925,120.00
14	Adigala to Adigala T/S		
	Total	2,971,840.00	23,096,736.00

B. Overall Simulink Model of the Static System

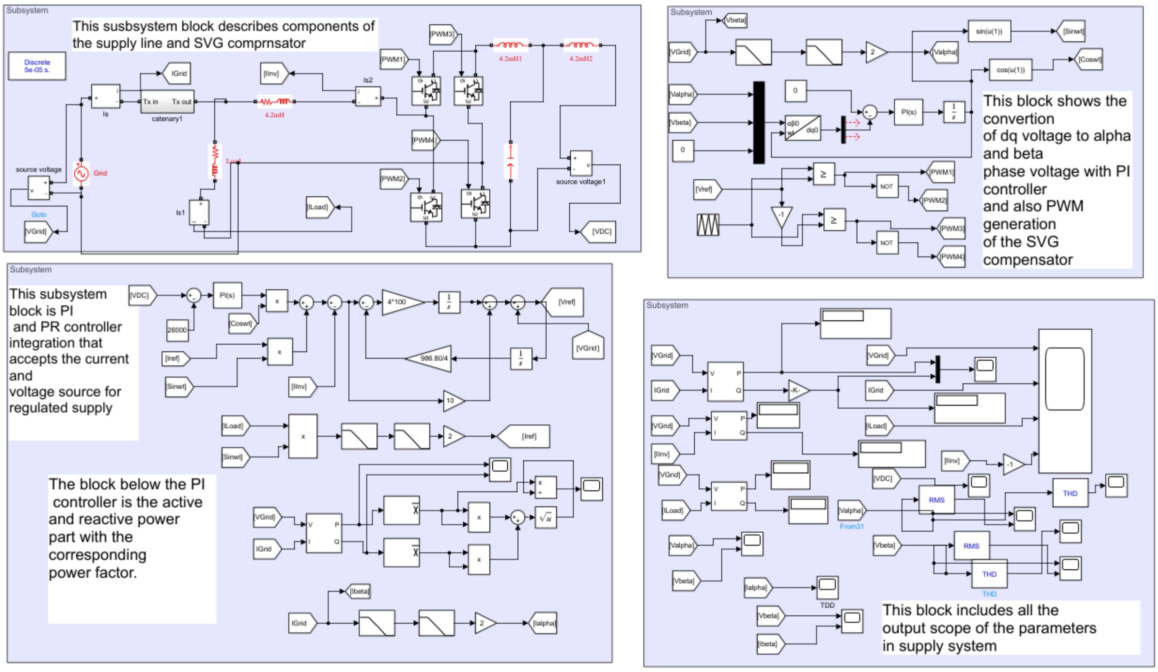

C.Overall Simulink Model of the Static System

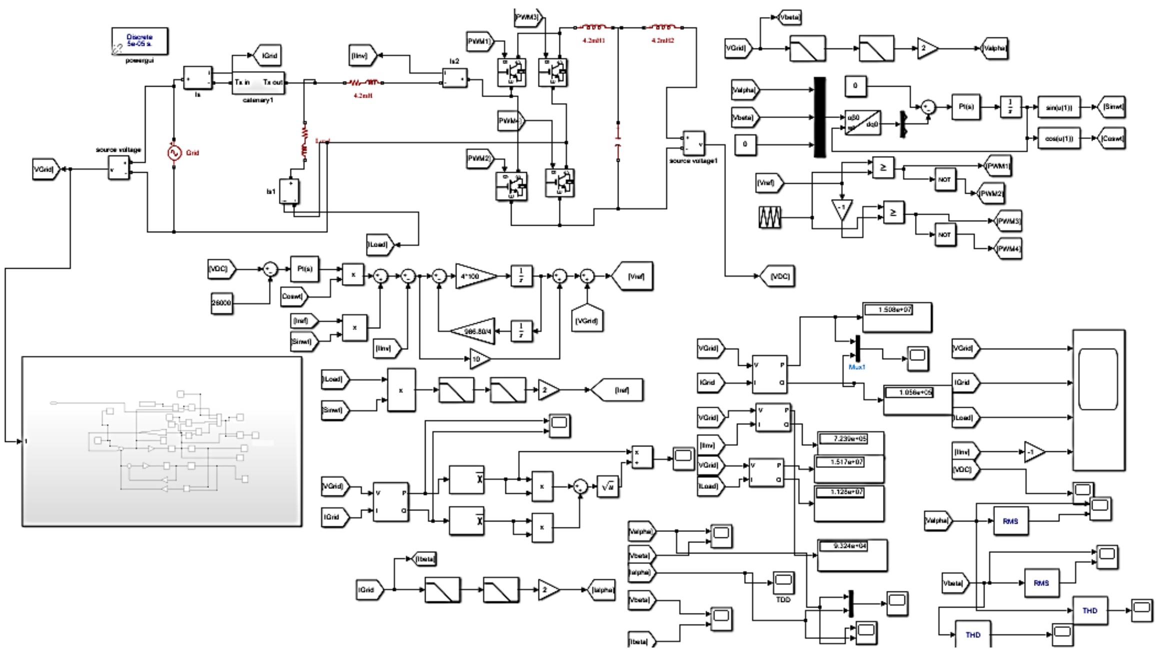

D. Train Dynamic Model

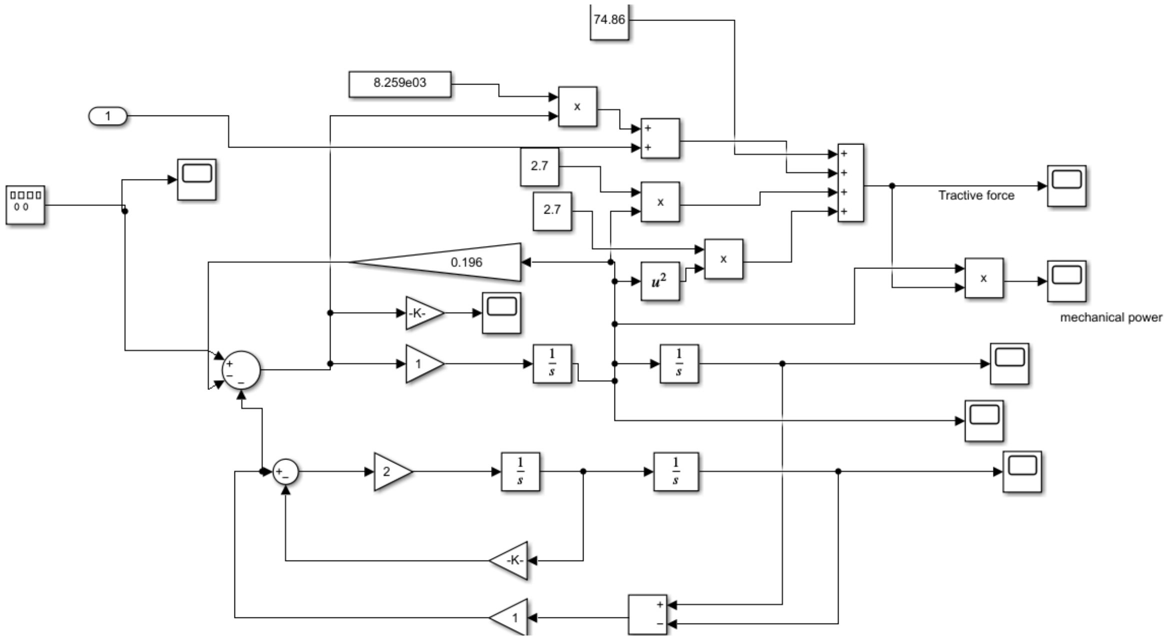

E. Matlab Partial Code for PSO tuning PI Parameter

```
%%the objective function for optimization of PSO
% Measures a performance index from the simulink model
function objfunc=  EvalObj(x)
% Updates the values of Kp, Ki and Kd in Simulink model
workspace
simulink_model= 'aytonew_PI';
load_system(simulink_model);
gains= get_param(simulink_model,'modelworkspace');
popsize= size(x,1);
objfunc= zeros(popsize,1);

    % Simulates the simulink model to get the outputs
    simOut= sim(simulink_model,'SaveOutput','on');

    % Retrieves time t and error e
    t= simOut.find('t');
    e= simOut.find('e');
```

```
    % Calculate a performance index using the trapezoidal
integration rule
    n= length(e);
    ae= abs(e);
    objfunc(k)= 0;
    for i= 2:n
        stepsize= t(i)-t(i-1);
        objfunc(k)=  objfunc(k)+0.5*(ae(i-1)+ae(i))*stepsize;
% IAE
    end
end
%Tune the gains of the PID controller using the PSO
function Tune_aytonew_PI
rng default % Initialize the random number generator
options                                                             =
optimoptions('particleswarm','PlotFcn',@pswplotbestf);
options.MaxIterations= 30;
options.SwarmSize= 20;
nvar= 4;
LB=  [0.0001  0.0001  0.0001  1];  %  Lower  bound  of  tuning
parameters
UB= [10 70 1 1]; % Upper bound of tuning parameters
[x,fval]= particleswarm(@EvalObj,nvar,LB,UB,options)
```